AD_____

Award Number: W81XWH-09-2-0113

TITLE: Advancing Individualized Medicine by Understanding Phenotypic Integration Using the Human Skeleton as a Model System

PRINCIPAL INVESTIGATOR: Karl J. Jepsen, Ph.D.

CONTRACTING ORGANIZATION: Mount Sinai Medical Center
New York, NY 10029

REPORT DATE: September 2011

TYPE OF REPORT: Annual

PREPARED FOR: U.S. Army Medical Research and Materiel Command
Fort Detrick, Maryland 21702-5012

REPORT DOCUMENTATION PAGE

Form Approved
OMB No. 0704-0188

1. REPORT DATE	2. REPORT TYPE	3. DATES COVERED
September 2011	Annual	1 September 2010 – 31 August 2011

4. TITLE AND SUBTITLE

Advancing Individualized Medicine by Understanding Phenotypic Integration Using the Human Skeleton as a Model System

5a. CONTRACT NUMBER

5b. GRANT NUMBER
W81XWH-09-2-0113

5c. PROGRAM ELEMENT NUMBER

6. AUTHOR(S)

Karl J. Jepsen

E-Mail: karl.jepsen1@gmail.com

5d. PROJECT NUMBER

5e. TASK NUMBER

5f. WORK UNIT NUMBER

7. PERFORMING ORGANIZATION NAME(S) AND ADDRESS(ES)

Mount Sinai Medical Center
New York, NY 10029

8. PERFORMING ORGANIZATION REPORT NUMBER

9. SPONSORING / MONITORING AGENCY NAME(S) AND ADDRESS(ES)
U.S. Army Medical Research and Materiel Command
Fort Detrick, Maryland 21702-5012

10. SPONSOR/MONITOR'S ACRONYM(S)

11. SPONSOR/MONITOR'S REPORT NUMBER(S)

12. DISTRIBUTION / AVAILABILITY STATEMENT
Approved for Public Release; Distribution Unlimited

13. SUPPLEMENTARY NOTES

14. ABSTRACT
Susceptibility to common, heritable diseases is generally thought to originate at the genetic-level, and most studies seek genomic variants or altered molecular networks to develop novel diagnostics and treatments to reduce disease risk on a personalized basis. We show that fracture susceptibility in human tibiae and femora can also arise at a higher-level of biological organization, a phenomenon that may be difficult to predict from genetic information alone, because it involved biomechanical tradeoffs, constraints on cellular activity, and a network of compensatory trait interactions defining organ-level function. Importantly, we also identified a novel level of biological control regulating the degree of internal remodeling affecting young adult tibiae and aging femora. Limited compensation at this level of biological organization may be a public health concern, not only because of the increased fracture susceptibility, but also because it is unclear to what extent prophylactic treatments can circumvent intrinsic cellular constraints to establish a higher degree of functional equivalence among individuals. Thus, the funds supporting our research efforts have significantly advanced our understanding of bone by identifying a "flaw" or limitation in the functional adaptation process that may contribute to fracture risk and by discovering biological controls regulating internal remodeling that have not previously been reported.

15. SUBJECT TERMS
Individualized medicine; functional in-equivalence; phenotypic integration; biological limitations; stress fractures; bone strength

16. SECURITY CLASSIFICATION OF:			17. LIMITATION OF ABSTRACT	18. NUMBER OF PAGES	19a. NAME OF RESPONSIBLE PERSON
a. REPORT	b. ABSTRACT	c. THIS PAGE			USAMRMC
U	U	U	UU	86	19b. TELEPHONE NUMBER *(include area code)*

Table of Contents

Introduction

Trauma associated with warfare affects multiple physiological systems and often in very complex ways. Recent advances revealed that physiological systems rely on compensatory changes among traits to establish and maintain function. The compensatory changes among traits is called phenotypic integration. An important, emergent property of phenotypic integration is that an individual acquires a specific set of adult traits. Although acquiring a specific set of traits establishes system function for normal "daily" conditions, the downside is that not all sets of traits will perform well under extreme conditions. Consequently, certain individuals will be susceptible to health risks under extreme conditions despite being perfectly healthy under daily conditions. Tolerance to extreme conditions is expected to vary among individuals and among physiological systems. We postulate that phenotypic integration is central to health and disease, because it is directly involved in establishing a person's response to genetic and environmental perturbations. Knowing how multiple traits and their interactions respond to the environment and/or medical treatment regimens will improve the physicians ability to treat complex systems more effectively and on an individualized basis.

The skeleton has proven to be a remarkable model to study phenotypic integration. Phenotypic integration in the skeletal system results from biological processes that adapt structure and matrix quality to achieve a particular functional endpoint. Consequently, the set of traits acquired by an individual during growth provides insight into system-level biology. We propose to investigate phenotypic integration for the femoral neck, an important fracture site associated with significant morbidity and mortality. We propose to identify the compensatory trait interactions resulting in trait sets that are functional for both daily activities as well as during an extreme condition such as a fall. We hypothesize that variation in femoral neck width will be compensated by coordinated changes in traits specifying cortical thickness, trabecular architecture, and mineralization. This integrative, top-down systems approach is a major departure from conventional reductionist approaches, and offers the advantage of advancing personalized medicine well in advance of identifying the genetic variants that are responsible for variation in skeletal strength and fragility.

From Statement of Work: In year 1, a peripheral Quantitative Computed Tomography (pQCT) scanner will be purchased and modified to acquire full three-dimensional images over the entire proximal femur. A validation study will be conducted to determine the accuracy and repeatability for measuring bone morphology and tissue-mineral density using the customized 3-D pQCT system. Optimal scanning parameters will be identified to improve accuracy and repeatability.

In year 2, three-dimensional, high-resolution images of the proximal femur will be constructed for an existing collection of cadaveric femora from adult men and women. Each bone image will be calibrated to convert grayscale values to tissue-mineral content values. Morphological and compositional bone traits will be quantified for the femoral mid-shaft and femoral neck. Phenotypic integration will be examined using Path Analysis to evaluate how variation in age, sex, and external bone size are compensated by functional interactions among traits specifying marrow expansion, trabecular architecture, and tissue-mineral density. Quantitative measures of bone function will be obtained by mechanically loading femora in the mid-stride position to evaluate stiffness under daily load conditions. The femora will then be loaded to failure in the fall position to evaluate the strength and toughness (fragility) under an extreme load condition. The Path Models will identify the pattern of trait sets and thus the compensatory interactions among traits required to establish and maintain mechanical function for this population.

Nearly all objectives have been accomplished. We found that it was not necessary to create 3D volumes from the pQCT images to quantify the traits contributing to whole bone mechanical function. We were able to explain nearly 65% of the variation in bone strength based on a few (select) traits measured from 2D images of the femoral neck. This is an important outcome because of the cost savings involved in predicting strength from 2D rather than 3D images.

Body

This report is divided into two sections. The first section describes the results of a collaborative project involving the US DoD and the UK Military in which we analyzed data from pQCT images generated for the tibia of nearly 700 individuals and answered a very important question, "does the adaptation process in bone lead to functionally equivalent outcomes across a population of healthy individuals?" This study was recently accepted into the Journal of Bone and Mineral Research. Athough this collaborative study was not described in the Statement of Work, the line of research is directly related to our mission of understanding bone as a complex system. In addition to answering the question stated above, we also reported a novel finding that there is a biological control mechanism regulating internal remodeling that has not been previously reported. We found that the degree of internal remodeling is highly dependent on whether a person has slender (narrow relative to length) or robust (wide relative to length) tibia. Slender tibiae showed reduced internal remodeling compared to robust tibiae. This finding is mentioned here because a similar outcome was discovered during our analysis of the proximal human femur (second section).

In the second section of this report, we describe our progress in studying the human proximal femur, a major site of fractures. This study provided important new insight into how the functional adaptation process works across a population as well as how robustness is associated with age related bone loss. The results indicated that slender femora are constructed with a different set of traits compared to robust femora and that segregating femora by the natural variation in robustness provided a model to identify predictable differences in age related bone loss. Importantly, slender femora showed very little age-related bone loss compared to robust femora, which showed a significant amount of bone loss with aging. This finding is entirely consistent with our discovery from the analysis of the human tibiae, and is important clinically because it means that we can now personalized treatments to the biological needs of the individuals (i.e., anti-resorptive treatments may be more effective in individuals with robust bones and less effective in individuals with slender bones). Taken together, clinical diagnoses and treatments will benefit from a better understanding of these bone-size specific structural and bone-loss patterns. Thus, studying bone as a complex system and using an integrative scientific approach has proven to be an extremely effective method to answer hard questions regarding bone functionality and for discovering novel biological controls that may affect how individuals are treated prophylactically to reduce fracture risk.

Section 1. Biological constraints that limit compensation of a common skeletal trait variant lead to inequivalence of tibial function among healthy young adults

The following text is taken from a manuscript that was accepted to the Journal of Bone and Mineral Research and that involves an international collaboration among investigators studying bone adaptation and stress fracture risk in men and women engaged in military training (see Reportable Outcomes for author list). Details of Methodology can be found in a copy of the accepted manuscript provided in Appendix 2. We applied the same ideas about phenotypic integration that we proposed for the femoral neck to the tibia. This study has significantly advanced our understanding of how biological limitations affect skeletal function. We found highly predictable patterns in the way traits covary to establish function among individuals, but tibiae that are slender relative to body size are less stiff relative to applied loads compared to robust bones. This functional in-equivalence is highly predictable based on simple measures acquired using pQCT. This study has re-focused the analysis we conducted for the femoral neck, such that, we also tested for functional equivalence in the femoral neck.

Introduction

Physiological systems, like bone, tolerate many genetic and environmental factors by adjusting traits in a highly coordinated, compensatory manner to establish organ-level function. This ubiquitous process is critical for population-wide fitness and occurs at all levels of biological organization (1-3), including interactions among systems (4). Trait variants that are commonly expressed in a population are expected to be adequately compensated to have survived the pressures of natural selection (5). However, the amount of variation in system function tolerated by a population is not fully understood (6). For most systems, individual traits are nonlinearly related to organ-level function, and intrinsic boundaries on cellular activity could limit the degree to which adaptive processes can adjust traits, resulting in functional disparity or inequivalence among individuals. Functional inequivalence associated with a common trait variant could be a public health concern if system performance is limited and susceptibility to common diseases is increased for a predictable segment of the population.

We studied how biological constraints that limit compensation of a common skeletal trait variant lead to functional inequivalence among healthy, young adults. To be functional, bones must be sufficiently stiff and strong to support the loads incurred during daily activities. The adaptive process that adjusts traits to match bone stiffness with these loads occurs primarily during growth (7) with continued modifications throughout life (8). This process is well understood for the population-average bone. However, two people with similar body sizes can acquire widely varying bone sizes, ranging from slender (narrow relative to length) to robust (wide relative to length) (Figure 1). Bone robustness is a common, heritable (9) morphological variant established by approximately 2-years of age (10). Because bone stiffness is proportional to the fourth power of width, small variations in width must be compensated by large, coordinated changes in other traits (11,12) to maximize stiffness while minimizing mass (13), otherwise slender bones would be weak and prone to fracturing, whereas robust bones would be bulky and metabolically expensive to maintain and move through space. Slender bones are generally assumed to be less strong than robust bones (14,15), but just how much variation in function is tolerated among healthy individuals and whether this variation stems from limited functional compensation are not known. We hypothesized that the nonlinear relationship between bone width and whole bone stiffness is too severe for bone cells to compensate slender and robust bones equivalently. Our goals were to determine if adaptive processes establish a uniform level of skeletal function across a healthy population and to identify biological constraints that limit the ability of the skeletal system to fully compensate the normal range in robustness.

Figure 1. Representative pQCT images of slender and robust tibial cross-sections taken at the 38 and 66% anatomical sites. Measures of morphology are shown for clarification.

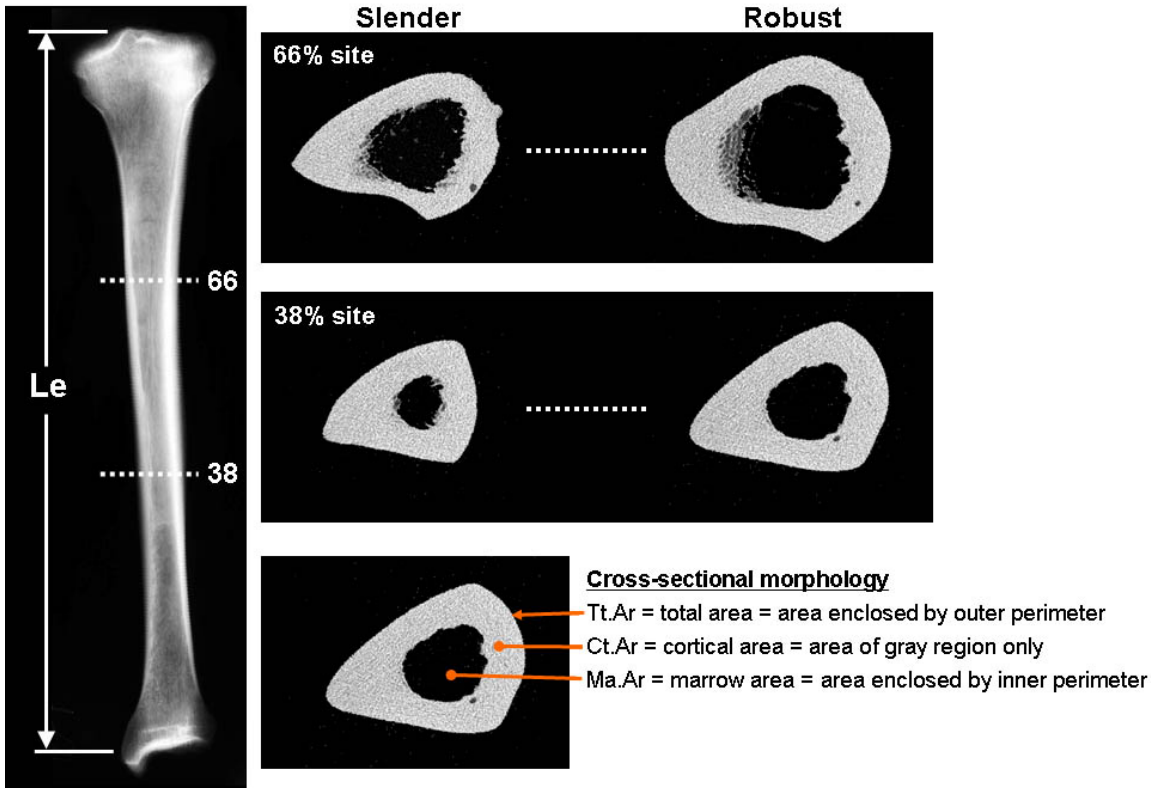

Study participants

A total of 730 women (20.8 ± 3.1 years old) and men (21.4 ± 3.4 years old) from the United States and the United Kingdom volunteered to participate in this study, all with informed consent. The average BMI for those with recorded height was 23.4 ± 2.9 kg/m^2 for women and 23.7 ± 2.8 kg/m^2 for men. For the US cohort, 347 individuals (321 women, 26 men) were enrolled through the Naval Station Great Lakes (Great Lakes, Illinois, USA), the Physical Therapy Department at Oakland University (Rochester, Michigan, USA), and the University of Connecticut (Storrs, Connecticut, USA). Individuals recruited into the US cohort were healthy and had no prior participation in organized sports. For the UK cohort, 383 individuals were recruited through the Army Training Centre in Pirbright, England (148 women, 100 men) and the Infantry Training Centre in Catterick, England (135 men). These individuals all passed rigorous medical entry assessments. The only criteria for excluding individuals from the study was image quality. A few individuals moved during pQCT scanning, resulting in tibial cross-sections with small streaks in the image. Each image was scored for image quality by one individual (CN) prior to quantifying cross-sectional morphology. Those with motion artifacts near the region of interest were removed from the analysis. In addition, data for one woman from the US cohort with unusually robust bones (> 5 standard deviations from the mean) were excluded, because her traits generated excessively large residuals that affected most regression analyses. Of the total number of individuals enrolled, 696 individuals (442 women, 254 men) had valid information regarding anthropometric and morphological traits that were absent of motion artifacts from which functional equivalence was tested. Individuals were from various racial and ethnic backgrounds, but were primarily Caucasian. All datasets were combined and segregated by sex only.

Validation studies

Because whole bone bending stiffness depends on both morphology and tissue-quality, a validation study was conducted using cadaveric tibiae to determine how Ct.TMD determined by pQCT relates to matrix mineralization and porosity, both of which affect X-ray attenuation and define tissue-modulus. A linear regression analysis revealed that none of the traits of interest (robustness, TtAr, CtAr, MaAr, CtTMD, Le, J, E) changed significantly with age (R^2 = 0.0 - 0.1, p-value = 0.1 - 0.9), and this was true for the 25, 38, 50, 66, and 75% anatomical sites. Linear regression analysis showed that Ct.TMD correlated positively with ash content (R^2=0.34, p<0.007) and negatively with porosity (R^2=0.51, p<0.0004) and pore density (R^2=0.35, p<0.006). Pore density correlated significantly with porosity (R^2=0.40, p<0.003), as expected. Multiple linear regression analysis showed that 63% of the variation in Ct.TMD was explained by ash content, porosity, and pore density (Table 1). Tissue-modulus determined by conventional 4-point bending tests correlated positively with Ct.TMD (R^2=0.27, p<0.0004), as expected.

Table 1. Multiple linear regression analysis

EQUATION	R^2 (adj)	p-value
Ct.TMD = 668 - 7.20 %Porosity + 977 %Ash Content	0.60	0.0001
Ct.TMD = 657 - 4.84 %Porosity + 1046 Ash Content - 2.70 Ct.Po.N	0.63	0.0001

Further examination revealed significant negative correlations between robustness and Ct.TMD (Figure 2A) and ash content (Figure 2B), as expected. Surprisingly, a significant positive correlation was observed between porosity and robustness (Figure 2C), which remained significant after accounting for age effects by partial regression analysis (R^2=0.42, p<0.04). The slope of the tissue-modulus versus robustness regression (Figure 2D) was not significantly different between the live human cohort and the cadaveric data (p<0.84, ANCOVA), confirming that our method of estimating E from Ct.TMD replicated the full range of variation in tissue-modulus expected for the live human cohort. A small difference in the y-intercepts between regressions was expected because of differences in attenuation associated with imaging cadaveric tibiae in water compared to acquiring images for tibiae of living humans with surrounding muscle, fat, and skin.

Finally, the whole bone 4-point bending tests showed that EI measured at the 38% site correlated best (i.e., slope closest to 1) with bending stiffness measured in the P-A and L-M directions (Figure 2E). This was confirmed by conducting a Bland Altman analysis, which compared the difference between EI measured directly by 4-point bending to EI measured by pQCT at each of the 5 anatomical sites. The data points for the 25 and 38% sites were on average 0.3 SD away from the average of the two methods, whereas data for the 50, 66, and 75% sites were on average 1.0, 2.4, and 3.4 SDs, respectively, from the average of the two methods. The regression between the Difference and the Average showed that the 38% site had the lowest R^2-value (p<0.1) and the p-value was not significant (p<0.11). This regression was borderline significant for the 25% site (negative slope, R^2=0.14, p<0.06) and highly significant (all positive slopes, R^2=0.72-0.92, all p<0.0001) for the 50, 66, and 75% sites, indicating that stiffer bones were underestimated by pQCT data measured at the 25% site and overestimated by pQCT data measured at the 50, 66, and 75% sites. Thus, EI measured at the 38% site was the only site to show good agreement between methods and consistent predictability across all stiffness values. Thus, we show that EI calculated from pQCT images accurately estimated whole bone bending stiffness.

Figure 2. **A)** Ct.TMD, **B)** ash content, and **C)** porosity correlated significantly with tibial robustness measured at the 66% anatomical site. **D)** Tissue-modulus measured directly for the cadaveric tibiae correlated negatively with robustness. The slope of this line was not significantly different from that of the entire live human cohort ($p<0.84$, ANCOVA), where E was estimated from Ct.TMD measured by pQCT. **E)** Bending stiffness (EI) estimated from pQCT images acquired at the 38% site accurately predicted whole bone bending stiffness of cadaveric tibiae (n=13) loaded to failure in conventional 4-point bending tests in the postero-anterior (P-A) and latero-medial (L-M) directions. Tissue-stiffness, E, was estimated from tissue-mineral density (Ct.TMD) and I was calculated about the PA- and ML-axes from the pQCT images.

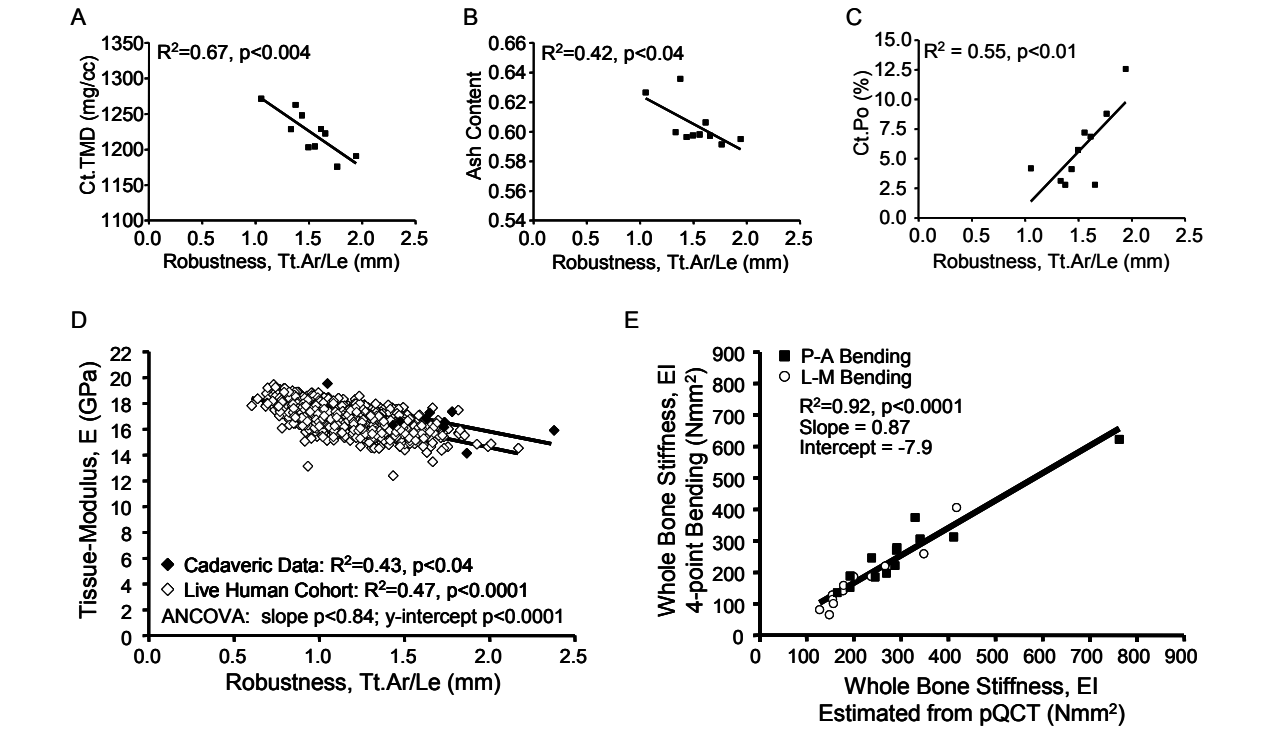

Functional equivalence

Morphological traits were quantified for tibial diaphyses using peripheral Quantitative Computed Tomography, pQCT (XCT 2000 or 3000; Stratec Medizintechnik, Pforzheim, Germany), as described previously (16). Tibial robustness (total cross-sectional area / tibial length) was normally distributed ($p>0.10$, Kolmogorov-Smirnov test) and varied ~2-fold among men and women (Figure 3A). Further, robustness increased modestly with BW-Le (Figure 3B), and significant differences in the y-intercept ($p<0.0001$, ANCOVA) indicated the greater tibial robustness for men was independent of a measure of body size, consistent with sexually dimorphic growth patterns.

To test for functional equivalence, we determined whether the relationship between whole bone bending stiffness and the applied loads depend on robustness. Whole bone stiffness increased with applied loads (Figure 3C), and the R^2-values suggested our study population tolerated a modest degree of variation in bone stiffness. Because the slope of the regressions for EI versus robustness was significantly different between men and women ($p<0.017$, ANCOVA), we tested for sex-specific effects by correcting EI for BW-Le by regression analysis. When men and women were compared at a common BW-Le (260.2 kg cm), male tibiae were 40.9% stiffer relative to applied loads compared to female tibiae ($p<0.0001$, t-test). Importantly,

bone stiffness correlated significantly with robustness for both sexes after accounting for BW-Le (Figure 3D). Tibiae that were slender relative to BW-Le were as much as 2-3 times less stiff relative to applied loads compared to robust tibiae. This analysis confirmed that the variation in robustness was not fully compensated by the underlying biology, resulting in functional inequivalence among individuals, as hypothesized.

Figure 3. Tibial robustness (Tt.Ar/Le) measured at the 66% anatomical site **A)** varied widely among women (solid line) and men (dashed line), and **B)** increased modestly with BW-Le for women (R^2=0.10) and men (R^2=0.08). Differences in the y-intercept (ANCOVA, p<0.0001) indicated that men have more robust tibiae relative to BW-Le compared to women. C) Whole bone bending stiffness (EI) increased significantly with BW-Le for women (R^2=0.38) and men (R^2=0.38). **D)** Whole bone bending stiffness correlated significantly with robustness for women (R^2=0.40) and men (R^2=0.37) after accounting for BW-Le by partial regression analysis. All linear regressions were significant at p<0.0001.

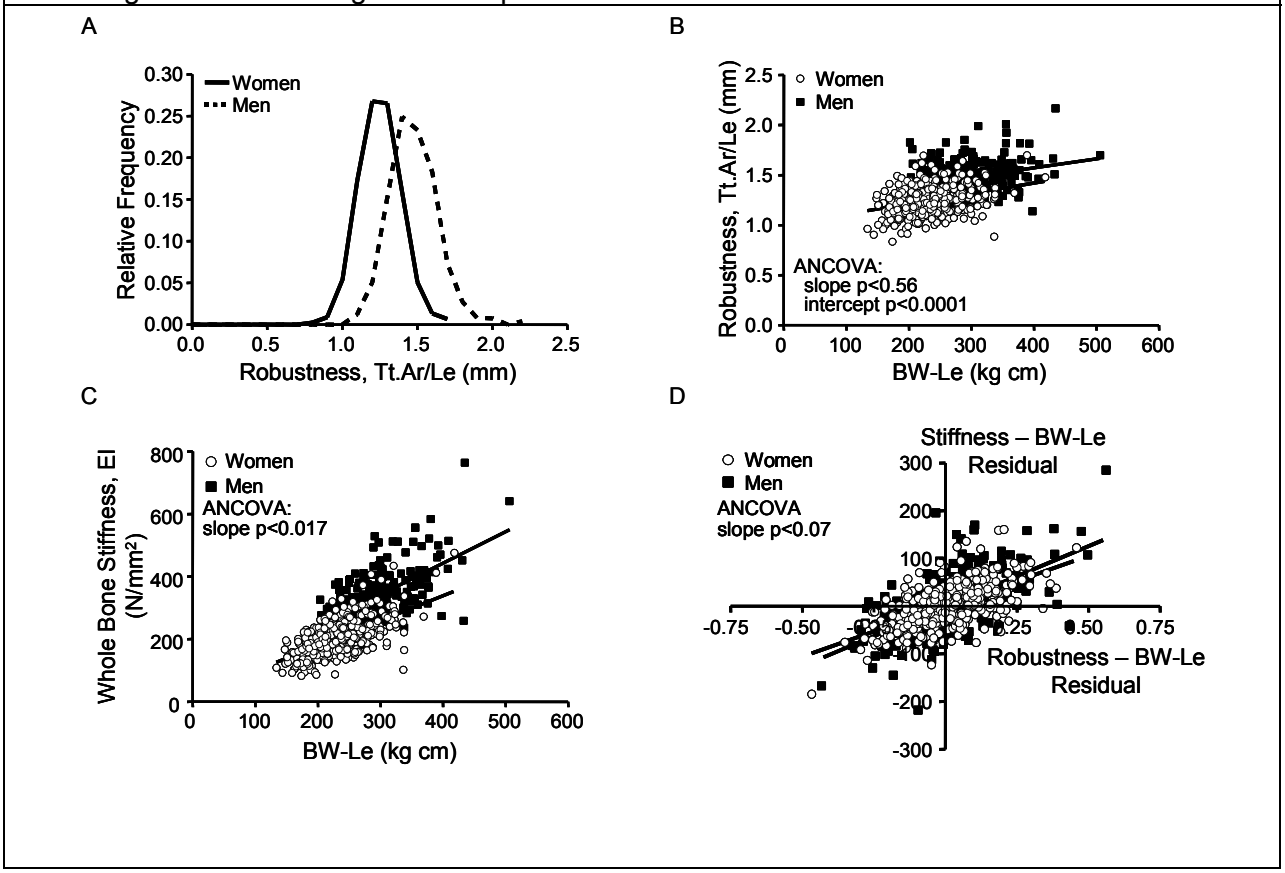

Interactions among traits contributing to whole bone stiffness

To identify biological constraints limiting the degree of compensation permissible in human long bone, we first determined whether individuals in our study population used a similar strategy to compensate for a common, heritable trait like robustness. In general, bone cells are expected to coordinate traits in a non-random manner to establish function for any given person. If all individuals were to use a similar biological strategy to compensate for robustness, then functionally related traits would correlate across a population and, because many traits are involved, these correlations would resemble a network of trait interactions (2,17,18). Robustness, relative cortical area (cortical area/total area), and tissue-stiffness, which are functionally interacting traits shown previously to contribute to long bone function (18), exhibited

a well defined trajectory in a 3-D plot (Figures 4A, B). Path Analysis was used to determine how this pattern of trait interactions contributed to the variation in whole bone stiffness. The significant goodness-of-fit criteria for the Path Model (Chi-square test p-value = 0.39; RMSEA = 0.000) confirmed that traits covaried in a highly consistent manner among individuals (Figure 4C). Similar networks were found when analyzing the male and female data separately (not shown). Some trait-trait interactions were expected based on mathematical associations (e.g., the interactions among Ct.Ar, Robustness, and RCA), whereas other interactions were indicative of biological associations (e.g., the interaction between RCA and E). Removing or reversing the arrow between RCA and E resulted in loss of goodness-of-fit for the model, suggesting the interaction between the amount of bone and tissue-modulus is a critical component of the functional adaptation process. The network and the reduced structural equations indicated that individuals with slender bones relative to BW-Le acquired a proportionally greater relative cortical area and tissue-modulus to establish stiffness, whereas individuals with robust bones established stiffness by acquiring a proportionally lower relative cortical area and tissue-modulus. The reduced form equations showed that the network of trait interactions explained 73% of the variation in whole bone stiffness and that Ct.Ar and robustness had similar relative contributions to whole bone bending stiffness.

Figure 4. An emergent trajectory was observed among robustness, tissue-stiffness, and relative cortical area for **A)** women and **B)** men. Symbols: open circles = 38% anatomical site; filled circles = 66% anatomical site. **C)** The Path Model, which included data for both men and women, showed significant goodness-of-fit criteria. The reduced structural equations revealed that 73% of the variation in whole bone stiffness was explained by BW-Le, robustness, and cortical area. Arrows: solid = positive association; dashed = negative association. Abbreviations: E = tissue-stiffness; Ct.Ar = cortical area; RCA = relative cortical area = Ct.Ar/Tt.Ar; Tt.Ar = total cross-sectional area.

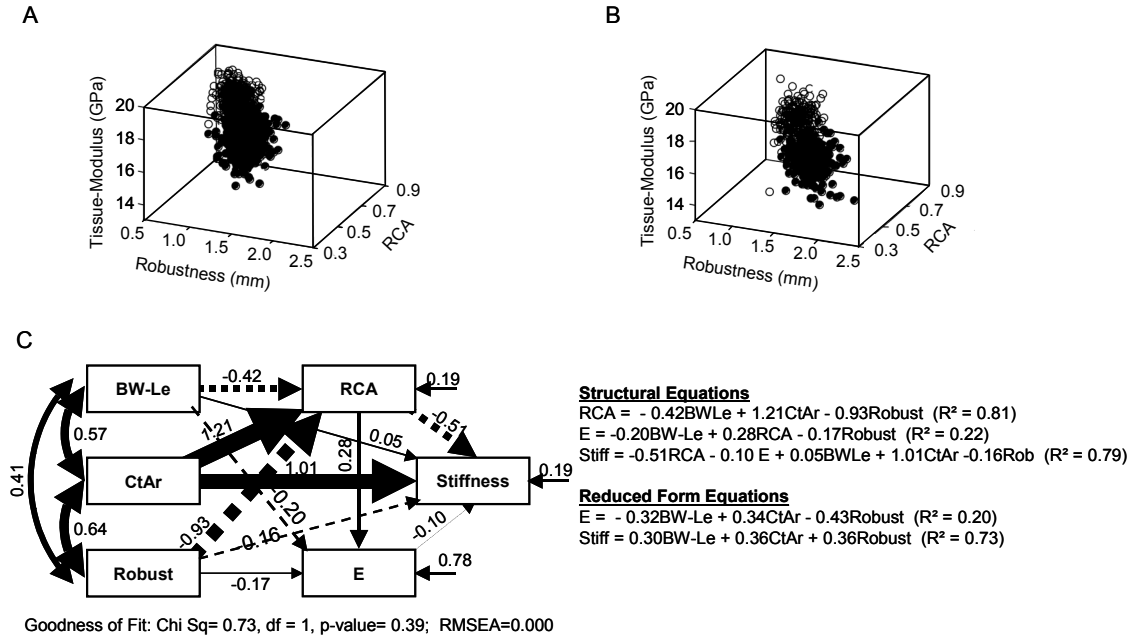

Biological constraints limiting compensation

Because the Path Analysis indicated that individuals in our study population utilized a similar biological strategy to mechanically compensate robustness, we could identify common boundaries on cellular activity or 'biological constraints' that limited the degree of compensation permissible in human long bone and that were responsible for the functional inequivalence. The two major compensatory traits contributing to function included the amount of bone (cortical area) and tissue-modulus. Cortical area measured at the 38% (Women R^2=0.36, Men R^2=0.38) and 66% (Women R^2=0.25, Men R^2=0.31) anatomical sites correlated positively with BW-Le for both sexes ($p<0.0001$ for all regressions). Men exhibited a significantly greater amount of bone (10-11%) compared to women across the full range in body size (ANCOVA, intercept $p<0.0001$). After accounting for BW-Le, we found that cortical area correlated positively with robustness at both the 38% (Figure 5A) and 66% sites (Figure 5B), indicating that tibiae which were slender relative to BW-Le were constructed with less bone tissue relative to BW-Le compared to robust tibiae. To further compensate for robustness, osteoblasts and osteoclasts must also adjust tissue-modulus. Both men and women showed significant negative correlations between tissue-modulus and robustness (Figure 5C), indicating that osteoblasts compensated slender tibiae with greater tissue-modulus. We estimated the regression between tissue-modulus and robustness required to equilibrate function among individuals by iteratively modifying the relationship between tissue-modulus and Ct.TMD until the slope of the partial regression between EI and robustness was not significantly different from zero or the R^2 value was less than 0.01 (i.e., satisfying the null hypothesis). The regressions required to establish functional equivalence for men and women are shown in Figure 5C. These regressions do not represent biologically realistic outcomes, because they would result in excessively large tissue-modulus values for slender bones and extremely low tissue-modulus values for robust bones.

Discussion

Functional compensation is a biological process critical for system health and homeostasis, because it allows individuals to tolerate many genetic and environmental factors leading to variation in one trait through coordinated, compensatory changes in other traits. Approximately 70 years ago, Waddington proposed that functional compensation or 'buffering' suppresses phenotypic variation and establishes functional equivalence, or 'constancy of the wild type,' across a population (5). However, we now know this concept cannot be generalized to all physiological systems, as inter-individual variation in lung size (4,19), heart size (20), and arterial morphology (21,22) are associated with disparity in system performance, overall fitness, and disease-risk. The current results were consistent with these studies, showing that compensation of tibial robustness, a common, heritable morphological variant, was imperfect and led to functional inequivalence among nearly 700 young adult women and men, as hypothesized. In contrast to prior studies showing functional equivalence of mastication among different species of soricid shrews expressing variable mandibular morphologies (23), herein we found functional inequivalence when studying the inter-individual variation in morphology of long bones within a single species.

The functional inequivalance was predictable based on robustness and the amount of disparity among individuals was substantial; tibiae that were slender for BW-Le were as much as 2-3 times less stiff relative to BW-Le compared to tibiae that were robust relative to BW-Le. The relationship between whole bone stiffness and the applied loads is important because it defines tissue-level strains, which are thought to drive functional adaptation (24). Although BW-Le is traditionally used as a measure of the loads applied to bone (25,26), other aspects of activity (e.g., type, intensity, duration, age of onset of training) that are thought to be involved in the functional adaptation process during growth are expected to vary among individuals. Whether activity levels during growth varied predictably with bone robustness for members of our study population and would explain a portion of the functional inequivalence observed here,

however, remains unclear. Functional inequivalence relative to robustness means that bone cells could not adjust traits like cortical area and tissue-modulus to the degree needed to fully compensate the nonlinear relationship between bone width and whole bone bending stiffness. The functional inequivalence reported in Figure 3D was not limited to bending loads, but was also found when assuming tibiae were loaded in compression (data not shown). Although long bones of modern populations are comparatively more slender and weaker than archaeological populations (27,28), it is unclear if the degree of functional inequivalence has changed over time and whether modern diets and exercise habits contributed to the substantial disparity in function observed for the young adult population examined here. Further, the vast majority of individuals in our study population were Caucasian, and it remains to be determined if the degree of functional inequivalence varies with race or ethnic background. Future work could also include measuring the amount of subcortical bone and determining whether this compartment varies in a predictable way with robustness and may reduce some of the functional equivalence reported here.

Figure 5. Cortical area correlated positively with robustness for both the **A)** 38% (Women R^2=0.58, Men R^2=0.53) and **B)** 66% (Women R^2=0.29, Men R^2=0.17) anatomical sites after accounting for BW-Le by partial regression analysis. All linear regressions were significant at p<0.0001. **C)** Tissue-modulus estimated from pQCT correlated negatively with robustness at the 38 and 66% sites for women (R^2=0.42) and men (R^2=0.33). The relationship between tissue-modulus and robustness required to establish functional equivalence is shown for women (short-dashed line) and men (long-dashed line). All linear regressions were significant at p<0.0001.

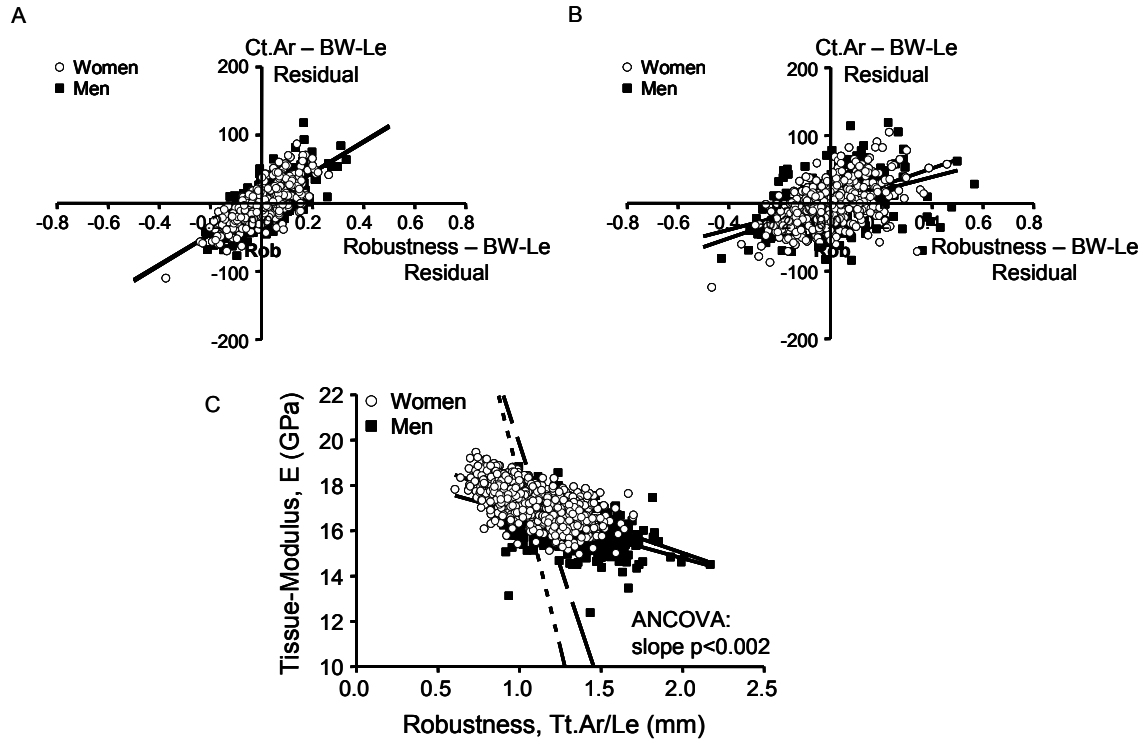

The results provided important insight into the biological constraints that limited the degree of compensation. The disparity in cortical area relative to robustness (Figure 5A,B) may affect

measures like BMD, but would contribute only modestly to the functional inequivalence because further addition of mineralized tissue to the inner surface of slender tibiae would have minimal mechanical benefits. The limited range in tissue-modulus (range/average = 36.7%) did not fully compensate the wide range in moment of inertia (279%) and thus was an important determinant of the functional inequivalence reported here (Figure 5C). Limited compensation at this level of biological organization may be a public health concern, not only because it means a predictable segment of the population has a functional deficit, but also because it remains to be determined to what extent prophylactic treatments can circumvent these intrinsic cellular constraints to establish a higher degree of functional equivalence among individuals.

Our analysis indicated that bone cells adjusted tissue-modulus to compensate for robustness, but only within a very narrow range compared to that observed for bones from different species with widely varying loading demands (29). This constraint, however, may be advantageous, because extracellular matrix modifications that increase tissue-modulus (e.g., mineralization) generally occur at the expense of increased tissue-brittleness. Slender tibiae would be extremely brittle if mineralized to the degree needed to establish the same level of functionality as robust tibiae (Figure 7). Thus, the skeletal system may have evolved to tolerate a modest degree of functional inequivalence relative to robustness, possibly to avoid developing an excessively fragile bone that is prone to fracturing under daily activities and that would decrease individual fitness and survival. This biomechanical tradeoff may be an important factor defining the range in robustness values and the degree of functional inequivalence tolerated by a modern population.

The significant correlation between EI derived from pQCT and EI measured directly from 4-point bending of cadaveric tibiae (Figure 2E) confirmed that we accurately estimated whole bone bending stiffness for our study population. We used EI as the measure of bending stiffness, rather than the more commonly used strength-related parameters like bone mineral density (BMD), section modulus, the bone strength index (BSI), and the strength-strain index (SSI). BMD is useful clinically for diagnosing osteoporosis, but does not provide the details of structure and tissue-quality required to assess functional inequivalence. Morphological indices like section modulus do not consider the variation in tissue-quality which we show in the current study and in prior work (11,12) is a critical component of the functional adaptation process. Both BSI and SSI incorporate Ct.TMD as a measure of tissue-quality. However, because small changes in bone density correspond to large changes in tissue-modulus (30), it was important to use EI as a measure of bending stiffness to test whether the variation in E was sufficiently large to compensate the variation in moment of inertia. We found that EI measured at the 38% site was an accurate predictor of whole bone bending stiffness (Figure 2E), which is consistent with prior work showing that tibial architecture at the 33% site was well adapted to anterior-posterior bending loads (31). Although further work is needed to establish a standard conversion between Ct.TMD and E, our method replicated the range in E for the live human cohort and confirmed the relationship between robustness and E was accurately estimated from pQCT (Figure 2D). The small difference in the y-intercept between the regressions for the cadaveric data and the live human cohort did not affect the outcome of our study, because the partial regression analysis and the Path Analysis relied on the variation in E relative to robustness, not the magnitude of E.

Although functional inequivalence was observed for both sexes, we also found functional disparity between men and women (Figure 3C), consistent with prior work (31). The stiffness of tibiae relative to BW-Le was 40.9% lower for women compared to men, indicating the 14.8% reduction in robustness of female tibiae was not compensated to the same degree as male tibiae, despite a 7% greater tissue-modulus for female tibiae (Figure 5C; $p<0.0001$, t-test). Consistent with the results of others (32), women showed 10-11% less Ct.Ar relative to BW-Le compared to men (data not shown) which contributed in part to the functional disparity between sexes. This disparity in tibial stiffness relative to body size may help explain why women sustain

approximately 5-times more stress fractures than men during gender-integrated military training regimens (33), and why fracture incidence is greater for elderly women compared to men (34). Prior work by others demonstrated that sex-differences in strength-related morphological parameters are not fully eliminated even after adjusting for body size (32,35).

Anecdotally, young adult men and women expressing the full range in bone robustness successfully perform daily activities (e.g., walk, run, stand), indicating that functional inequivalence is generally tolerated, likely because bone has large safety factors that minimize fracture risk under normal loading conditions (36). However, our concern is that safety factors are often exceeded under extreme loading conditions, such as falls in the elderly and the intense, repetitive exercise combined with prolonged load carriage typical of military training. Young adults with reduced stiffness relative to body size have proportionally weaker bones that would be expected to experience greater tissue strains during intense exercise, increasing matrix damage and the probability of developing a stress fracture (37). This functional inequivalence may help explain why having a slender tibia relative to body size is an important risk factor for stress fractures in military recruits (14,15) and athletes (38). Although slender bones are generally assumed to be weaker than robust bones (14,15), it was important to formally test this assumption in the context of the skeletal system's ability to compensate a common trait variant. Prior work did not consider the compensatory changes in morphology and tissue-quality that accompany the natural variation in robustness. Functional inequivalence may also be problematic in the ever-growing elderly population, because it means individuals begin the aging process at different starting points. Individuals with slender bones relative to body size would be expected to reach a fracture-risk threshold earlier in life if they lose bone mass on a structure with a pre-existing functional deficit. To the extent which functional inequivalence in the tibial diaphysis extends to other skeletal sites, our results may help explain why bone slenderness is a consistent indicator of fracture risk in the elderly (39,40). However, to generalize the results of this study to the hip, which shows a high incidence of age-related fragility fractures, would require testing how cortical and trabecular traits are adjusted to compensate for the natural variation in femoral neck width, whether proximal femora with slender and robust necks have the same strength during a fall to the side, and whether proximal femora with slender necks show the same age-related bone loss pattern as proximal femora with robust necks.

Our analysis also showed that nearly 700 young adult men and women with different genetic backgrounds and life histories exhibited highly significant functional trait interactions. The network of trait interactions shown in the Path Model (Figure 4C) highlighted the biological complexity of a relatively simple, tubular system. Unlike multivariate approaches such as multiple regression or principal components analysis which make no specific assumption about the underlying biology, we used Path Analysis to test whether traits that are functionally related during growth would show correlations among adult structures consistent with the idea that bone maximizes stiffness using minimum mass (13). The network, which explained 79% of the variation in whole bone stiffness and was consistent with that reported for a small cadaveric cohort (18), indicated that young adult men and women in our study population acquired highly predictable trait sets during growth and thus shared important aspects of a negative feedback control mechanism responsible for coordinating traits to establish function. In contrast to man-made systems where highly variable morphologies and materials are combined to establish function, biological systems like bone work with limited resources and must adjust the amount, location, and organization of a narrow range of building blocks (e.g., mineral, collagen, proteoglycan, water) to achieve the degree of variation in morphology and tissue-quality required to establish function across a population. These cellular constraints, which were responsible for functional inequivalence, appear to also limit the number of possible functional trait sets that can be acquired during growth. That is, individuals with slender bones coordinated Ct.Ar and tissue-modulus in fairly similar ways to establish function; likewise, the same can be

said for individuals with robust bones. The limited range in functional trait sets acquired during growth explained why we saw a consistent pattern in the way traits covaried across a young adult population. Although the larger number of traits in corticocancellous structures increases the possibility that compensation of robustness can occur using a wider range of trait sets, relatively similar functional trait-interactions have been observed for the human femoral neck (41) and mouse vertebral body (42).

Figure 6. A schematic diagram was constructed based on the results of the Path Model (Figure 4C) and the association between Ct.Ar and robustness (Figure 5A,B) to illustrate how variation in cortical area is superimposed on the variation in robustness. Tibial diaphyses are represented as idealized circular cross-sections, with gray-values representing the variation in tissue-modulus. With body size effects removed, cortical area varies with robustness, with slender tibia showing lower Ct.Ar than robust tibia. In addition, there is variation in Ct.Ar for any given robustness value. These relationships hold for men and women, despite sex-specific differences in robustness and Ct.Ar. Thus, the natural variation in robustness is associated with specific changes in cortical area and tissue-modulus that need to be considered when seeking genomic and/or environmental factors regulating bone function.

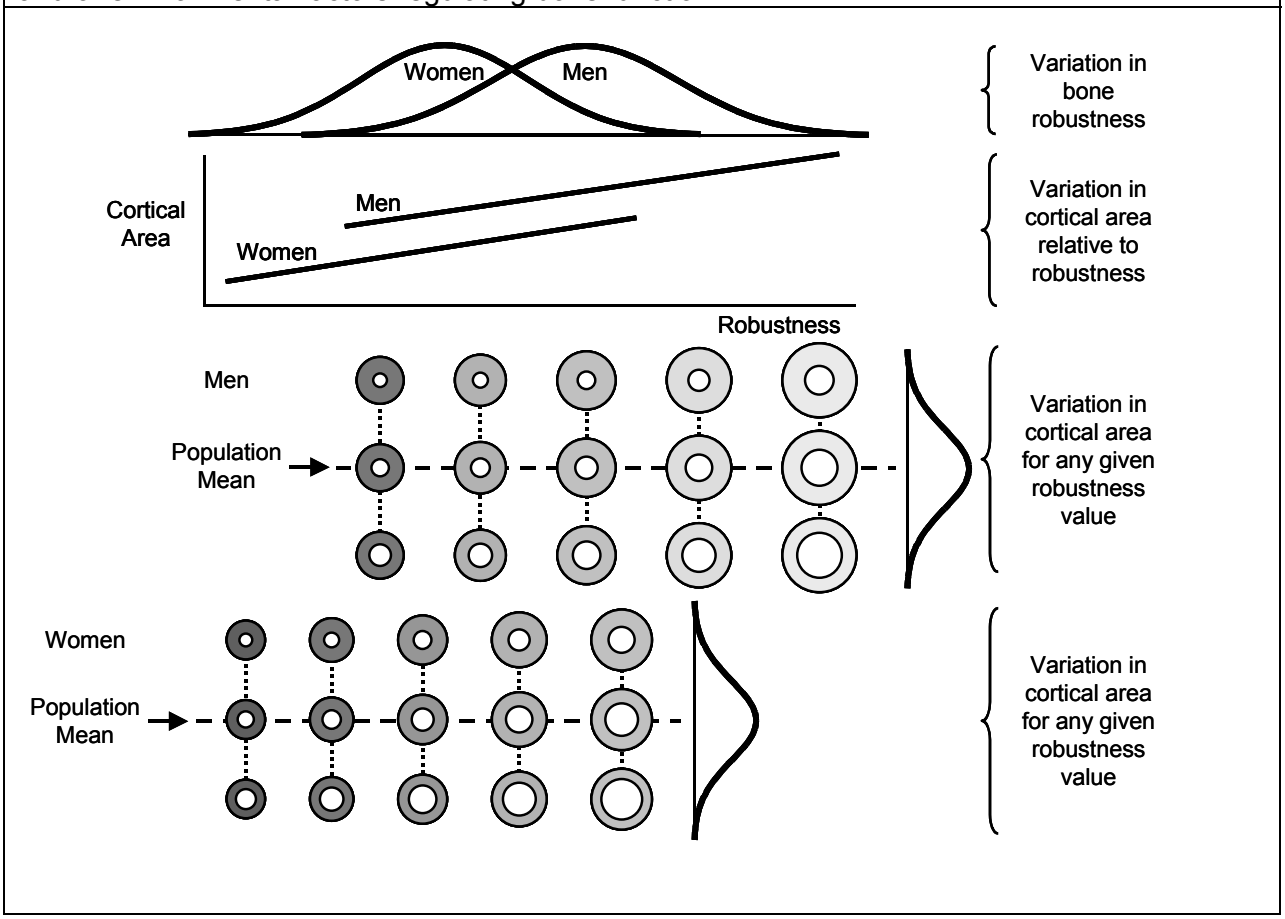

The Path Model also showed that variation in compensatory traits were superimposed on the variation in robustness. This is an important outcome of this study and one worth illustrating to better convey the concept. Figure 6 was constructed to illustrate how cortical area varied among individuals. A similar diagram could be constructed for tissue-modulus. First, cortical area varied relative to robustness, with slender tibiae having less Ct.Ar compared to robust tibiae. Second, there was inter-individual variation in Ct.Ar for any given robustness value. This

is important because it means that traits like Ct.Ar should be adjusted for body size and robustness to identify genetic and/or environmental factors affecting the inter-individual variation in measures related to bone mass (43). Although the Path Analysis revealed a highly predictable pattern for nearly 700 individuals, additional data from a more diverse population would be required to establish norms for these compensatory relationships. It is important to note that having slender bones does not necessarily indicate a failure to adapt. Although periosteal expansion during early growth may be modified by extreme loading conditions (44), it is unclear to what extent variation in the normal range of loading affects an individual's skeletal robustness. Based on our data, we would argue that genetic and/or environmental variants that impair the functional adaptation process may affect robustness but would primarily affect the compensatory traits that accompany robustness, i.e., Ct.Ar and E. A poorly adapted bone, whether slender or robust, would have reduced Ct.Ar and reduced E compared to population mean for that particular robustness value. Identifying individuals with poorly adapted bones would require establishing population norms for how traits covary relative to external size and then adjusting an individual's acquired trait set for their robustness.

Although the limited range in E was an important determinant of the functional inequivalence (Figure 5C), the Path Model showed that E was not a major determinant of the inter-individual variation in whole bone bending stiffness. This is likely because the variation in E at a single anatomical site is small compared to the variation in cortical area. Further, prior work in mouse bone showed that E covaries closely with periosteal expansion rate early in life (45). Consequently, the contribution of E to the variation in whole bone stiffness may be masked in the multivariate model by its association with robustness. In contrast, Ct.Ar develops throughout growth and may be more susceptible to environmental perturbations, thereby showing greater inter-individual variation relative to robustness and making a dominant contribution to the variation in whole bone stiffness (46,47).

The validation study provided important insight into the manner by which the skeletal system adjusts tissue-quality to compensate for robustness. Variation in Ct.TMD depended on both mineralization and porosity, consistent with expectations of acquiring pQCT images with a 0.4-0.5 mm pixel size. Although 63% of the variation in Ct.TMD was explained by ash content, porosity, and pore density (Table 1), we suspect the 37% unexplained variance could be due in part to measurement error, particularly for ash content and Ct.TMD. Although these two particular traits vary predictably with bone size, they show little variation among individuals. Consequently, small measurement errors would then contribute substantially to the unexplained variance. The unexplained variance could also be explained by properties that were not measured. In addition to ash content and porosity, X-ray attenuation could be affected by material heterogeneity, components of mineralization not accounted for by traditional ash content measures, and possibly the organic component of bone tissue. The negative correlations between robustness and Ct.TMD (Figure 2A,B) and between robustness and E (Figure 2D, 5C) are consistent with prior work (11,12,18). A surprising outcome was finding that porosity was also highly significantly correlated with robustness (Figure 2C). Unlike prior work (18,48), we assessed porosity and robustness at the same anatomical site in the current study, enabling us to see a strong association between these two traits that remained significant after correcting for age. Thus, the higher tissue-modulus of slender bones resulted from increased mineralization and reduced porosity, whereas at the other extreme the reduced tissue-modulus of robust bones resulted from reduced mineralization and increased porosity. This suggested that bone cells coordinately modulate both mineralization and porosity to regulate tissue-modulus, thereby expanding the range of variation in E that can be achieved across a population beyond a strict dependence on varying matrix mineralization alone. Because tissue density correlated positively with ash content (not shown), modulating tissue-quality by varying mineralization and porosity would have the added benefit of increasing the mass of slender bones while minimizing the mass of robust bones (13). It is unclear from our current study if

there are additional levels of compensation that modulate tissue-modulus, such as collagen orientation (49,50) and cross-linking (51), but certainly these factors should be examined in future work. The validation study was limited to available young adult and middle-aged tibiae, which are difficult to acquire. The limited number of samples did not allow us to test for a sex-specific effect.

Because our analysis purposely selected vascular pores from within the cortex, the positive correlation between porosity and robustness (Figure 2C) suggested that internal BMU-based remodeling may be suppressed in slender bones and stimulated in robust bones. These results suggested that internal remodeling may not only be regulated locally by factors such as matrix damage (52), but also globally by factors associated with the compensation of bone robustness. This intriguing outcome is worth confirming with a larger collection of tibiae combined with histological techniques that provide dynamic measures of bone turnover (53). Whether the internal remodeling of slender tibiae is suppressed during the intense physical exercise typical of military training and contributes to stress fracture incidence has yet to be tested.

In conclusion, intrinsic limitations on cellular activity and biomechanical tradeoffs established boundaries on tissue-modulus and cortical area that prevented adaptive processes from fully compensating the nonlinear relationship between tibial width and whole bone bending stiffness. The limited variation in trait values constrained the range of functional trait sets that could be acquired by individuals with diverse genetic backgrounds and life histories, resulting in an emergent network of trait interactions. Susceptibility to common, heritable diseases is generally thought to originate at the genetic-level, and most studies seek genomic variants or altered molecular networks to develop novel diagnostics and treatments to reduce disease risk (54). Herein, we showed that predictable functional deficits may also arise at a higher-level of biological organization, a phenomenon that may be difficult to predict from genetic information alone, because it involved biomechanical tradeoffs, constraints on cellular activity, regulation of internal remodeling, and a network of compensatory trait interactions defining organ-level function. Limited compensation at this level of biological organization may be a public health concern, and it remains to be determined how the functional inequivalence reported in this study relates to fracture susceptibility.

Section 2. Inter-individual variation in femoral neck width is associated with the acquisition of predictable sets of morphological and tissue-quality traits and differential bone loss patterns

The following is text taken from a manuscript that is being prepared for submission to the journal Bone. Details of Methodology can be found in a copy of the manuscript provided in Appendix 1. This paper reports the major findings of our analysis of the proximal femur. The text shows the influence of our analysis of the human tibiae (section 1) in that we now address functional inequivalence and the dependence of internal remodeling on the natural variation in bone size. These two concepts were not included in the original proposal and represent a major advance in our understanding of bone and will lead to novel hypotheses that can be developed into NIH RO1-level grants.

Introduction

Identifying skeletal trait variants that increase the risk of hip fractures is critical for reducing the associated morbidity, mortality, and cost (55). These variants are typically identified by comparing the average traits measured for a group of fracture cases to those of age- and sex-matched non-fracture controls. This approach only allows for a dichotomous outcome, such that physical traits contributing to fracture risk can be either greater than or less than the population average. Thus, it is not surprising that studies using this approach found that fracture cases had either a narrow (39,40) or wide (56,57) femoral neck compared to age- and sex-matched controls. However, despite finding small differences (2-3%) in bone width between fracture and non-fracture groups, these studies also showed that individuals at increased risk of fracturing express the full range of variation in bone size. Thus, it is unclear whether we are missing opportunities to identify and treat individuals using such an approach.

We propose that developing a better understanding of how a complex system like bone establishes and maintains mechanical function will benefit efforts to identify traits contributing to fracture risk. The inter-individual variation in robustness, a measure of bone width relative to length, provides a model to systematically evaluate how morphological and tissue-quality traits are coordinated to establish whole bone mechanical function. The functional adaptation process that matches structure to applied loads (i.e., Wolff's Law) is understood for the typical bone, but how this process works across a population of individuals expressing the normal variation in external size is not fully understood. All morphological traits are expected to be mechanically sensitive, including external size (44). Despite this, some individuals are genetically prone to having narrow bones, independent of height and weight, and this should not be viewed as a failure to adapt mechanically to applied loads. Rather, because external size is nonlinearly related to whole bone stiffness, the inter-individual variation in external size should be associated with large compensatory changes in morphological and tissue-quality traits in order for all individuals in a population to have functionally adapted bones that support physiological loads. Thus, variation in the degree to which a person functionally adapts their skeleton is expected to depend on the particular set of traits acquired during growth.

Prior work in mouse (12) and human (18) long bone identified compensatory interactions among morphological and tissue-quality traits that accompany the natural variation in bone robustness. Compensatory interactions among traits are not limited to long bones, but have also been identified in corticocancellous structures like the vertebral body (42) and the proximal femur (41). The functional adaptation process is more complex in structures like the proximal femur, because it involves compensatory interactions among morphological and tissue-quality traits for both cortical bone and trabecular bone. Work by others showed that narrow femoral necks are accompanied with a thicker cortical shell and greater vBMD compared to wide necks (41), suggesting the functional adaptation process maximizes stiffness in slender femora (narrow relative to length) and minimizes mass in robust femora (wide relative to length). Thus,

to be functional, slender femora must acquire a different set of traits than robust femora. However, the morphological and tissue quality differences in these robustness-specific trait sets are not fully understood.

The idea that individuals acquire sets of traits specific to external size is important, because it may complicate our understanding of the aging process in several ways. First, although slender and robust structures are expected to acquire different sets of traits by adulthood, it is unclear whether slender and robust femora show similar age-related bone loss patterns. Second, the bone-width specific trait sets acquired during growth and maintained with aging were based on femora being adapted to compensate loads incurred during daily activities, but it is unclear how these trait sets differentially affect bone strength during a fall to the side. Third, it is unclear if biological processes can adjust morphological and tissue-quality traits to the degree needed to fully compensate the nonlinear relationship between width and whole bone stiffness. Failure to fully compensate bone width would lead to functional inequivalence (i.e., slender femora being less stiff and strong compared to robust femora), which may result in slender femora experiencing greater tissue-strains compared to robust femora, thereby potentially affecting cell mediated bone loss patterns. In this study, we conducted a biomechanical analysis to test the hypotheses that variation in external size of the femur is associated with predictable compensatory changes in morphology and tissue-quality and that slender and robust femora age differently.

Sample population

The sample population included 49 female cadaveric femora. The population was normally distributed with respect to age (Kolmogorov-Smirnov test > 0.10), which ranged from 29 - 93 years with a mean and standard deviation of 68.2 $\pm$ 14.6 years. Race/ethnicity, body weight, and body height were available only for a small subset of the cohort and thus could not be considered in the analysis. Except for cause of death, medical history was unavailable and consequently femora could not be segregated for prior use of prophylactic treatments affecting bone formation and/or resorption. Cause of death was wide ranging, but no individuals died subsequent to hip fracture, and radiographs confirmed that femora showed no evidence of a prior fracture.

Bone morphology

Gross morphological traits of the proximal femur (Figure 7) were measured from plain film radiographs using previously published methods (58). Radiographs were acquired using a Hewlett Packard X-Ray imaging system (model 43805; Faxitron X-ray, Linconshire, Illinois USA) with an aluminum step wedge (model 117; Gammex, Middleton Wisconsin USA) included for exposure calibration. Radiographic exposure was set at 1mA and 50kV for a duration of 0.7 minutes on a direct exposure film packet (Kodak TL; Eastman Kodak, Rochester, New York USA). The femoral shaft was held in an antero-posterior position with a clamp so the femoral neck axis was visually perpendicular to the X-ray beam. Direct exposure film was digitized using an Epson high resolution scanner (model 10000 XL; Expression Series, Long Beach, California USA) and analyzed with image analysis software (ImageJ, version 1.44f, U.S. National Institutes of Health, Bethesda, Maryland USA). Femoral Neck Axis Length (NAL) was measured as the linear distance from the lateral aspect of the greater trochanter to the apex of the femoral head passing through the center of the femoral head. Femoral Head Diameter was obtained by fitting a circle to the outline of the femoral head. Neck Shaft Angle (NSA) was measured as the angle formed between the neck axis and the shaft axis. The trochanter-to-trochanter distance was measured as the distance from the apex of the greater trochanter to the apex of the lesser trochanter.

Morphological traits were quantified using peripheral Quantitative Computed Tomography, pQCT (XCT2000L, Stratec Medizintechnik, Pforzheim, Germany). This small-bore computed

tomography scanner acquires cross-sectional images with an in-plane pixel size of 0.16 mm x 0.16 mm. Measurement quality was assured daily by conducting a calibration scan using a standard phantom with known densities. Scans were obtained for the full length of the femoral neck, from the greater trochanter to the femoral head. The femoral neck was aligned perpendicular to the beam by holding the femoral shaft at a complementary angle to the neck shaft angle. The scanned region was fully submerged in saline solution. Because cortical and trabecular traits vary along the femoral neck (41), we chose the narrow neck region to standardize the analysis site among the cadaveric cohort. Intra-rater repeatability was demonstrated by measuring traits at two distinct times using the same hardware and software. The cortex was manually segregated from trabecular bone. Femoral neck traits were analyzed using ImageJ, and these included total cross-sectional area (Tt.Ar), marrow area (Ma.Ar), cortical area (Ct.Ar), cortical tissue mineral density (Ct.TMD), marrow bone mineral density (Ma.BMD), robustness (Tt.Ar/NAL), and relative cortical area (RCA=Ct.Ar/Tt.Ar). Grayscale values of the cortical and trabecular regions were converted to Ct.TMD and Ma.BMD, respectively, using calibration constants derived from the phantom. No significant difference was found between repeat measures for Tt.Ar ($p<0.81$, t-test), Ma.Ar ($p<0.48$, t-test), Ct.Ar ($p<0.19$, t-test), RCA ($p<0.88$, t-test), NAL ($p<0.77$, t-test) Ct.TMD ($p<0.96$, t-test), and Ma.BMD ($p<0.61$, t-test).

Figure 7. Radiographic images of the slender and robust femora and the associated cross-sections derived from pQCT depict the natural variation in bone size that exists among individuals. The center image shows how neck axis length was measured.

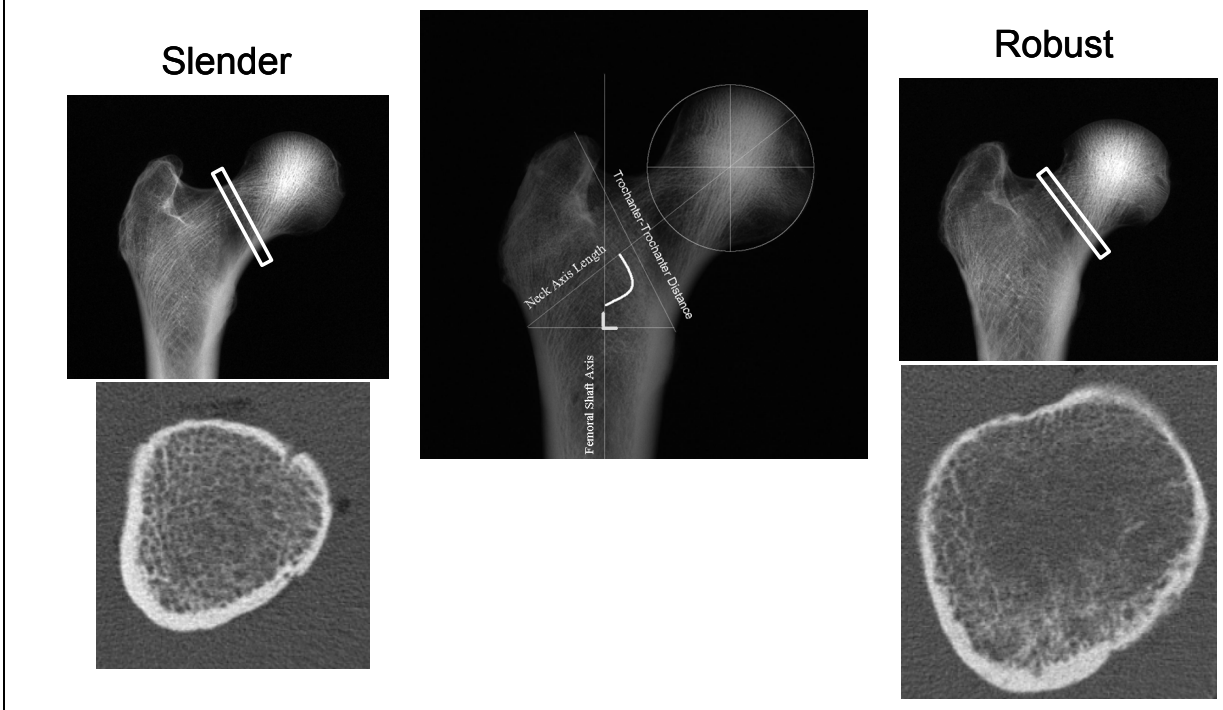

Inter-individual variation in femoral neck robustness

Although variation in external size of the femoral neck could be measured by width or total cross-sectional area, we found that using these absolute trait values was not sufficient for our purposes because a small individual with a robust bone may have the same width or total cross-sectional area as a large individual with a slender bone. We compared different ways of calculating external size to identify a geometric measure of the neck that differentiated these outcomes. Because the femoral neck has a non-circular cross-sectional morphology and external size varies continually along the neck, we used total cross-sectional area at the narrow neck region as a measure of transverse size since no single width measure would represent size alone. We normalized total area by neck axis length (NAL) as a measure of femoral neck robustness. Total cross-sectional area increased with neck axis length ($R^2 = 0.34$, $p<0.0001$), as expected (Figure 8A). For any given neck axis length, total area varied by as much as 50-75% among individuals indicating that cross-sectional area varied widely relative to neck length. Residuals calculated from this regression correlated significantly with the ratio, Tt.Ar/NAL ($R^2 = 0.94$, $p<0.0001$) (Figure 8B), such that individuals with a negative Tt.Ar-NAL residual were characterized as slender, whereas those with a positive Tt.Ar-NAL residual were characterized as robust. This confirmed that the ratio, Tt.Ar/NAL, could be used as a measure of robustness to differentiate slender from robust femora even though this ratio does not take the y-intercept of the linear regression between Tt.Ar and NAL into consideration. Robustness (Tt.Ar/NAL) was normally distributed ($p>0.10$, Kolmogorov-Smirnov test) and varied widely among women (Figure 8C), showing a coefficient of variation of 14.9%. Linear regression analysis revealed that robustness correlated weakly with age ($R^2 = 0.04$, $p>0.20$) and neck shaft angle ($R^2 = 0.025$, $p>0.27$). Tt.Ar/NAL correlated positively with alternative measures of robustness such as femoral head diameter/NAL ($R^2 = 0.24$, $p<0.0005$) and Tt.Ar/neck length ($R^2=0.70$, $p<0.001$). We chose to use Tt.Ar/NAL as a measure of femoral neck robustness, because the lack of distinct anatomic markers delineating the beginning and end of the neck region made neck length a less reliable measure compared to NAL.

Correlations between bone morphology and tissue quality

To determine how the natural variation in robustness was compensated to establish function, we tested whether RCA, Ct.TMD, and Ma.BMD varied with robustness. Accounting for age effects using partial regression analysis revealed significant negative correlations between RCA and robustness (Figure 9A), Ct.TMD and robustness (Figure 9B), and Ma.BMD and robustness (Figure 9C). MicroCT images were used to quantify cortical thickness in the superior and inferior aspects of the narrow neck region for a subset of the femora (n=24). Ct.Th correlated negatively with robustness for both the superior and inferior regions (Figure 9D), and was significant only for the superior region ($R^2 = 0.28$, $p<0.008$), but not for the inferior neck region ($R^2 = 0.04$, $p<0.34$). Further analysis of the apical Ct.Th showed no significant correlation between superior Ct.Th and age ($R^2 = 0.06$, $p<0.24$) or inferior Ct.Th and age ($R^2 = 0.005$, $p<0.73$).

A validation study was conducted using a subset of the femora (n=26) to relate the Ma.BMD determined by pQCT to indices of trabecular architecture determined using microCT. Ma.BMD correlated positively with BV/TV ($R^2 = 0.66$, $p<0.0001$), Tb.Th ($R^2 = 0.66$, $p<0.0001$), Tb.N ($R^2 = 0.42$, $p<0.001$), and Tb.TMD ($R^2 = 0.48$, $p<0.001$; Figure 10B). Because the trabecular traits are inter-related, we also performed a multivariate analysis and found that BV/TV alone was the strongest predictor of Ma.BMD ($p<0.005$), and adding Tb.Th, Tb.N, and Tb.TMD to the regression did not greatly improve the predictability of the multivariate model ($R^2 = 0.68$, $p<0.0001$) over the univariate regressions. We further tested, albeit indirectly, whether the Ct.TMD determined by pQCT could also be used as an indicator of tissue-quality. Ct.TMD measured by pQCT correlated positively with Ct.TMD determined by microCT ($R^2 = 0.53$, $p<0.001$) (Figure 10A), and the overall TMD (cortical + trabecular) determined by microCT

correlated significantly with ash content (R^2 = 0.40, p<0.0001) (Figure 10C). This indirect validation suggested that variation in Ct.TMD measured by pQCT reflected differences in tissue-quality. Taken together, these results indicated that more robust femoral necks had a thinner cortical shell, a less mineralized cortical shell, and reduced trabecular BV/TV, whereas slender femoral necks had a proportionally thicker cortical shell, a more highly mineralized cortex, and greater trabecular BV/TV.

Figure 8. A) Variation in total cross-sectional area as a function of neck axis length. **B)** Robustness (Tt.Ar/Le) was plotted against residuals from the Tt.Ar-Le regression to determine if the ratio differentiated slender from robust femora. **C)** Robustness was normally distributed across our cadaveric cohort.

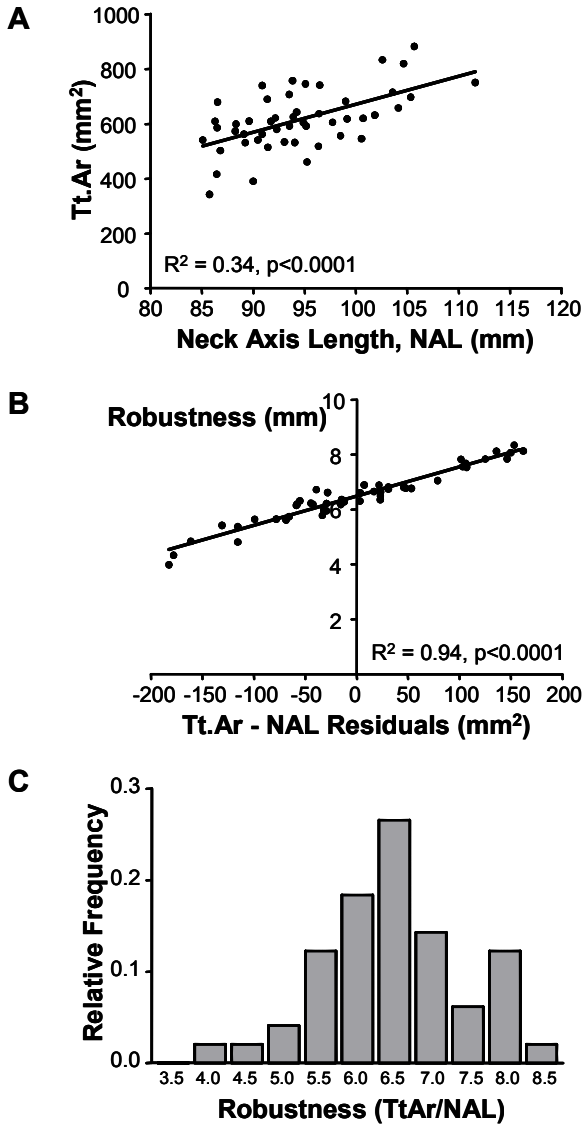

Figure 9. Partial regression analyses were conducted to take the effects of age into consideration, showing that **A)** relative cortical area (RCA = Ct.Ar/Tt.Ar), **B)** Ct.TMD, **C)** Ma.BMD, and **D)** Ct.Th all correlate negatively with robustness.

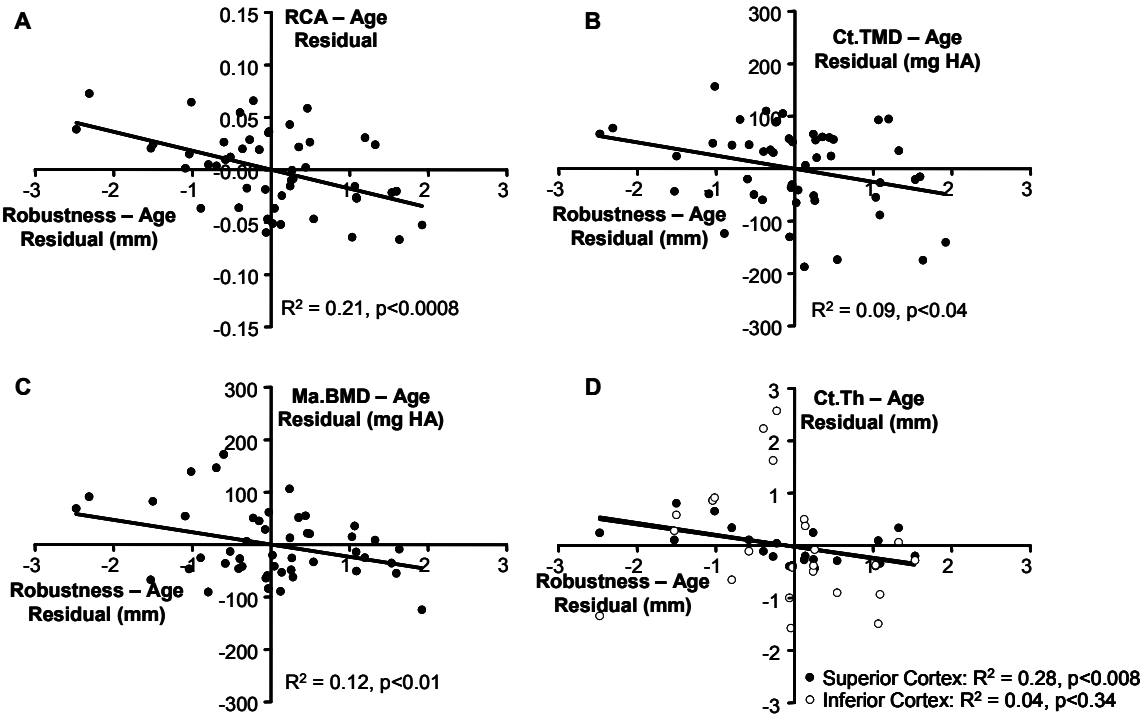

Path Analysis

Path analysis was conducted to assess the functional interactions among morphological and tissue-level traits. The Path Model included age, robustness, Ct.Ar, RCA, Ct.TMD, and Ma.BMD. The χ^2 and RMSEA values both indicated there was an excellent fit between the data and the model (Figure 11). The Path coefficients were calculated based on Z-transformed data and thus reflect the number of standard deviation changes in a trait arising from a 1 standard deviation change in robustness. When all the direct and indirect paths were taken into consideration, a 1 SD increase in robustness was associated with a 0.71 SD decrease in RCA, a 0.47 SD decrease in Ct.TMD, and a 0.44 SD decrease in Ma.BMD. The Path Model confirmed the univariate results indicating that robust femoral necks tended to have a cortex that occupied proportionally less space, had a lower degree of cortical mineralization, and lower trabecular bone mass. The goodness of fit for the Path Model failed (i.e., p-value for χ^2 <0.05, RMSEA > 0.1) when the arrow between RCA and Ct.TMD was removed or reversed, suggesting there is an important interaction among external size, the amount of bone, and tissue-quality.

Figure 10. A validation study confirmed that **A)** Ct.TMD measured by pQCT correlated significantly with Ct.TMD measured by microCT, **B)** Ma.BMD measured by pQCT correlated significantly with Tb.TMD measured by microCT, and **C)** the overall TMD (cortical + trabecular) correlated significantly with ash content.

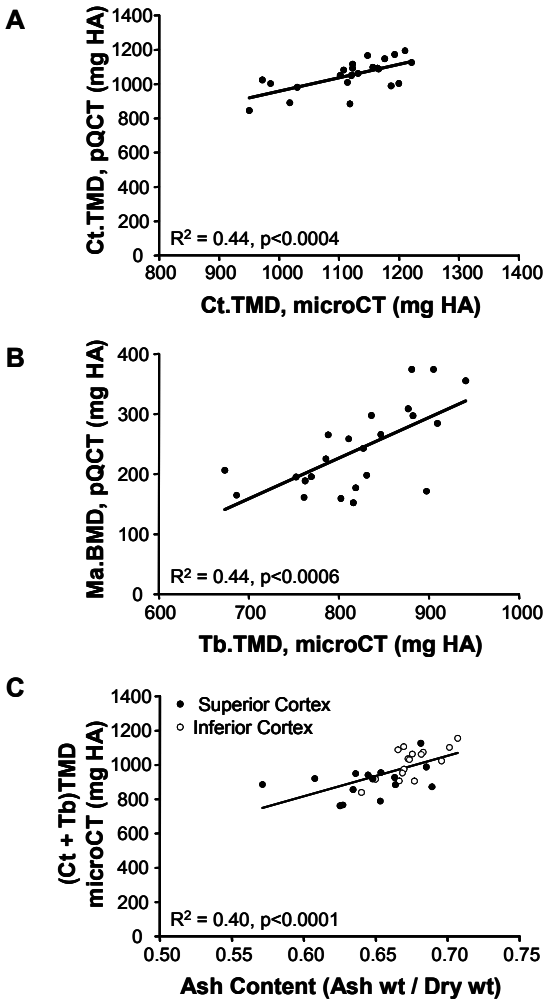

Age-related bone loss

Individuals were stratified into robustness tertiles to evaluate whether robust femora aged differently compared to slender femora. There was no difference in age between robust (n=17; 64.0±8.6 years) and slender (n=17; 69.9±17.2 years) tertiles ($p<0.25$, t-test). The robust and slender tertiles differed with respect to Tt.Ar ($p<0.0001$, t-test), but not NAL ($p<0.19$, t-test), suggesting the variation in robustness resulted largely from differences in transverse expansion rather than axial growth of the neck. The slender tertile showed a significantly greater RCA compared to the robust tertile ($p<0.01$, t-test), which was expected based on the results of the univariate and multivariate analyses. Although the cortex occupied proportionally greater space for the slender tertile, the slender tertile had a lower Ct.Ar compared to the robust tertile ($p<0.018$, t-test), indicating that slender femoral necks were constructed with a lower absolute amount of cortical bone. Linear regression analysis of the entire cohort (Figure 12A, C, E) revealed that Ct.Ar ($R^2 = 0.06$, $p<0.08$), Ct.TMD ($R^2 = 0.20$, $p<0.11$), and Ma.BMD ($R^2 = 0.10$, $p<0.05$) decreased with age, as expected. However, stratifying the data into robustness tertiles

revealed that slender femora aged differently compared to robust femora. Ct.Ar decreased significantly with age for the robust tertile (R^2 = 0.29, p<0.05), but not for the slender tertile (R^2 = 0.02, p>0.58). The slopes of the Ct.Ar - age regressions were significantly different between robust and slender tertiles (p<0.012, ANCOVA), suggesting that slender and robust femoral necks exhibited differential rates of cortical bone loss with aging (Figure 12B). Likewise, Ct.TMD (R^2=0.48, p<0.01) and Ma.BMD (R^2=0.34, p<0.05) decreased significantly with age for the robust tertile, but not for the slender tertile (R^2 = 0.0005-0.09, p<0.25). The slopes of the mineral density - age regressions were significantly different between robust and slender tertiles for Ct.TMD (p<0.005, ANCOVA), but not Ma.BMD (Figures 12D, F). This suggested that slender and robust femoral necks exhibited differential rates of cortical tissue-mineral loss with aging, but showed fairly similar losses in trabecular mineral density.

Figure 11. The results of the Path Analysis show a significant goodness of fit for the hypothesized interactions among cortical and trabecular traits (morphological as well as tissue-quality).

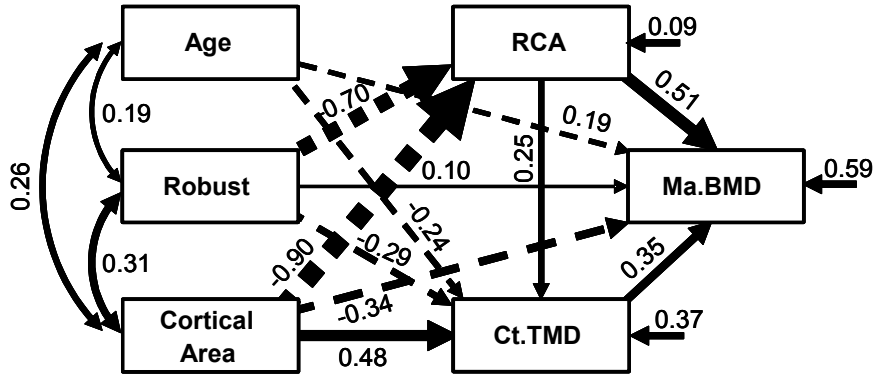

Goodness of Fit Criteria: Chi Sq=0.90, p<0.34; RMSEA=0.000

Reduced Form Structural Equations

RCA = 0.0 Age – 0.70 Robust + 0.90 CtAr (R^2=0.91)

CtTMD = -0.24 Age – 0.47 Robust + 0.71 CtAr (R^2=0.62)

MaBMD = -0.28 Age – 0.43 Robust + 0.37 CtAr (R^2=0.32)

Bone mechanics

Whole bone mechanical tests were conducted to test how acquisition of robustness-specific trait sets affected bone stiffness and maximum load during a simulated fall-to-the-side. Linear regression analysis applied to the entire cohort showed that maximum load (R^2 = 0.19, p<0.004) but not stiffness (R^2 = 0.05, p<0.18) decreased with age. A multiple regression analysis (Table 2), also applied to the entire cohort, indicated that 63.1% of the variation in maximum load was explained by robustness, Ct.Ar, Ct.TMD, Ma.BMD, and age (R^2 = 0.631, p<0.0001). Of these variables, only Ct.Ar and Ma.BMD were significant contributors, accounting for the majority of the variation in maximum load (Table 2). When segregating the data into robustness tertiles, femora in the robust tertile showed a 31% greater stiffness (p<0.05, t-test) and 13% greater maximum load (p<0.3, t-test) compared to slender femora (Figure 13). Maximum load decreased with age for both tertiles and the slope of this regression was ~2-fold greater (not significant) for the robust tertile compared to the slender tertile.

Figure 12. Age-related changes in **A)** Ct.Ar of the shell, **C)** Ct.TMD, and **E)** Ma.BMD are shown for the entire population. These same regressions were segregated for robust and slender tertiles and are shown in **B, D,** and **F** for comparison. Segregating based on robustness tertile showed significant differences in the regressions for Ct.Ar and Ct.TMD versus age.

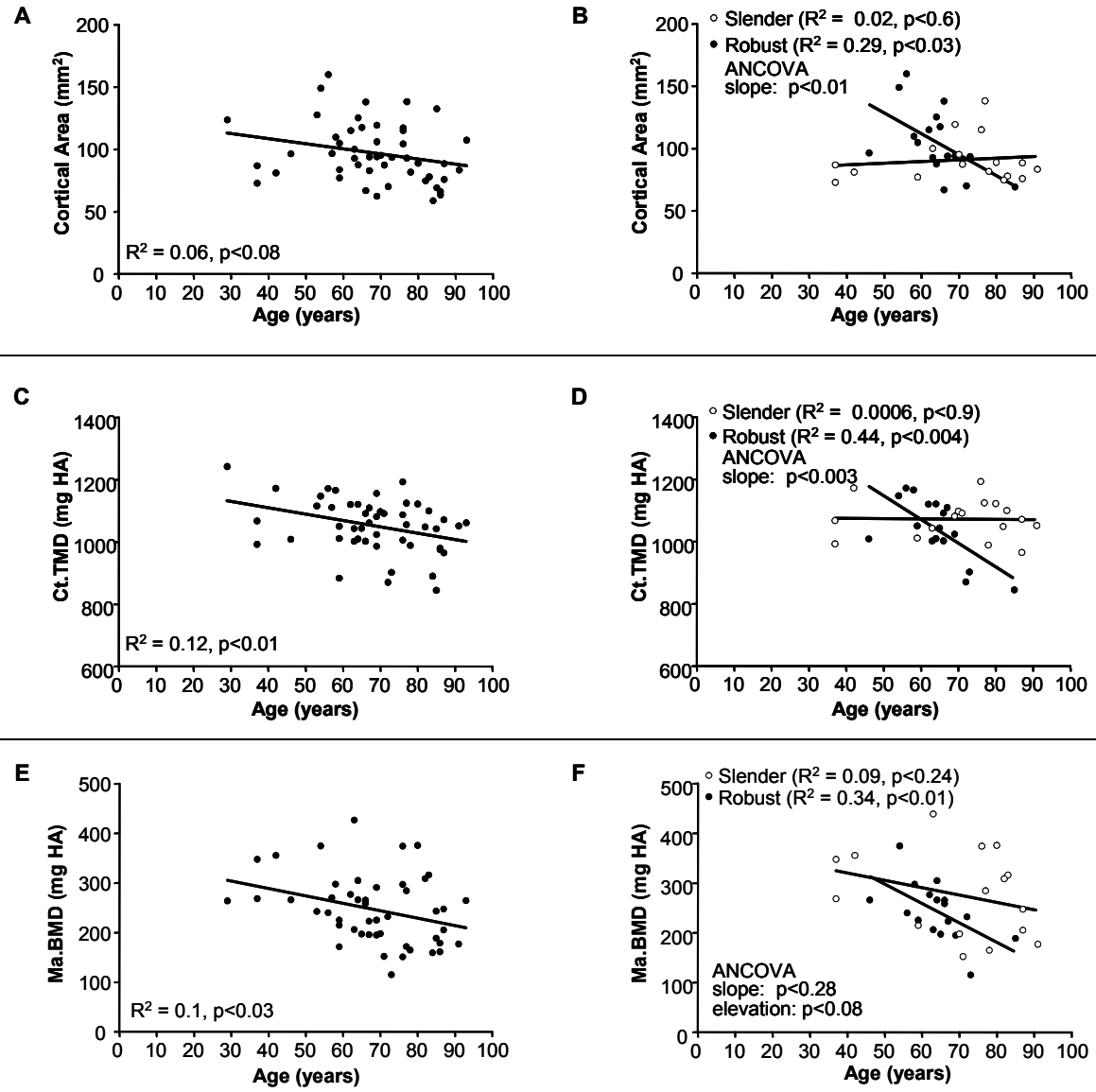

Table 2. Multiple regression analysis

Equation	R^2 - adj	p-value
Max Load = -3175 - 20.9 Age + 212 Robustness + **23.6 Ct.Ar** + 3.39 Ct.TMD + **6.41 Ma.BMD**	63.1%	0.0001
Max Load = -1161 + **34.9 Ct.Ar** + **8.05 Ma.BMD**	58.9%	0.0001

Bold font indicates traits making significant (p<0.05) contributions to the variation in Max Load

Figure 13. Age-changes in **A)** stiffness and **C)** maximum load measured in a fall to the side direction are shown for the entire cohort. The robust tertile showed a greater loss in **B)** stiffness and **D)** maximum load compared to slender. However, these regression were not significantly different.

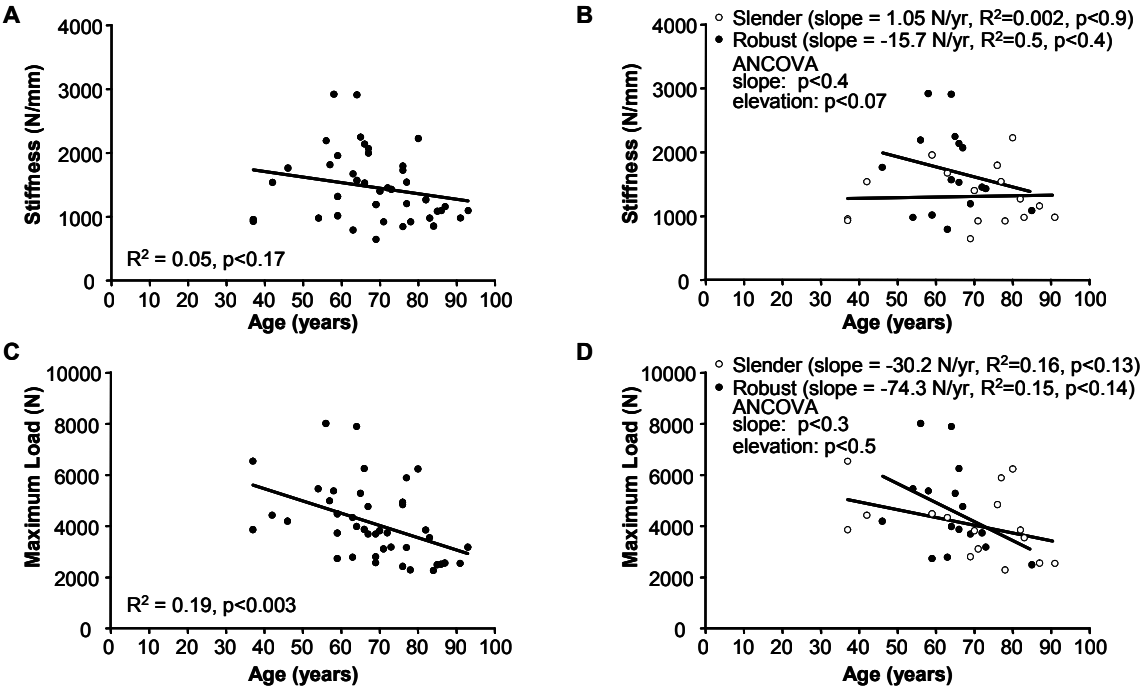

Discussion

We used the variation in external size (robustness) as a model to better understand how adult bone traits interact to establish function. Robustness is a trait established early in life (10,59) which provided us the opportunity to systematically categorize bone in a biologically relevant manner (43). Other research has highlighted how individual traits in the femoral neck such as Ct.Th, matrix mineralization, and Ct.Ar (60-63) may contribute to fracture risk. Our study of 49 female cadaveric femora, contributed to this literature by showing that the functional adaptation process results in a predictable network of compensatory interactions among tissue quality and morphological traits associated with the natural variation in robustness of the femoral neck. Univariate analysis demonstrated negative correlations ($p<0.05$) between RCA and robustness ($R^2 = 0.2$), Ct.TMD and robustness ($R^2 = 0.1$), and Ma.BMD and robustness ($R^2 = 0.1$). Multivariate path analysis confirmed these findings, demonstrating that increased robustness was associated with a decrease in RCA, a decrease in Ct.TMD, and a decrease in Ma.BMD. Further, after validating pQCT information using microCT, we found that robust femoral necks had a thinner and less mineralized cortical shell and reduced trabecular BV/TV, whereas slender femoral necks had a proportionally thicker and more highly mineralized cortical shell and greater trabecular BV/TV. Taken together, our data indicated that slender bones are constructed in a different manner than robust bones. The particular set of traits acquired by individuals in our study cohort were consistent with the idea that bone cells adjust traits to

maximize stiffness while minimizing mass (13). However, differences in Ct.Ar among robust and slender tertiles in young adulthood (Figure 12B) indicated that individuals do not acquire the same mass, but a mass that is specific to their particular femoral neck robustness. This is important because it makes interpreting BMD values difficult, such that a small change in BMD for a robust bone may mean something different compared to a small change in BMD for a slender bone. The impact of these robustness specific trait sets on clinical measures like BMD have yet to be established.

The predictable pattern of trait variation associated with robustness suggested that individuals in our study population used a common biological strategy to build functional proximal femora. Whether robustness directs cortical or trabecular development in early life remains to be determined. Furthermore, whether trabecular traits influence adaptation in cortical traits or whether an individual's cortical traits lead to adaptation in trabecular traits is not well understood. In spite of this, previous research has elucidated that external size is established early in life (10) and our findings suggest that adult cortical and trabecular trait patterns predictably correlate with an early established phenotype. These finding may contribute to assessing bone strength and fracture risk, by inviting the option of not only comparing individual traits to the population mean, which is the traditional approach, but also comparing traits relative to their peers with similar robustness to analyze how well adapted the bone trait sets are for a given size.

Slender and robust structures acquired different sets of traits by adulthood in order to maximize stiffness and minimize mass. Since robust and slender phenotypes employed different strategies to build functional proximal femora, we hypothesized that they would experience age related bone loss at different rates. The current literature elucidates a number of factors associated with age related bone loss, but variation in adult bone size is not a recognized factor. In our population, robust and slender femora showed significantly different bone loss patterns. In particular, the robust tertile showed a significant and negative correlation with age for Ct.Ar (R^2=0.29, $p<0.03$), Ma.BMD (R^2=0.34, $p<0.01$), and Ct.TMD (R^2=0.4, $p<0.003$). In contrast, femora in the slender tertile did not show these age related changes (all $R^2<0.09$ and $p>0.2$). Slender femora appeared to retain cortical area, whereas robust femora lost significant amounts of cortical area with age. This suggested that resorption rates may differ based on bone size. This is consistent with recent work in our lab showing that internal bone remodeling rates in young adult human tibiae correlate with robustness (Jepsen et al, JBMR accepted for publication). Thus, robustness may be a global factor influencing internal remodeling. Although our cross-sectional study does not provide the data to explain why internal remodeling depends on external size, we suspect that the functional adaptation process does not fully compensate slender bones, leading to greater in situ strains during normal daily activities. These greater tissue strains may act as a stimulus to suppress internal remodeling in order to maintain a stiffness level that is adequate to support physiological loads. Differences in the y-intercept of the stiffness-age regression, albeit borderline significant, supports this theory. This intriguing hypothesis is worth testing in future studies.

The pattern of bone loss in the femoral neck may place robust femora at increased risk of fracturing during a fall to the side, since robust femora typically have a thinner superior cortex, a structural feature implicated in fracture risk (62). This is consistent with studies showing that having a wide femoral neck combined with a thin cortical shell is a risk factor for fractures (56). Both robust and slender tertiles showed loss of Ma.BMD with age, which we showed was highly correlated with trabecular BV/TV, an important determinant of trabecular stiffness and strength. Unlike prior work which assumed robust and slender femoral necks were constructed with a similar amount of bone (41), the age-regressions in our study suggested that robust and slender femora have a different Ct.Ar early in life, but then differential resorption resulted in the two tertiles showing similar amounts of bone in older age. The biological mechanism explaining the robustness-specific bone loss patterns is unclear. Our limited cohort size did not allow us to

conclude whether biological processes adjusted traits (e.g., Ct.Ar, Ma.BMD) to fully compensate the nonlinear relationship between width and stiffness to equilibrate function between slender and robust femora. Segregating femora by the natural variation in robustness provided a model to identify predictable differences in the age related bone loss. These findings may invite the opportunity to intervene and treat a subset of a population which is expected to experience an increased rate of age related bone loss.

Our conclusions are based on a cross sectional study utilizing 49 female cadaveric femora. Given the cross-sectional nature of this study, longitudinal changes in morphology and tissue quality could not be examined. Age-related bone loss is influenced by a number of factors. Variables that may affect bone loss such as lifestyle, diet, and medications were not available for a majority of our samples and could not be controlled for in the current study. Since external size is not a previously recognized factor affecting bone loss, we do not expect that individuals with slender and robust bones would have been subjected to different prophylactic treatments. As such, the regressions shown in Figure 12 are more likely to reflect how the natural variation in bone size affects bone loss rather than a systematic bias resulting from differential treatment. Future studies evaluating the relationship between bone structure and morphology should be of a prospective nature to better elucidate the association between morphology and bone loss while ruling out secular changes. This research analysis was limited to the narrow neck region of the femoral neck and further work is needed to confirm that similar associations are observed at other sites along the femoral neck. Although the 49 femora provided ample power to test for functional interactions among morphological and tissue-quality traits, the tertile analysis consisted of a relatively small sample size. Despite this, we observed significant differences between tertiles in how certain traits change over time. However, we did not have sufficient power to detect a significant difference in how bone strength changed over time. Future studies employing a larger cadaveric cohort combined with a prospective clinical study are needed to confirm these age-related changes and to determine whether differences in the loss of strength with aging are meaningful. We suspect that slender femora show increased risk of fracturing (39, Szulc, 2006 #617) because the bones are under-designed (i.e., naturally weaker because of the failure to fully compensate the reduced width), whereas robust femora are at increased risk of fracturing later in life (56) because of the greater loss in cortical shell area. Thus, slender and robust femora may be at risk of fracturing for fundamentally different biological reasons. This is an important outcome of this study and one certainly worth investigating in a larger clinical cohort using high resolution imaging techniques (e.g., CT, MRI).

In conclusion, this study provided new insight into how the functional adaptation process works across a population. The natural variation in robustness was accompanied by specific and predictable changes in cortical and trabecular traits in the femoral neck. Robust femoral necks had a thinner and less mineralized cortical shell and reduced trabecular BV/TV, while slender femoral necks had a proportionally thicker and more highly mineralized cortical shell and greater trabecular BV/TV. We suspect that a common biological strategy is driving a patterned adaptation across the population. Understanding this variation and its implications on biomechanical strength is critical for advancing our ability to identify individuals at increased risk of fracturing. The second major finding of our study demonstrated that segregating femora by robustness provided a model to identify predictable differences in the way bone ages. In particular, robust femora lost significant amounts of cortical area with age while slender femora tended to retain cortical area with age. Understanding what extrinsic and intrinsic variables contribute to age related bone loss and thus regulate internal remodeling may contribute to clinical diagnostics and treatment therapies and allow us to better identify individuals are at increased risk of bone loss.

Key Research Accomplishments

1. We purchased and validated the pQCT system for acquiring images of human tibiae and proximal femora.

2. We established a protocol for acquiring reproducible pQCT images of the femoral neck.

3. We linked stress fracture risk to buffering mechanisms within the skeletal system. Through an ongoing collaboration with Col. Rachel Evans, PhD (Center for the Intrepid, San Antonio, TX, USA) and Dr. Charles Negus (L-3 Jaycor, San Diego, CA., USA), we demonstrated that cellular constraints within complex systems limit the degree of buffering that is required to fully compensate natural variation in bone morphology. These cellular limitations resulted in functional inequivalence across a population of over 700 men and women that was predictable based on bone robustness and that contributed to increased risk of developing a stress fracture during basic training. Thus, we showed that the natural variation in bone robustness was associated with predictable functional deficits that were attributable to cellular constraints limiting the amount of compensation permissible in human long bone.

4. We established imaging protocols for scanning and analysis of the proximal human femur.

5. We acquired images for approximately 50 human femora, quantified the morphological traits, and validated that traits measured by pQCT provide reliable measures of tissue-quality.

6. We conducted univariate and multivariate statistical analyses on the current dataset. The regressions indicated that the proximal human femur shows similar patterns of trait covariation as that observed for the human tibia, that slender femora are less stiff and strong compared to robust femora, and importantly that individuals with slender femora age differently compared to individuals with robust femora.

7. Thus, we show that studying bone as a complex system and using the natural variation in external size as a way to systematically evaluate how the system adjusts itself to establish function provided an important approach to answering fundamental questions about bone and providing novel insight into biological control mechanisms that not have been discovered using conventional reductionist approaches. The data derived from this study will provide the basis for developing new grants (e.g., NIH RO1) focusing on this novel discovery of a global control mechanism regulating internal remodeling.

Individuals supported by this grant:

Karl J. Jepsen, Principal Investigator (10% annual salary support)

Philip Nasser, Research Coordinator (25% annual salary support)

G. Felipe Duarte, Medical Student (supported research efforts; salary covered by other funds)

Yan Epelboym, Medical Student (supported research efforts; salary covered by other funds)

Reportable Outcomes

Directly related to funds

Jepsen KJ, Centi A, Duarte GF, Galloway K, Goldman H, Hampson N, Lappe JM, Cullen DM, Greeves J, Izard R, Nindl BC, Kraemer WJ, Negus CH, Evans RK. Biological constraints that limit compensation of a common skeletal trait variant lead to inequivalence of tibial function among healthy young adults. *J Bone Miner Res,* in press, 2011 (see Appendix 2)

Epelboym Y, Gendron N, Mayer J, Fusco J, Nasser P, Gross G, Ghillani, Jepsen KJ. Inter-individual variation in femoral neck width is associated with the acquisition of predictable sets of morphological and tissue-quality traits and differential bone loss patterns. To be submitted to Bone, Fall 2011. (see Appendix 1)

Indirectly related to funds, but relavent to current research approach

Bhola S, Chen J, Fusco J, Duarte GF, Andarawis-Puri N, Ghillani R, Jepsen KJ, Variation in childhood skeletal robustness is an important determinant of adult bone mass. *Bone*, in press, 2011.

Williams JC, Tommasini SM, Laudier D, Levy R, Schaffler MB, Terranova CJ, Ghillani R, Jepsen KJ. Network theory reveals differential bone loss patterns in the proximal femur. Osteoporosis International, submitted Oct, 2010. In revision

Rachel Grimes, Karl J. Jepsen, Jennifer L. Fitch, Thomas A. Einhorn, Louis C. Gerstenfeld. The transcriptome of fracture healing defines mechanisms of coordination of skeletal and vascular development during endochondral bone formation. *J Bone Miner Res,* in press, July 2011

2. Abstracts

Jepsen KJ, Courtland HW, Nadeau JH. Genetically-determined phenotype covariation networks control bone strength. 7th International Conference on Pathways, Networks, and Systems Medicine, Corfu Chandris. Corfu, Greece

Karl J. Jepsen, G. Felipe Duarte, Amanda Antczak, Yael Arbel, Amir Hadid, Ran Yanovich, Rachel Evans, Charles Negus, Daniel S. Moran. Building a weak skeleton relative to body size during growth increases fracture risk in adults. American Society of Bone and Mineral Research; Toronto, Ontario, Canada; October 2010

G. Felipe Duarte, N. Remi Gendron, Philip Nasser, Richard Ghillani, Rachel Evans, Charles Negus, Karl J. Jepsen. The pattern of compensatory trait interactions defining variation in skeletal function among individuals is recapitulated within a single bone. American Society of Bone and Mineral Research; Toronto, Ontario, Canada; October 2010

Epelboym Y, Ghillani R, Laudier D, Jepsen KJ. Patterns of skeletal trait interactions that may prove useful in prognosticating bone health. ASBMR 2011 Topical Meeting, Forum on Aging and Skeletal Health, December 16, 2010. Bethesda, Maryland. (Note: Yan Epelboym received a Young Investigator Award for this poster)

Duarte GF, Gendron NR, Nasser P, Ghillani R, Jepsen KJ. The pattern of compensatory trait interactions defining variation in skeletal function among individuals is recapitulated within a single bone. Annual meeting of the Orthopaedic Research Society, Long Beach, CA 2011.

Hampson N., Duarte GF, Gendron R, Kalidindi SR, Jepsen KJ, Goldman HM. Porosity, mineralization and morphology interactions at the human tibial cortex. American Society of Bone and Mineral Research; San Diego, CA. September 2011.

Epelboym Y, Gendron NR, Mayer J, Fusco J, Nasser P, Gross G, Ghillani R, Jepsen KJ. Functional interactions among morphological and tissue-quality traits in the proximal femur. Submitted to the annual meeting of the Orthopaedic Research Society, to be held in San Francisco, CA 2012.

Epelboym Y, Gendron NR, Mayer J, Fusco J, Nasser P, Gross G, Ghillani R, Jepsen KJ. Effects of the iInter-individual variation in femoral neck width on age-related bone loss and strength. Submitted to the annual meeting of the Orthopaedic Research Society, to be held in San Francisco, CA 2012.

Jepsen KJ. The path less traveled: insights into complex systems learned from a function-based analysis of the skeleton. Invited talk for platform presentation. 10th International Conference on Pathways, Networks, and Systems Medicine, Rhodes, Greece. July 2012.

Conclusion

Susceptibility to common, heritable diseases is generally thought to originate at the genetic-level, and most studies seek genomic variants or altered molecular networks to develop novel diagnostics and treatments to reduce disease risk on a personalized basis. We show that fracture susceptibility in human tibiae and femora can also arise at a higher-level of biological organization, a phenomenon that may be difficult to predict from genetic information alone, because it involved biomechanical tradeoffs, constraints on cellular activity, and a network of compensatory trait interactions defining organ-level function. Importantly, we also identified a novel level of biological control regulating the degree of internal remodeling affecting young adult tibiae and aging femora. Limited compensation at this level of biological organization may be a public health concern, not only because of the increased fracture susceptibility, but also because it is unclear to what extent prophylactic treatments can circumvent intrinsic cellular constraints to establish a higher degree of functional equivalence among individuals. Functional inequivalence associated with a common trait variant may not be unique to bone, as most traits are nonlinearly related to organ-level function through engineering principles in many physiological systems. Thus, the funds supporting our research efforts have significantly advanced our understanding of bone by identifying a "flaw" or limitation in the functional adaptation process that may contribute to fracture risk and by discovering biological controls regulating internal remodeling that have not previously been reported.

References

1. Rutherford SL, Lindquist S 1998 Hsp90 as a capacitor for morphological evolution. Nature **396**(6709)**:**336-42.
2. Nadeau JH, Burrage LC, Restivo J, Pao YH, Churchill G, Hoit BD 2003 Pleiotropy, homeostasis, and functional networks based on assays of cardiovascular traits in genetically randomized populations. Genome Res **13**(9)**:**2082-91.
3. Marder E, Goaillard JM 2006 Variability, compensation and homeostasis in neuron and network function. Nat Rev Neurosci **7**(7)**:**563-74.
4. Hopkins SR, Harms CA 2004 Gender and pulmonary gas exchange during exercise. Exerc Sport Sci Rev **32**(2)**:**50-6.
5. Waddington CH 1942 Canalization of development and the inheritance of acquired characters. Nature **14:**563-565.
6. Goaillard JM, Taylor AL, Schulz DJ, Marder E 2009 Functional consequences of animal-to-animal variation in circuit parameters. Nat Neurosci **12**(11)**:**1424-30.
7. Ruff C 2005 Growth tracking of femoral and humeral strength from infancy through late adolescence. Acta Paediatr **94**(8)**:**1030-7.
8. Smith RW, Walker RR 1964 Femoral expansion in aging women: Implications for osteoporosis and fractures. Science **145:**156-157.
9. Susanne C, Defrise-Gussenhoven E, Van Wanseele P, Tassin A 1983 Genetic and environmental factors in head and face measurements of Belgian twins. Acta Genet Med Gemellol (Roma) **32**(3-4)**:**229-38.
10. Pandey N, Bhola S, Goldstone A, Chen F, Chrzanowski J, Terranova CJ, Ghillani R, Jepsen KJ 2009 Inter-individual variation in functionally adapted trait sets is established during post-natal growth and predictable based on bone robusticity. J Bone Miner Res **24**(12)**:**1969-1980.
11. Tommasini SM, Nasser P, Schaffler MB, Jepsen KJ 2005 Relationship between bone morphology and bone quality in male tibias: implications for stress fracture risk. J Bone Miner Res **20**(8)**:**1372-80.
12. Jepsen KJ, Hu B, Tommasini SM, Courtland H-W, Price C, Terranova CJ, Nadeau JH 2007 Genetic randomization reveals functional relationships among morphologic and tissue-quality traits that contribute to bone strength and fragility. Mamm Genome **18**(6-7)**:**492-507.
13. Currey JD, Alexander RM 1985 The thickness of the walls of tubular bones. Journal of Zoology, London **206:**453-468.
14. Milgrom C, Giladi M, Simkin A, Rand N, Kedem R, Kashtan H, Stein M, Gomori M 1989 The area moment of inertia of the tibia: a risk factor for stress fractures. J Biomech **22**(11-12)**:**1243-8.
15. Beck TJ, Ruff CB, Shaffer RA, Betsinger K, Trone DW, Brodine SK 2000 Stress fracture in military recruits: gender differences in muscle and bone susceptibility factors. Bone **27**(3)**:**437-44.
16. Evans RK, Negus C, Antczak AJ, Yanovich R, Israeli E, Moran DS 2008 Sex differences in parameters of bone strength in new recruits: beyond bone density. Med Sci Sports Exerc **40**(11 Suppl)**:**S645-53.
17. Wright S 1921 Correlation and causation. Journal of Agricultural Research **20:**557-585.
18. Tommasini SM, Nasser P, Hu B, Jepsen KJ 2008 Biological Co-adaptation of Morphological and Composition Traits Contributes to Mechanical Functionality and Skeletal Fragility. J Bone Miner Res **23**(2)**:**236-246.

19. Tawhai MH, Hoffman EA, Lin CL 2009 The lung physiome: merging imaging-based measures with predictive computational models. Wiley Interdiscip Rev Syst Biol Med **1**(1)**:**61-72.
20. Nash M, Hunter P 2000 Computational mechanics of the heart. J Elasticity **61:**113-141.
21. Lee SW, Antiga L, Spence JD, Steinman DA 2008 Geometry of the carotid bifurcation predicts its exposure to disturbed flow. Stroke **39**(8)**:**2341-7.
22. Markl M, Wegent F, Zech T, Bauer S, Strecker C, Schumacher M, Weiller C, Hennig J, Harloff A 2010 In vivo wall shear stress distribution in the carotid artery: effect of bifurcation geometry, internal carotid artery stenosis, and recanalization therapy. Circ Cardiovasc Imaging **3**(6)**:**647-55.
23. Young RL, Haselkorn TS, Badyaev AV 2007 Functional equivalence of morphologies enables morphological and ecological diversity. Evolution **61**(11)**:**2480-92.
24. Frost HM 1987 Bone "mass" and the "mechanostat": a proposal. Anat Rec **219**(1)**:**1-9.
25. Selker F, Carter DR 1989 Scaling of long bone fracture strength with animal mass. J Biomech **22**(11-12)**:**1175-83.
26. Ruff C 2003 Growth in bone strength, body size, and muscle size in a juvenile longitudinal sample. Bone **33**(3)**:**317-29.
27. Ruff CB 2005 Mechanical determinants of bone form: insights from skeletal remains. J Musculoskelet Neuronal Interact **5**(3)**:**202-12.
28. Nowlan NC, Jepsen KJ, Morgan EF 2011 Smaller, weaker, and less stiff bones evolve from changes in subsistence strategy. Osteoporos Int **22**(6)**:**1967-80.
29. Currey JD 1979 Mechanical properties of bone tissues with greatly differing functions. J Biomech **12**(4)**:**313-9.
30. Currey JD 1984 Effects of differences in mineralization on the mechanical properties of bone. Philos Trans R Soc Lond B Biol Sci **304**(1121)**:**509-18.
31. Rittweger J, Beller G, Ehrig J, Jung C, Koch U, Ramolla J, Schmidt F, Newitt D, Majumdar S, Schiessl H, Felsenberg D 2000 Bone-muscle strength indices for the human lower leg. Bone **27**(2)**:**319-26.
32. Nieves JW, Formica C, Ruffing J, Zion M, Garrett P, Lindsay R, Cosman F 2005 Males have larger skeletal size and bone mass than females, despite comparable body size. J Bone Miner Res **20**(3)**:**529-35.
33. Friedl KE 2005 Biomedical research on health and performance of military women: accomplishments of the Defense Women's Health Research Program (DWHRP). J Womens Health (Larchmt) **14**(9)**:**764-802.
34. Cummings SR, Kelsey JL, Nevitt MC, O'Dowd KJ 1985 Epidemiology of osteoporosis and osteoporotic fractures. Epidemiol Rev **7:**178-208.
35. Looker AC, Beck TJ, Orwoll ES 2001 Does body size account for gender differences in femur bone density and geometry? J Bone Miner Res **16**(7)**:**1291-9.
36. Currey JD 2003 How well are bones designed to resist fracture? J Bone Miner Res **18**(4)**:**591-8.
37. Burr DB, Forwood MR, Fyhrie DP, Martin RB, Schaffler MB, Turner CH 1997 Bone microdamage and skeletal fragility in osteoporotic and stress fractures. J Bone Miner Res **12**(1)**:**6-15.
38. Franklyn M, Oakes B, Field B, Wells P, Morgan D 2008 Section modulus is the optimum geometric predictor for stress fractures and medial tibial stress syndrome in both male and female athletes. Am J Sports Med **36**(6)**:**1179-89.
39. Albright F, Smith PH, Richardson AM 1941 Post-menopausal osteoporosis. Its clinical features. JAMA **116:**2465-2474.
40. Szulc P, Munoz F, Duboeuf F, Marchand F, Delmas PD 2006 Low width of tubular bones is associated with increased risk of fragility fracture in elderly men--the MINOS study. Bone **38**(4)**:**595-602.

41. Zebaze RM, Jones A, Knackstedt M, Maalouf G, Seeman E 2007 Construction of the femoral neck during growth determines its strength in old age. J Bone Miner Res **22**(7)**:**1055-61.
42. Tommasini SM, Hu B, Nadeau JH, Jepsen KJ 2009 Phenotypic integration among trabecular and cortical bone traits establishes mechanical functionality of inbred mouse vertebrae. J Bone Miner Res **24**(4)**:**606-620.
43. Jepsen KJ, Courtland H-W, Nadeau JH 2010 Genetically-determined phenotype covariation networks control bone strength. J Bone Miner Res **25**(7)**:**1581-1593.
44. Kannus P, Haapasalo H, Sankelo M, Sievanen H, Pasanen M, Heinonen A, Oja P, Vuori I 1995 Effect of starting age of physical activity on bone mass in the dominant arm of tennis and squash players. Ann Intern Med **123**(1)**:**27-31.
45. Jepsen KJ, Hu B, Tommasini SM, Courtland H-W, Price C, Cordova M, Nadeau JH 2009 Phenotypic integration of skeletal traits during growth buffers genetic variants affecting the slenderness of femora in inbred mouse strains. Mamm Genome **20**(1)**:**21-33.
46. Liu D, Manske SL, Kontulainen SA, Tang C, Guy P, Oxland TR, McKay HA 2007 Tibial geometry is associated with failure load ex vivo: a MRI, pQCT and DXA study. Osteoporos Int **18**(7)**:**991-7.
47. Kontulainen SA, Johnston JD, Liu D, Leung C, Oxland TR, McKay HA 2008 Strength indices from pQCT imaging predict up to 85% of variance in bone failure properties at tibial epiphysis and diaphysis. J Musculoskelet Neuronal Interact **8**(4)**:**401-9.
48. Ural A, Vashishth D 2006 Interactions between microstructural and geometrical adaptation in human cortical bone. J Orthop Res **24**(7)**:**1489-98.
49. Skedros JG, Dayton MR, Sybrowsky CL, Bloebaum RD, Bachus KN 2006 The influence of collagen fiber orientation and other histocompositional characteristics on the mechanical properties of equine cortical bone. J Exp Biol **209**(Pt 15)**:**3025-42.
50. Goldman HM, Bromage TG, Thomas CD, Clement JG 2003 Preferred collagen fiber orientation in the human mid-shaft femur. Anat Rec **272A**(1)**:**434-45.
51. Brama PA, TeKoppele JM, Bank RA, Barneveld A, van Weeren PR 2002 Biochemical development of subchondral bone from birth until age eleven months and the influence of physical activity. Equine Vet J **34**(2)**:**143-9.
52. Bentolila V, Boyce TM, Fyhrie DP, Drumb R, Skerry TM, Schaffler MB 1998 Intracortical remodeling in adult rat long bones after fatigue loading. Bone **23**(3)**:**275-81.
53. Goldman HM, McFarlin SC, Cooper DM, Thomas CD, Clement JG 2009 Ontogenetic patterning of cortical bone microstructure and geometry at the human mid-shaft femur. Anat Rec (Hoboken) **292**(1)**:**48-64.
54. Schadt EE 2009 Molecular networks as sensors and drivers of common human diseases. Nature **461**(7261)**:**218-23.
55. Melton LJ, 3rd, Wahner HW, Richelson LS, O'Fallon WM, Riggs BL 1986 Osteoporosis and the risk of hip fracture. Am J Epidemiol **124**(2)**:**254-61.
56. Rivadeneira F, Zillikens MC, De Laet CE, Hofman A, Uitterlinden AG, Beck TJ, Pols HA 2007 Femoral neck BMD is a strong predictor of hip fracture susceptibility in elderly men and women because it detects cortical bone instability: the Rotterdam Study. J Bone Miner Res **22**(11)**:**1781-90.
57. LaCroix AZ, Beck TJ, Cauley JA, Lewis CE, Bassford T, Jackson R, Wu G, Chen Z 2010 Hip structural geometry and incidence of hip fracture in postmenopausal women: what does it add to conventional bone mineral density? Osteoporos Int **21**(6)**:**919-29.
58. Chappard C, Bousson V, Bergot C, Mitton D, Marchadier A, Moser T, Benhamou CL, Laredo JD 2010 Prediction of femoral fracture load: cross-sectional study of texture analysis and geometric measurements on plain radiographs versus bone mineral density. Radiology **255**(2)**:**536-43.

59. Kimura K 1976 Growth of the second metacarpal according to chronological age and skeletal maturation. Anat Rec **184**(2)**:**147-57.
60. Crabtree N, Loveridge N, Parker M, Rushton N, Power J, Bell KL, Beck TJ, Reeve J 2001 Intracapsular hip fracture and the region-specific loss of cortical bone: analysis by peripheral quantitative computed tomography. J Bone Miner Res **16**(7)**:**1318-28.
61. Loveridge N, Power J, Reeve J, Boyde A 2004 Bone mineralization density and femoral neck fragility. Bone **35**(4)**:**929-41.
62. Mayhew PM, Thomas CD, Clement JG, Loveridge N, Beck TJ, Bonfield W, Burgoyne CJ, Reeve J 2005 Relation between age, femoral neck cortical stability, and hip fracture risk. Lancet **366**(9480)**:**129-35.
63. Johannesdottir F, Poole KE, Reeve J, Siggeirsdottir K, Aspelund T, Mogensen B, Jonsson BY, Sigurdsson S, Harris TB, Gudnason VG, Sigurdsson G 2011 Distribution of cortical bone in the femoral neck and hip fracture: a prospective case-control analysis of 143 incident hip fractures; the AGES-REYKJAVIK Study. Bone **48**(6)**:**1268-76.

APPENDICES

Appendix 1
Epelboym Y, Gendron N, Mayer J, Fusco J, Nasser P, Gross G, Ghillani, Jepsen KJ. Inter-individual variation in femoral neck width is associated with the acquisition of predictable sets of morphological and tissue-quality traits and differential bone loss patterns. To be submitted to Bone, Fall 2011.

Note: Section 2 in the Final Report was copied from the following manuscript. This is provided as evidence of work in progress toward submitting this paper to the journal Bone during the Fall of 2011.

Appendix 2 (begins on page 69)
Jepsen KJ, Centi A, Duarte GF, Galloway K, Goldman H, Hampson N, Lappe JM, Cullen DM, Greeves J, Izard R, Nindl BC, Kraemer WJ, Negus CH, Evans RK. Biological constraints that limit compensation of a common skeletal trait variant lead to inequivalence of tibial function among healthy young adults. *J Bone Miner Res,* in press, 2011

Inter-individual variation in femoral neck width is associated with the acquisition of predictable sets of morphological and tissue-quality traits and differential bone loss patterns

[1]Yan Epelboym, [1]Nicholas Gendron, [1]Jillian Mayer, [1]Joseph Fusco, [1]Philip Nasser, [2]Gary Gross, [1]Richard Ghillani, [1]Karl J Jepsen

[1] Mount Sinai School of Medicine, NY, New York, USA
[2] The Procter & Gamble Company, West Chester, OH USA

E-mail addresses:

yan.epelboym@gmail.com, remigendron@gmail.com, mayerjillian@gmail.com, joseph.fusco@mssm.edu, philip.nasser@mssm.edu, gross.gj@pg.com, righi@att.net, karl.jepsen1@gmail.com

Correspondence:

Karl J. Jepsen, PhD
Leni & Peter W. May, Department of Orthopaedics
Mount Sinai School of Medicine, Box 1188
One Gustave Levy Place
New York, NY 10029
karl.jepsen@mssm.edu

Abstract

A better understanding of femoral neck structure and age related bone loss will benefit research aimed at reducing fracture risk. We used the natural variation in robustness (measure of bone width relative to length) to analyze how the femoral neck adjusts traits to compensate for robustness, and whether variation in robustness is associated with variable rates of bone loss. Forty-nine female cadaveric femora (29-93 years of age) were evaluated for gross morphological traits (neck axis length, NAL), as well as more localized morphological and tissue level traits using pQCT, microCT, and ashing studies in the narrow neck region of the femoral neck. To test for trait interactions in relation to robustness, bivariate regression analyses and Path Analyses were conducted. Robustness was normally distributed ($p>0.10$, K-S test) and varied widely among women with a coefficient of variation of 14.9%. Age-adjusted partial regression analysis revealed significant negative correlations ($p<0.05$) between RCA and robustness ($R^2 = 0.2$), Ct.TMD and robustness ($R^2 = 0.1$), and Ma.BMD and robustness ($R^2 = 0.1$); these results were confirmed by multivariate path analysis. Tertile analysis based on robustness showed significantly different bone loss patterns when comparing slender vs. robust tertiles. Femora in the robust tertile showed significant negative correlations with age for Ct.Ar ($R^2=0.29$, $p<0.03$), Ma.BMD ($R^2=0.34$, $p<0.01$), and Ct.TMD ($R^2=0.4$, $p<0.003$). However, femora in the slender tertile did not show these age related changes (all $R^2<0.09$ and $p>0.2$). This study provided important new insight into how the functional adaptation process works across a population as well as how robustness is associated with age related bone loss. The results indicated that slender femora are constructed with a different set of traits compared to robust femora and that segregating femora by the natural variation in robustness provided a model to identify predictable differences in age related bone loss. Clinical diagnoses and treatments would benefit from a better understanding of these bone-size specific structural and aging patterns.

Introduction

Identifying skeletal trait variants that increase the risk of hip fractures is critical for reducing the associated morbidity, mortality, and cost (1). These variants are typically identified by comparing the average traits measured for a group of fracture cases to those of age- and sex-matched non-fracture controls. This approach only allows for a dichotomous outcome, such that physical traits contributing to fracture risk can be either greater than or less than the population average. Thus, it is not surprising that studies using this approach found that fracture cases had either a narrow (2,3) or wide (4,5) femoral neck compared to age- and sex-matched controls. However, despite finding small differences (2-3%) in bone width between fracture and non-fracture groups, these studies also showed that individuals at increased risk of fracturing express the full range of variation in bone size. Thus, it is unclear whether we are missing opportunities to identify and treat individuals using such an approach.

We propose that developing a better understanding of how a complex system like bone establishes and maintains mechanical function will benefit efforts to identify traits contributing to fracture risk. The inter-individual variation in robustness, a measure of bone width relative to length, provides a model to systematically evaluate how morphological and tissue-quality traits are coordinated to establish whole bone mechanical function. The functional adaptation process that matches structure to applied loads (i.e., Wolff's Law) is understood for the typical bone, but how this process works across a population of individuals expressing the normal variation in external size is not fully understood. All morphological traits are expected to be mechanically sensitive, including external size (6). Despite this, some individuals are genetically prone to having narrow bones, independent of height and weight, and this should not be viewed as a failure to adapt mechanically to applied loads. Rather, because external size is nonlinearly related to whole bone stiffness, the inter-individual variation in external size should be associated with large compensatory changes in morphological and tissue-quality traits in order for all individuals in a population to have functionally adapted bones that support physiological

loads. Thus, variation in the degree to which a person functionally adapts their skeleton is expected to depend on the particular set of traits acquired during growth.

Prior work in mouse (7) and human (8) long bone identified compensatory interactions among morphological and tissue-quality traits that accompany the natural variation in bone robustness. Compensatory interactions among traits are not limited to long bones, but have also been identified in corticocancellous structures like the vertebral body (9) and the proximal femur (10). The functional adaptation process is more complex in structures like the proximal femur, because it involves compensatory interactions among morphological and tissue-quality traits for both cortical bone and trabecular bone. Work by others showed that narrow femoral necks are accompanied with a thicker cortical shell and greater vBMD compared to wide necks (10), suggesting the functional adaptation process maximizes stiffness in slender femora (narrow relative to length) and minimizes mass in robust femora (wide relative to length). Thus, to be functional, slender femora must acquire a different set of traits than robust femora. However, the morphological and tissue quality differences in these robustness-specific trait sets are not fully understood.

The idea that individuals acquire sets of traits specific to external size is important, because it may complicate our understanding of the aging process in several ways. First, although slender and robust structures are expected to acquire different sets of traits by adulthood, it is unclear whether slender and robust femora show similar age-related bone loss patterns. Second, the bone-width specific trait sets acquired during growth and maintained with aging were based on femora being adapted to compensate loads incurred during daily activities, but it is unclear how these trait sets differentially affect bone strength during a fall to the side. Third, it is unclear if biological processes can adjust morphological and tissue-quality traits to the degree needed to fully compensate the nonlinear relationship between width and whole bone stiffness. Failure to fully compensate bone width would lead to functional inequivalence (i.e., slender femora being less stiff and strong compared to robust femora), which may result in slender

femora experiencing greater tissue-strains compared to robust femora, thereby potentially affecting cell mediated bone loss patterns. In this study, we conducted a biomechanical analysis to test the hypotheses that variation in external size of the femur is associated with predictable compensatory changes in morphology and tissue-quality and that slender and robust femora age differently.

Methods

Sample Population

The sample population included 49 female cadaveric femora. The population was normally distributed with respect to age (Kolmogorov-Smirnov test > 0.10), which ranged from 29 - 93 years with a mean and standard deviation of 68.2 $\pm$ 14.6 years. Race/ethnicity, body weight, and body height were available only for a small subset of the cohort and thus could not be considered in the analysis. Except for cause of death, medical history was unavailable and consequently femora could not be segregated for prior use of prophylactic treatments affecting bone formation and/or resorption. Cause of death was wide ranging, but no individuals died subsequent to hip fracture, and radiographs confirmed that femora showed no evidence of a prior fracture.

Bone Morphology

Gross morphological traits of the proximal femur (Figure 1) were measured from plain film radiographs using previously published methods (11). Radiographs were acquired using a Hewlett Packard X-Ray imaging system (model 43805; Faxitron X-ray, Linconshire, Illinois USA) with an aluminum step wedge (model 117; Gammex, Middleton Wisconsin USA) included for exposure calibration. Radiographic exposure was set at 1mA and 50kV for a duration of 0.7 minutes on a direct exposure film packet (Kodak TL; Eastman Kodak, Rochester, New York USA). The femoral shaft was held in an antero-posterior position with a clamp so the femoral

neck axis was visually perpendicular to the X-ray beam. Direct exposure film was digitized using an Epson high resolution scanner (model 10000 XL; Expression Series, Long Beach, California USA) and analyzed with image analysis software (ImageJ, version 1.44f, U.S. National Institutes of Health, Bethesda, Maryland USA). Femoral Neck Axis Length (NAL) was measured as the linear distance from the lateral aspect of the greater trochanter to the apex of the femoral head passing through the center of the femoral head. Femoral Head Diameter was obtained by fitting a circle to the outline of the femoral head. Neck Shaft Angle (NSA) was measured as the angle formed between the neck axis and the shaft axis. The trochanter-to-trochanter distance was measured as the distance from the apex of the greater trochanter to the apex of the lesser trochanter.

Cross-sectional morphology and tissue-mineral density

Morphological traits were quantified using peripheral Quantitative Computed Tomography, pQCT (XCT2000L, Stratec Medizintechnik, Pforzheim, Germany). This small-bore computed tomography scanner acquires cross-sectional images with an in-plane pixel size of 0.16 mm x 0.16 mm. Measurement quality was assured daily by conducting a calibration scan using a standard phantom with known densities. Scans were obtained for the full length of the femoral neck, from the greater trochanter to the femoral head. The femoral neck was aligned perpendicular to the beam by holding the femoral shaft at a complementary angle to the neck shaft angle. The scanned region was fully submerged in saline solution.

Images of the femoral neck were acquired at 2 mm increments between the base of the head and the base of the trochanter. The cortex was manually segregated from trabecular bone. Femoral neck traits were analyzed using ImageJ, and these included total cross-sectional area (Tt.Ar), marrow area (Ma.Ar), cortical area (Ct.Ar), cortical tissue mineral density (Ct.TMD), marrow bone mineral density (Ma.BMD), robustness (Tt.Ar/NAL), and relative cortical area (RCA=Ct.Ar/Tt.Ar). Grayscale values of the cortical and trabecular regions were converted to

Ct.TMD and Ma.BMD, respectively, using calibration constants derived from the phantom. The grayscale value of cortical bone included bone voxels only, and consequently we referred to the mineral density as tissue-mineral density. The marrow space included both bone and non-bone voxels, and consequently we referred to the mineral density as bone mineral density. For this study, femoral neck traits were reported for the narrow neck region, which was defined as the site with the smallest total area (Tt.Ar). Because cortical and trabecular traits vary along the femoral neck (10), we chose the narrow neck region to standardize the analysis site among the cadaveric cohort. Intra-rater repeatability was demonstrated by measuring traits at two distinct times using the same hardware and software. No significant difference was found between repeat measures for Tt.Ar ($p<0.81$, t-test), Ma.Ar ($p<0.48$, t-test), Ct.Ar ($p<0.19$, t-test), RCA ($p<0.88$, t-test), NAL ($p<0.77$, t-test) Ct.TMD ($p<0.96$, t-test), and Ma.BMD ($p<0.61$, t-test).

Biological constraints affecting compensation

If individuals use a similar biological strategy to compensate for the variation in robustness to establish function during growth, then functionally related traits would be expected to correlate across an adult population (7,8,12). Prior work identified functional interactions among robustness, relative cortical area, and mineralization in mouse femora (7) and human tibiae (8). We postulated that the femoral neck will show similar compensatory trait interactions among robustness, cortical area, and tissue-quality. However, because the femoral neck also includes trabecular bone, we postulated that trabecular architectural traits, particularly those related to tissue-stiffness (e.g., BV/TV), will also covary with robustness. To test for these functional interactions, we conducted a series of univariate regression analyses to identify significant correlations among cortical and trabecular traits. We then conducted a multivariate analysis to test whether the cadaveric cohort exhibits a pattern in the way these traits covary. Multiple regression and principal components analysis test whether traits are related, but make no specific assumption about the underlying biology. We used Path Analysis because this

multivariate analysis allows us to not only test whether certain traits are related, but to also test the hypothesis that traits are related in a particular way that reflects a common biological strategy to build functional structures. We tested whether traits that are functionally related during growth would show correlations among adult structures consistent with the idea that bone maximizes stiffness using minimum mass (13).

For the Path Analysis, we arranged the traits and specified the direction of the arrows among the traits to test whether variation in robustness was accompanied by coordinated changes in the amount of cortical bone (CtAr, RCA), the mineral content of the cortical shell (Ct.TMD), and trabecular mass (Ma.BMD). Path coefficients, which represent the magnitude of the direct and indirect relationships among traits, were calculated using standardized (Z-transformed) data (LISREL v.8.8; Scientific Software International, Lincolnwood, IL, USA). Structural equations were constructed using the Path coefficients to specify the interconnected relationships. For traits with both direct and indirect connections, the structural equations were re-derived in terms of the independent traits (robustness, age, Ct.Ar) and these are reported as the reduced form equations. Observed and model-implied covariance matrices were compared using maximum likelihood estimation. Chi-squared values with an associated p-value greater than 0.05 indicate the model adequately fit the data. The Root Mean Square Error of Approximation (RMSEA), which is a measure of fit that is adjusted for population size and that takes the number of degrees of freedom of the model into consideration, was also reported as an additional fit index. For RMSEA, the p-value represents the significance of fit with $p < 0.05$ indicating a close fit.

Mechanical testing

To assess how the compensatory interactions among traits affect bone strength, 38 of the proximal femora were subjected to a conventional load condition that simulated a fall to the side (14). Femora were sectioned 4.5 inches inferior to the lesser trochanter to isolate the proximal

femur. The shaft was embedded in a square aluminum channel using orthodontic acrylic (Dentsply International, Milford, DE, USA) with the femoral neck in 15° of internal rotation. Impressions of the greater trochanter were made in a petri-dish filled with Bondo® (3M; Maplewood, MN, USA). This impression was necessary to distribute the load across the greater trochanter during testing. Femora were placed in a simulated fall configuration with 10° of rotation in the coronal plane and held in a custom designed fixture with the greater trochanter sitting in the pre-formed impression. A compressive force was applied to the femoral head through stainless steel hemispherical cups to simulate acetabular contact. The acetabular cups ranged in size from 20 – 29 mm radii in 1 mm increments, and each femoral head was matched to the best fitting cup size for testing. A 100 N preload was applied with an Instron 8511 materials test machine (Instron, Inc.; Norwood, MA USA) at 2 mm/second to assure proper sample seating. Testing was conducted at 100 mm/sec until fracture. Stiffness and maximum load were calculated from load-deflection curves.

Validation studies

Several validation studies were conducted to confirm that Ma.BMD and Ct.TMD provided measures of tissue-quality. First, we related Ma.BMD measured by pQCT to trabecular architectural traits measured by microComputed Tomography (microCT). For 26 of the proximal femora, the narrow neck region was identified visually, re-imaged by pQCT using the previously described protocols, and the corresponding 2 mm section was extracted using a diamond coated metallurgical saw (South Bay Technology, Inc.; San Clemente, CA, USA). The 2 mm section was hemisected into superior and inferior halves and imaged using a desktop micro-CT (GE eXplore Locus SP Specimen Scanner; GE Healthcare, London, Ontario, Canada). Images were obtained at 80kV (300 ms integration time) with a 0.010" Aluminum filter and reconstructed at a voxel size of 0.017 mm. The image volumes were individually thresholded (15) to segment bone from non-bone voxels, and cortical bone was manually segregated from trabecular bone.

Cortical thickness (Ct.Th), cortical tissue mineral density (Ct.TMD), trabecular tissue mineral density (Tb.TMD), bone volume fraction (BV/TV), trabecular number (Tb.N), trabecular thickness (Tb.Th), and trabecular separation (Tb.Sp) were measured. Cortical thickness (Ct.Th) was measured for the inferior and superior regions by manually measuring the thickness at the apex of the superior and inferior hemisections. Ma.BMD was related to trabecular bone volume fraction (BV/TV), trabecular thickness (Tb.Th), and trabecular number (Tb.N) by linear regression analysis.

Second, we related Ct.TMD to ash content. Ct.TMD measured by pQCT could not be directly related to ash content, because we were unable to physically separate the cortical shell from the trabecular bone to perform reliable ashing studies. We could not relate Ct.TMD directly to ash content because ashing was done for the entire hemisection, which includes and cortical and trabecular tissues, and variation in the ash content of the trabecular may obscure the association between Ct.TMD and ash content. As an alternative, we related Ct.TMD to ash content indirectly by using microCT data as an intermediate. For each hemisection, we digitally separated cortical and trabecular bone in the CT images and related Ct.TMD measured by pQCT to Ct.TMD measured by microCT. We then related the overall TMD (cortical + trabecular) measured by microCT to ash content. Ash content was measured for 15 samples using previously published methods (8). The femoral neck hemisections were defatted using a 1:1 volume ratio of ethanol/ether for 8 hours followed by a 2:1 volume ratio of chloroform/methanol for 8 hours. The methanol residue was removed by using two changes of pure chloroform for 1 hour each. Samples were dried under vacuum at 80°C for 24 hours to constant weight and weighed (dry weight). Finally, samples were ashed at 600°C for 18 hours and reweighed (ash weight). Ash content was calculated as the ash weight normalized by the dry weight.

Robustness-specific bone loss patterns

Linear regression analysis was used to test whether age related bone loss patterns varied with robustness. Femora were grouped by robustness values into a robust tertile (n=17) and a slender tertile (n=17). Cortical and trabecular traits were compared between the two tertiles (Student's t-test) and differences in how each trait changed with age were evaluated by ANCOVA.

Results

Inter-individual variation in femoral neck robustness

Although variation in external size of the femoral neck could be measured by width or total cross-sectional area, we found that using these absolute trait values was not sufficient for our purposes because a small individual with a robust bone may have the same width or total cross-sectional area as a large individual with a slender bone. We compared different ways of calculating external size to identify a geometric measure of the neck that differentiated these outcomes. Because the femoral neck has a non-circular cross-sectional morphology and external size varies continually along the neck, we used total cross-sectional area at the narrow neck region as a measure of transverse size since no single width measure would represent size alone. We normalized total area by neck axis length (NAL) as a measure of femoral neck robustness. Total cross-sectional area increased with neck axis length (R^2 = 0.34, p<0.0001), as expected (Figure 2A). For any given neck axis length, total area varied by as much as 50-75% among individuals indicating that cross-sectional area varied widely relative to neck length. Residuals calculated from this regression correlated significantly with the ratio, Tt.Ar/NAL (R^2 = 0.94, p<0.0001) (Figure 2B), such that individuals with a negative Tt.Ar-NAL residual were characterized as slender, whereas those with a positive Tt.Ar-NAL residual were characterized as robust. This confirmed that the ratio, Tt.Ar/NAL, could be used as a measure of robustness to

differentiate slender from robust femora even though this ratio does not take the y-intercept of the linear regression between Tt.Ar and NAL into consideration. Robustness (Tt.Ar/NAL) was normally distributed ($p>0.10$, Kolmogorov-Smirnov test) and varied widely among women (Figure 2C), showing a coefficient of variation of 14.9%. Linear regression analysis revealed that robustness correlated weakly with age ($R^2 = 0.04$, $p>0.20$) and neck shaft angle ($R^2 = 0.025$, $p>0.27$). Tt.Ar/NAL correlated positively with alternative measures of robustness such as femoral head diameter/NAL ($R^2 = 0.24$, $p<0.0005$) and Tt.Ar/neck length ($R^2=0.70$, $p<0.001$). We chose to use Tt.Ar/NAL as a measure of femoral neck robustness, because the lack of distinct anatomic markers delineating the beginning and end of the neck region made neck length a less reliable measure compared to NAL

Correlations between bone morphology and tissue quality

To determine how the natural variation in robustness was compensated to establish function, we tested whether RCA, Ct.TMD, and Ma.BMD varied with robustness. Accounting for age effects using partial regression analysis revealed significant negative correlations between RCA and robustness (Figure 3A), Ct.TMD and robustness (Figure 3B), and Ma.BMD and robustness (Figure 3C). MicroCT images were used to quantify cortical thickness in the superior and inferior aspects of the narrow neck region for a subset of the femora (n=24). Ct.Th correlated negatively with robustness for both the superior and inferior regions (Figure 3D), and was significant only for the superior region ($R^2 = 0.28$, $p<0.008$), but not for the inferior neck region ($R^2 = 0.04$, $p<0.34$). Further analysis of the apical Ct.Th showed no significant correlation between superior Ct.Th and age ($R^2 = 0.06$, $p<0.24$) or inferior Ct.Th and age ($R^2 = 0.005$, $p<0.73$).

A validation study was conducted using a subset of the femora (n=26) to relate the Ma.BMD determined by pQCT to indices of trabecular architecture determined using microCT. Ma.BMD correlated positively with BV/TV ($R^2 = 0.66$, $p<0.0001$), Tb.Th ($R^2 = 0.66$, $p<0.0001$), Tb.N ($R^2 =$

0.42, $p<0.001$), and Tb.TMD ($R^2 = 0.48$, $p<0.001$; Figure 4B). Because the trabecular traits are inter-related, we also performed a multivariate analysis and found that BV/TV alone was the strongest predictor of Ma.BMD ($p<0.005$), and adding Tb.Th, Tb.N, and Tb.TMD to the regression did not greatly improve the predictability of the multivariate model ($R^2 = 0.68$, $p<0.0001$) over the univariate regressions. We further tested, albeit indirectly, whether the Ct.TMD determined by pQCT could also be used as an indicator of tissue-quality. Ct.TMD measured by pQCT correlated positively with Ct.TMD determined by microCT ($R^2 = 0.53$, $p<0.001$) (Figure 4A), and the overall TMD (cortical + trabecular) determined by microCT correlated significantly with ash content ($R^2 = 0.40$, $p<0.0001$) (Figure 4C). This indirect validation suggested that variation in Ct.TMD measured by pQCT reflected differences in tissue-quality. Taken together, these results indicated that more robust femoral necks had a thinner cortical shell, a less mineralized cortical shell, and reduced trabecular BV/TV, whereas slender femoral necks had a proportionally thicker cortical shell, a more highly mineralized cortex, and greater trabecular BV/TV.

Path Analysis

Path analysis was conducted to assess the functional interactions among morphological and tissue-level traits. The Path Model included age, robustness, Ct.Ar, RCA, Ct.TMD, and Ma.BMD. The χ^2 and RMSEA values both indicated there was an excellent fit between the data and the model (Figure 5). The Path coefficients were calculated based on Z-transformed data and thus reflect the number of standard deviation changes in a trait arising from a 1 standard deviation change in robustness. When all the direct and indirect paths were taken into consideration, a 1 SD increase in robustness was associated with a 0.71 SD decrease in RCA, a 0.47 SD decrease in Ct.TMD, and a 0.44 SD decrease in Ma.BMD. The Path Model confirmed the univariate results indicating that robust femoral necks tended to have a cortex that occupied proportionally less space, had a lower degree of cortical mineralization, and lower trabecular

bone mass. The goodness of fit for the Path Model failed (i.e., p-value for χ^2 <0.05, RMSEA > 0.1) when the arrow between RCA and Ct.TMD was removed or reversed, suggesting there is an important interaction among external size, the amount of bone, and tissue-quality.

Age-related bone loss

Individuals were stratified into robustness tertiles to evaluate whether robust femora aged differently compared to slender femora. There was no difference in age between robust (64.0±8.6 years) and slender (69.9±17.2 years) tertiles ($p<0.25$, t-test). The robust and slender tertiles differed with respect to Tt.Ar ($p<0.0001$, t-test), but not NAL ($p<0.19$, t-test), suggesting the variation in robustness resulted largely from differences in transverse expansion rather than axial growth of the neck. The slender tertile showed a significantly greater RCA compared to the robust tertile ($p<0.01$, t-test), which was expected based on the results of the univariate and multivariate analyses. Although the cortex occupied proportionally greater space for the slender tertile, the slender tertile had a lower Ct.Ar compared to the robust tertile ($p<0.018$, t-test), indicating that slender femoral necks were constructed with a lower absolute amount of cortical bone. Linear regression analysis of the entire cohort (Figure 6) revealed that Ct.Ar ($R^2 = 0.06$, $p<0.08$), Ct.TMD ($R^2 = 0.20$, $p<0.11$), and Ma.BMD ($R^2 = 0.10$, $p<0.05$) decreased with age, as expected. However, stratifying the data into robustness tertiles revealed that slender femora aged differently compared to robust femora. Ct.Ar decreased significantly with age for the robust tertile ($R^2 = 0.29$, $p<0.05$), but not for the slender tertile ($R^2 = 0.02$, $p>0.58$). The slopes of the Ct.Ar - age regressions were significantly different between robust and slender tertiles ($p<0.012$, ANCOVA), suggesting that slender and robust femoral necks exhibited differential rates of cortical bone loss with aging (Figure 6B). Likewise, Ct.TMD ($R^2=0.48$, $p<0.01$) and Ma.BMD ($R^2=0.34$, $p<0.05$) decreased significantly with age for the robust tertile, but not for the slender tertile ($R^2 = 0.0005$-0.09, $p<0.25$). The slopes of the mineral density - age regressions were significantly different between robust and slender tertiles for Ct.TMD ($p<0.005$, ANCOVA), but

not Ma.BMD (Figures 6D, F). This suggested that slender and robust femoral necks exhibited differential rates of cortical tissue-mineral loss with aging, but showed fairly similar losses in trabecular mineral density.

Bone mechanics

Whole bone mechanical tests were conducted to test how acquisition of robustness-specific trait sets affected bone stiffness and maximum load during a simulated fall-to-the-side. Linear regression analysis applied to the entire cohort showed that maximum load (R^2 = 0.19, $p<0.004$) but not stiffness (R^2 = 0.05, $p<0.18$) decreased with age. A multiple regression analysis (Table 1), also applied to the entire cohort, indicated that 63.1% of the variation in maximum load was explained by robustness, Ct.Ar, Ct.TMD, Ma.BMD, and age (R^2 = 0.631, $p<0.0001$). Of these variables, only Ct.Ar and Ma.BMD were significant contributors, accounting for the majority of the variation in maximum load (Table 1). When segregating the data into robustness tertiles, femora in the robust tertile showed a 31% greater stiffness ($p<0.05$, t-test) and 13% greater maximum load ($p<0.3$, t-test) compared to slender femora (Figure 7). Maximum load decreased with age for both tertiles and the slope of this regression was ~2-fold greater (not significant) for the robust tertile compared to the slender tertile.

Discussion

We used the variation in external size (robustness) as a model to better understand how adult bone traits interact to establish function. Robustness is a trait established early in life (16,17) which provided us the opportunity to systematically categorize bone in a biologically relevant manner (18). Other research has highlighted how individual traits in the femoral neck such as Ct.Th, matrix mineralization, and Ct.Ar (19-22) may contribute to fracture risk. Our study of 49 female cadaveric femora, contributed to this literature by showing that the functional adaptation process results in a predictable network of compensatory interactions among tissue

quality and morphological traits associated with the natural variation in robustness of the femoral neck. Univariate analysis demonstrated negative correlations ($p<0.05$) between RCA and robustness ($R^2 = 0.2$), Ct.TMD and robustness ($R^2 = 0.1$), and Ma.BMD and robustness ($R^2 = 0.1$). Multivariate path analysis confirmed these findings, demonstrating that increased robustness was associated with a decrease in RCA, a decrease in Ct.TMD, and a decrease in Ma.BMD. Further, after validating pQCT information using microCT, we found that robust femoral necks had a thinner and less mineralized cortical shell and reduced trabecular BV/TV, whereas slender femoral necks had a proportionally thicker and more highly mineralized cortical shell and greater trabecular BV/TV. Taken together, our data indicated that slender bones are constructed in a different manner than robust bones. The particular set of traits acquired by individuals in our study cohort were consistent with the idea that bone cells adjust traits to maximize stiffness while minimizing mass (13). However, differences in Ct.Ar among robust and slender tertiles in young adulthood (Figure 6B) indicated that individuals do not acquire the same mass, but a mass that is specific to their particular femoral neck robustness. This is important because it makes interpreting BMD values difficult, such that a small change in BMD for a robust bone may mean something different compared to a small change in BMD for a slender bone. The impact of these robustness specific trait sets on clinical measures like BMD have yet to be established.

The predictable pattern of trait variation associated with robustness suggested that individuals in our study population used a common biological strategy to build functional proximal femora. Whether robustness directs cortical or trabecular development in early life remains to be studied. Furthermore, whether trabecular traits influence adaptation in cortical traits or whether an individual's cortical traits lead to adaptation in trabecular traits is not well understood. In spite of this, previous research has elucidated that external size is established early in life (17) and our findings suggest that adult cortical and trabecular trait patterns predictably correlate with an early established phenotype. These finding may contribute to

assessing bone strength and fracture risk, by inviting the option of not only comparing individual traits to the population mean, which is the traditional approach, but also comparing traits relative to their peers with similar robustness to analyze how well adapted the bone trait sets are for a given size.

Slender and robust structures acquired different sets of traits by adulthood in order to maximize stiffness and minimize mass. Since robust and slender phenotypes employed different strategies to build functional proximal femora, we hypothesized that they would experience age related bone loss at different rates. Current literature elucidates a number of factors associated with age related bone loss. However, based on the current body of research, it is unclear whether variation in bone size is associated with different age-related bone loss patterns in the femoral neck. In our population, robust and slender femora showed significantly different bone loss patterns. In particular, the robust tertile showed a significant and negative correlation with age for Ct.Ar (R^2=0.29, $p<0.03$), Ma.BMD (R^2=0.34, $p<0.01$), and Ct.TMD (R^2=0.4, $p<0.003$). In contrast, femora in the slender tertile did not show these age related changes (all $R^2<0.09$ and $p>0.2$). Slender femora appeared to retain cortical area, whereas robust femora lost significant amounts of cortical area with age. This suggested that resorption rates may differ based on bone size. This is consistent with recent work in our lab showing that internal bone remodeling rates in young adult human tibiae correlate with robustness (Jepsen et al, JBMR submitted). Thus, robustness may be a global factor influencing internal remodeling. Although our cross-sectional study does not provide the data to explain why internal remodeling depends on external size, we suspect that the functional adaptation process does not fully compensate slender bones, leading to greater in situ strains during normal daily activities. These greater tissue strains may act as a stimulus to suppress internal remodeling in order to maintain a stiffness level that is adequate to support physiological loads. Differences in the y-intercept of the stiffness-age regression, albeit borderline significant, supports this theory. This intriguing hypothesis is worth testing in future studies.

The pattern of bone loss in the femoral neck may place robust femora at increased risk of fracturing during a fall to the side, since robust femora typically have a thinner superior cortex, a structural feature implicated in fracture risk (21). This is consistent with studies showing that having a wide femoral neck combined with a thin cortical shell is a risk factor for fractures (4). Both robust and slender tertiles showed loss of Ma.BMD with age, which we showed was highly correlated with trabecular BV/TV, an important determinant of trabecular stiffness and strength. Unlike prior work which assumed robust and slender femoral necks were constructed with a similar amount of bone (10), the age-regressions in our study suggested that robust and slender femora have a different Ct.Ar early in life, but then differential resorption resulted in the two tertiles showing similar amounts of bone in older age. The biological mechanism explaining the robustness-specific bone loss patterns is unclear. Our limited cohort size did not allow us to conclude whether biological processes adjusted traits (e.g., Ct.Ar, Ma.BMD) to fully compensate the nonlinear relationship between width and stiffness to equilibrate function between slender and robust femora. Segregating femora by the natural variation in robustness provided a model to identify predictable differences in the age related bone loss. These findings may invite the opportunity to intervene and treat a subset of a population which is expected to experience an increased rate of age related bone loss.

Our conclusions are based on a cross sectional study utilizing 49 female cadaveric femora. Given the cross-sectional nature of this study, longitudinal changes in morphology and tissue quality could not be examined. Age-related bone loss is influenced by a number of factors. Variables that may affect bone loss such as lifestyle, diet, and medications were not available for a majority of our samples and could not be controlled for. Future studies evaluating the relationship between bone structure and morphology should be of a prospective nature to better elucidate the association between morphology and bone loss while ruling out secular changes. This research analysis was limited to the narrow neck region of the femoral neck and further work is needed to confirm that similar associations are observed at other sites along the femoral

neck. Although the 49 femora provided ample power to test for functional interactions among morphological and tissue-quality traits, the tertile analysis consisted of a relatively small sample size. Despite this, we observed significant differences between tertiles in how certain traits change over time. However, we did not have sufficient power to detect a significant difference in how bone strength changed over time. Future studies employing a larger cadaveric cohort combined with a prospective clinical study are needed to confirm these age-related changes and to determine whether differences in the loss of strength with aging are meaningful. We suspect that slender femora show increased risk of fracturing (2, Szulc, 2006 #617) because the bones are under-designed (i.e., naturally weaker because of the failure to fully compensate the reduced width), whereas robust femora are at increased risk of fracturing later in life (4) because of the greater loss in cortical shell area. Thus, slender and robust femora may be at risk of fracturing for fundamentally different biological reasons. This is an important outcome of this study and one certainly worth investigating in a larger clinical cohort using high resolution imaging techniques (e.g., CT, MRI).

In conclusion, this study provided new insight into how the functional adaptation process works across a population. The natural variation in robustness was accompanied by specific and predictable changes in cortical and trabecular traits in the femoral neck. Robust femoral necks had a thinner and less mineralized cortical shell and reduced trabecular BV/TV, while slender femoral necks had a proportionally thicker and more highly mineralized cortical shell and greater trabecular BV/TV. We suspect that a common biological strategy is driving a patterned adaptation across the population. Understanding this variation and its implications on biomechanical strength is critical for advancing our ability to identify individuals at increased risk of fracturing. The second major finding of our study demonstrated that segregating femora by robustness provided a model to identify predictable differences in the way bone ages. In particular, robust femora lost significant amounts of cortical area with age while slender femora tended to retain cortical area with age. Understanding what extrinsic and intrinsic variables

contribute to age related bone loss and thus regulate internal remodeling may contribute to clinical diagnostics and treatment therapies and allow us to better identify individuals are at increased risk of bone loss.

References

1. Melton LJ, 3rd, Wahner HW, Richelson LS, O'Fallon WM, Riggs BL 1986 Osteoporosis and the risk of hip fracture. Am J Epidemiol **124**(2)**:**254-61.
2. Albright F, Smith PH, Richardson AM 1941 Post-menopausal osteoporosis. Its clinical features. JAMA **116:**2465-2474.
3. Szulc P, Munoz F, Duboeuf F, Marchand F, Delmas PD 2006 Low width of tubular bones is associated with increased risk of fragility fracture in elderly men--the MINOS study. Bone **38**(4)**:**595-602.
4. Rivadeneira F, Zillikens MC, De Laet CE, Hofman A, Uitterlinden AG, Beck TJ, Pols HA 2007 Femoral neck BMD is a strong predictor of hip fracture susceptibility in elderly men and women because it detects cortical bone instability: the Rotterdam Study. J Bone Miner Res **22**(11)**:**1781-90.
5. LaCroix AZ, Beck TJ, Cauley JA, Lewis CE, Bassford T, Jackson R, Wu G, Chen Z 2010 Hip structural geometry and incidence of hip fracture in postmenopausal women: what does it add to conventional bone mineral density? Osteoporos Int **21**(6)**:**919-29.
6. Kannus P, Haapasalo H, Sankelo M, Sievanen H, Pasanen M, Heinonen A, Oja P, Vuori I 1995 Effect of starting age of physical activity on bone mass in the dominant arm of tennis and squash players. Ann Intern Med **123**(1)**:**27-31.
7. Jepsen KJ, Hu B, Tommasini SM, Courtland H-W, Price C, Terranova CJ, Nadeau JH 2007 Genetic randomization reveals functional relationships among morphologic and tissue-quality traits that contribute to bone strength and fragility. Mamm Genome **18**(6-7)**:**492-507.
8. Tommasini SM, Nasser P, Hu B, Jepsen KJ 2008 Biological Co-adaptation of Morphological and Composition Traits Contributes to Mechanical Functionality and Skeletal Fragility. J Bone Miner Res **23**(2)**:**236-246.
9. Tommasini SM, Hu B, Nadeau JH, Jepsen KJ 2009 Phenotypic integration among trabecular and cortical bone traits establishes mechanical functionality of inbred mouse vertebrae. J Bone Miner Res **24**(4)**:**606-620.
10. Zebaze RM, Jones A, Knackstedt M, Maalouf G, Seeman E 2007 Construction of the femoral neck during growth determines its strength in old age. J Bone Miner Res **22**(7)**:**1055-61.
11. Chappard C, Bousson V, Bergot C, Mitton D, Marchadier A, Moser T, Benhamou CL, Laredo JD 2010 Prediction of femoral fracture load: cross-sectional study of texture analysis and geometric measurements on plain radiographs versus bone mineral density. Radiology **255**(2)**:**536-43.
12. Cheverud JM 1982 Phenotypic, genetic, and environmental morphological integration in the cranium. Evolution **36**(3)**:**499-516.
13. Currey JD, Alexander RM 1985 The thickness of the walls of tubular bones. Journal of Zoology, London **206:**453-468.
14. Courtney AC, Wachtel EF, Myers ER, Hayes WC 1994 Effects of loading rate on strength of the proximal femur. Calcif Tissue Int **55**(1)**:**53-8.
15. Otsu N 1979 A threshold selection method from gray-level histograms. IEEE Transactions on Systems, Man, and Cybernetics **SMC-9**(1)**:**62-66.
16. Kimura K 1976 Growth of the second metacarpal according to chronological age and skeletal maturation. Anat Rec **184**(2)**:**147-57.
17. Pandey N, Bhola S, Goldstone A, Chen F, Chrzanowski J, Terranova CJ, Ghillani R, Jepsen KJ 2009 Inter-individual variation in functionally adapted trait sets is established during post-natal growth and predictable based on bone robusticity. J Bone Miner Res **24**(12)**:**1969-1980.

18. Jepsen KJ, Courtland H-W, Nadeau JH 2010 Genetically-determined phenotype covariation networks control bone strength. J Bone Miner Res **25**(7)**:**1581-1593.
19. Crabtree N, Loveridge N, Parker M, Rushton N, Power J, Bell KL, Beck TJ, Reeve J 2001 Intracapsular hip fracture and the region-specific loss of cortical bone: analysis by peripheral quantitative computed tomography. J Bone Miner Res **16**(7)**:**1318-28.
20. Loveridge N, Power J, Reeve J, Boyde A 2004 Bone mineralization density and femoral neck fragility. Bone **35**(4)**:**929-41.
21. Mayhew PM, Thomas CD, Clement JG, Loveridge N, Beck TJ, Bonfield W, Burgoyne CJ, Reeve J 2005 Relation between age, femoral neck cortical stability, and hip fracture risk. Lancet **366**(9480)**:**129-35.
22. Johannesdottir F, Poole KE, Reeve J, Siggeirsdottir K, Aspelund T, Mogensen B, Jonsson BY, Sigurdsson S, Harris TB, Gudnason VG, Sigurdsson G 2011 Distribution of cortical bone in the femoral neck and hip fracture: a prospective case-control analysis of 143 incident hip fractures; the AGES-REYKJAVIK Study. Bone **48**(6)**:**1268-76.

Table 1. Multiple regression analysis

Equation	R^2 - adj	p-value
Max Load = -3175 - 20.9 Age + 212 Robustness + **23.6 Ct.Ar** + 3.39 Ct.TMD + **6.41 Ma.BMD**	63.1%	0.0001
Max Load = -1161 + **34.9 Ct.Ar** + **8.05 Ma.BMD**	58.9%	0.0001

Bold font indicates traits making significant ($p<0.05$) contributions to the variation in Max Load

Figure 1. Radiographic images of the slender and robust femora and the associated cross-sections derived from pQCT depict the natural variation in bone size that exists among individuals. The center image shows how neck axis length was measured.

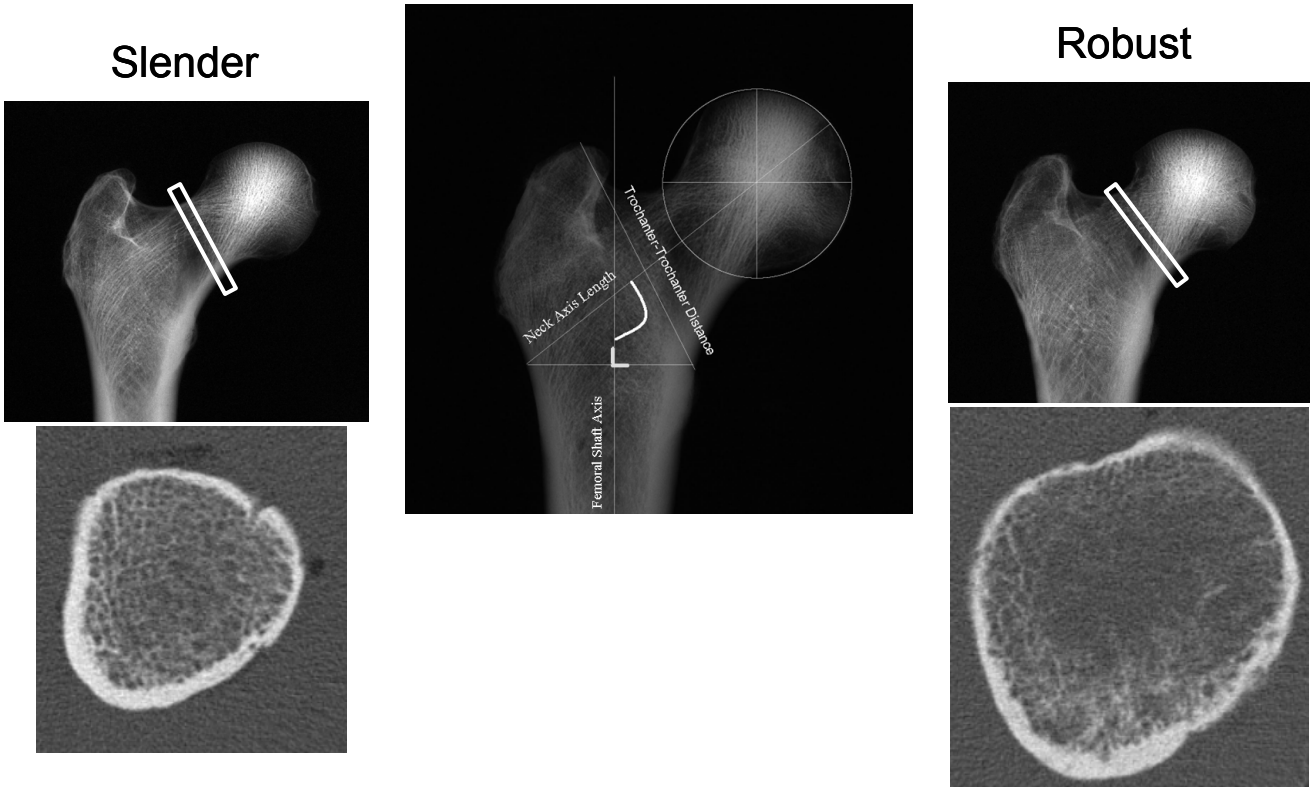

Figure 2. A) Variation in total cross-sectional area as a function of neck axis length. **B)** Robustness (Tt.Ar/Le) was plotted against residuals from the Tt.Ar-Le regression to determine if the ratio differentiated slender from robust femora. **C)** Robustness was normally distributed across our cadaveric cohort.

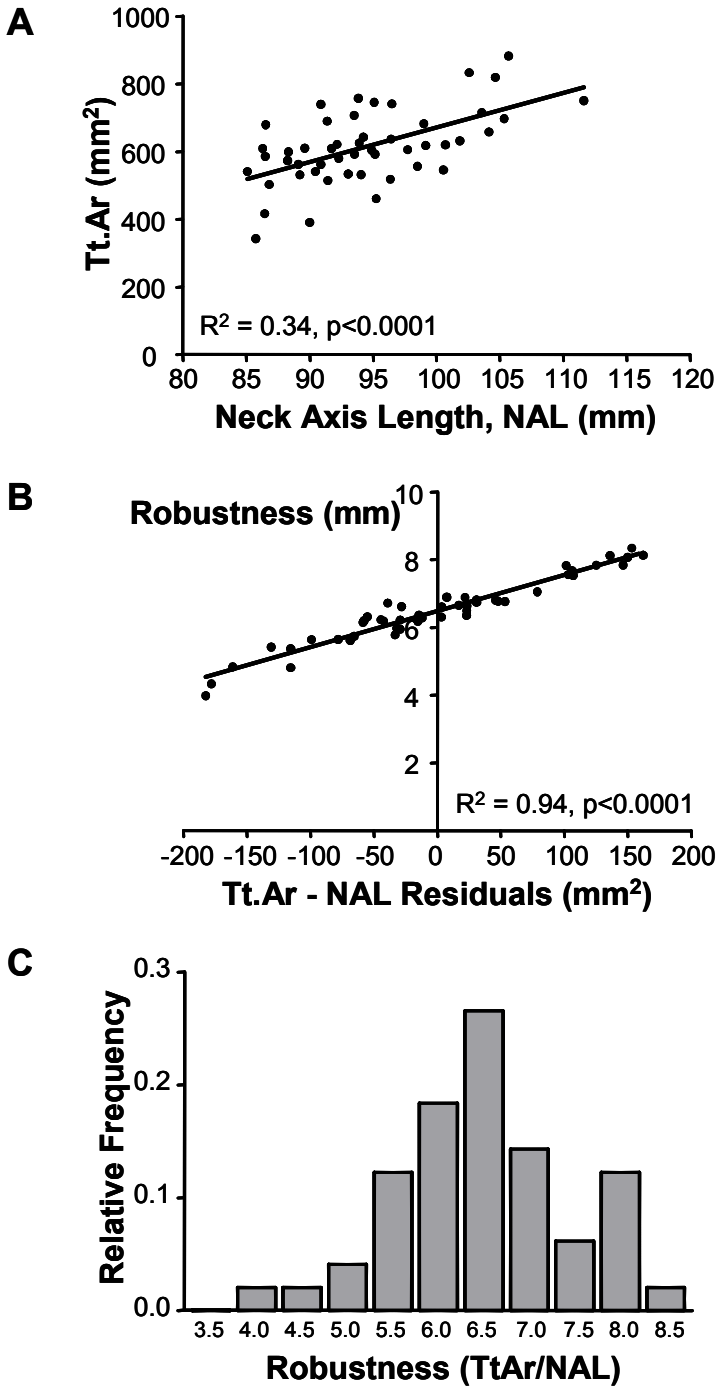

Figure 3. Partial regression analyses were conducted to take the effects of age into consideration, showing that **A)** relative cortical area (RCA = Ct.Ar/Tt.Ar), **B)** Ct.TMD, **C)** Ma.BMD, and **D)** Ct.Th all correlate negatively with robustness.

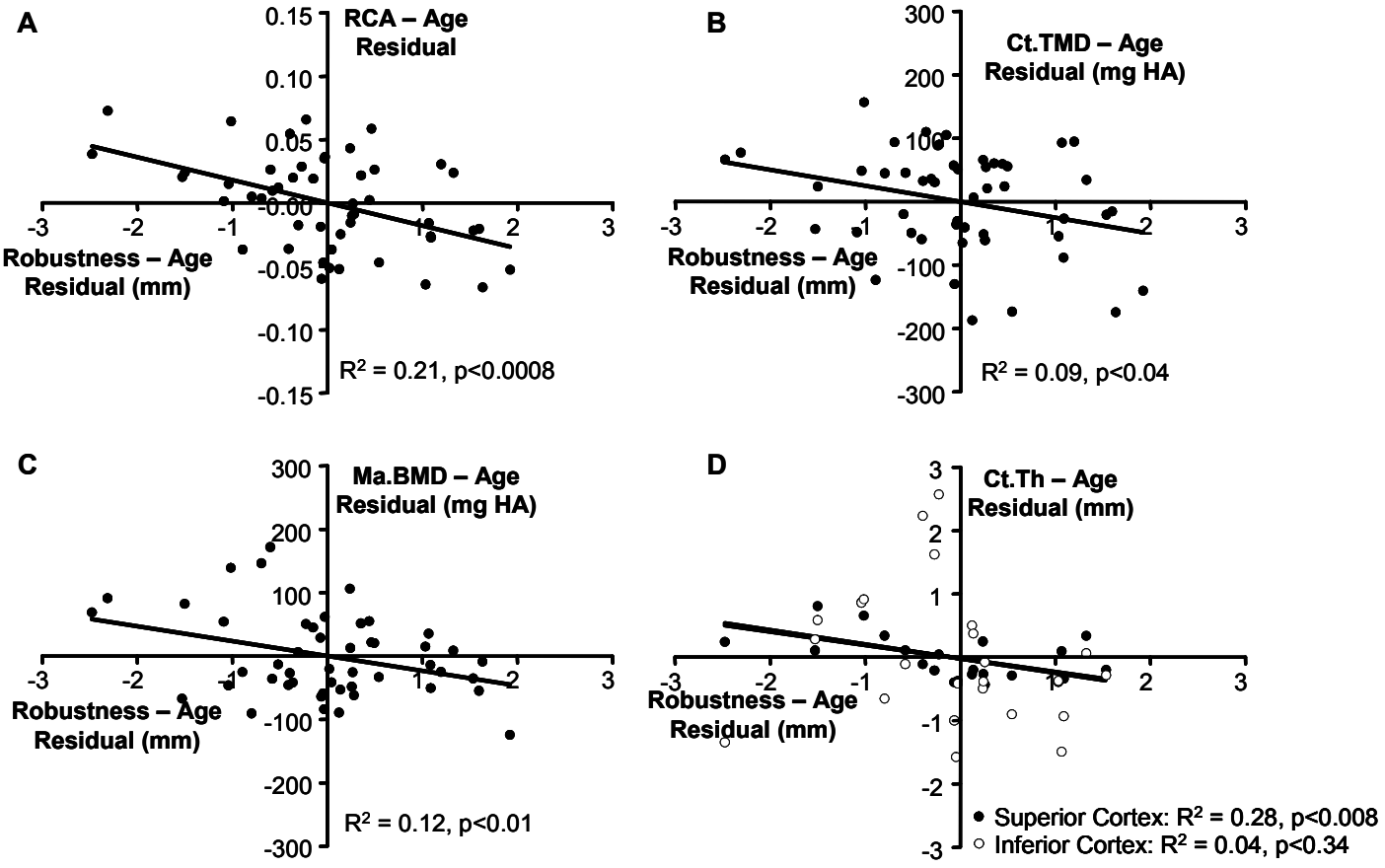

Figure 4. A validation study confirmed that **A)** Ct.TMD measured by pQCT correlated significantly with Ct.TMD measured by microCT, **B)** Ma.BMD measured by pQCT correlated significantly with Tb.TMD measured by microCT, and **C)** the overall TMD (cortical + trabecular) correlated significantly with ash content.

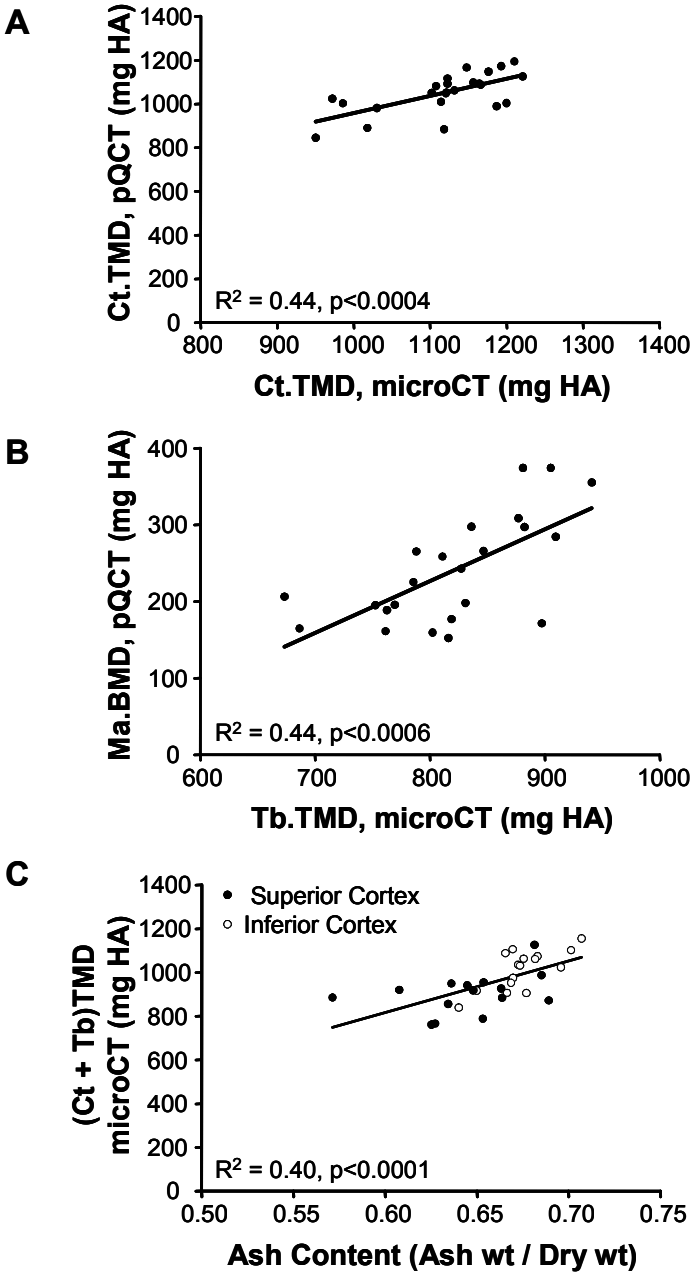

Figure 5. The results of the Path Analysis show a significant goodness of fit for the hypothesized interactions among cortical and trabecular traits (morphological as well as tissue-quality).

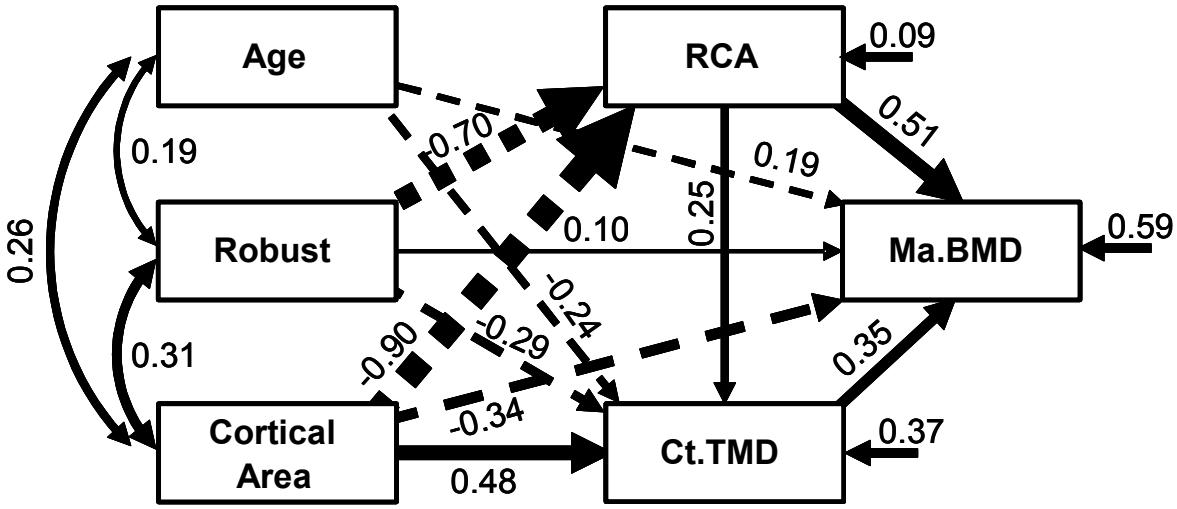

Goodness of Fit Criteria: Chi Sq=0.90, p<0.34; RMSEA=0.000

Reduced Form Structural Equations

RCA = 0.0 Age – 0.70 Robust + 0.90 CtAr (R^2=0.91)

CtTMD = -0.24 Age – 0.47 Robust + 0.71 CtAr (R^2=0.62)

MaBMD = -0.28 Age – 0.43 Robust + 0.37 CtAr (R^2=0.32)

Figure 6. Age-related changes in **A)** Ct.Ar of the shell, **C)** Ct.TMD, and **E)** Ma.BMD are shown for the entire population. These same regressions were segregated for robust and slender tertiles and are shown in **B, D,** and **F** for comparison. Segregating based on robustness tertile showed significant differences in the regressions for Ct.Ar and Ct.TMD versus age.

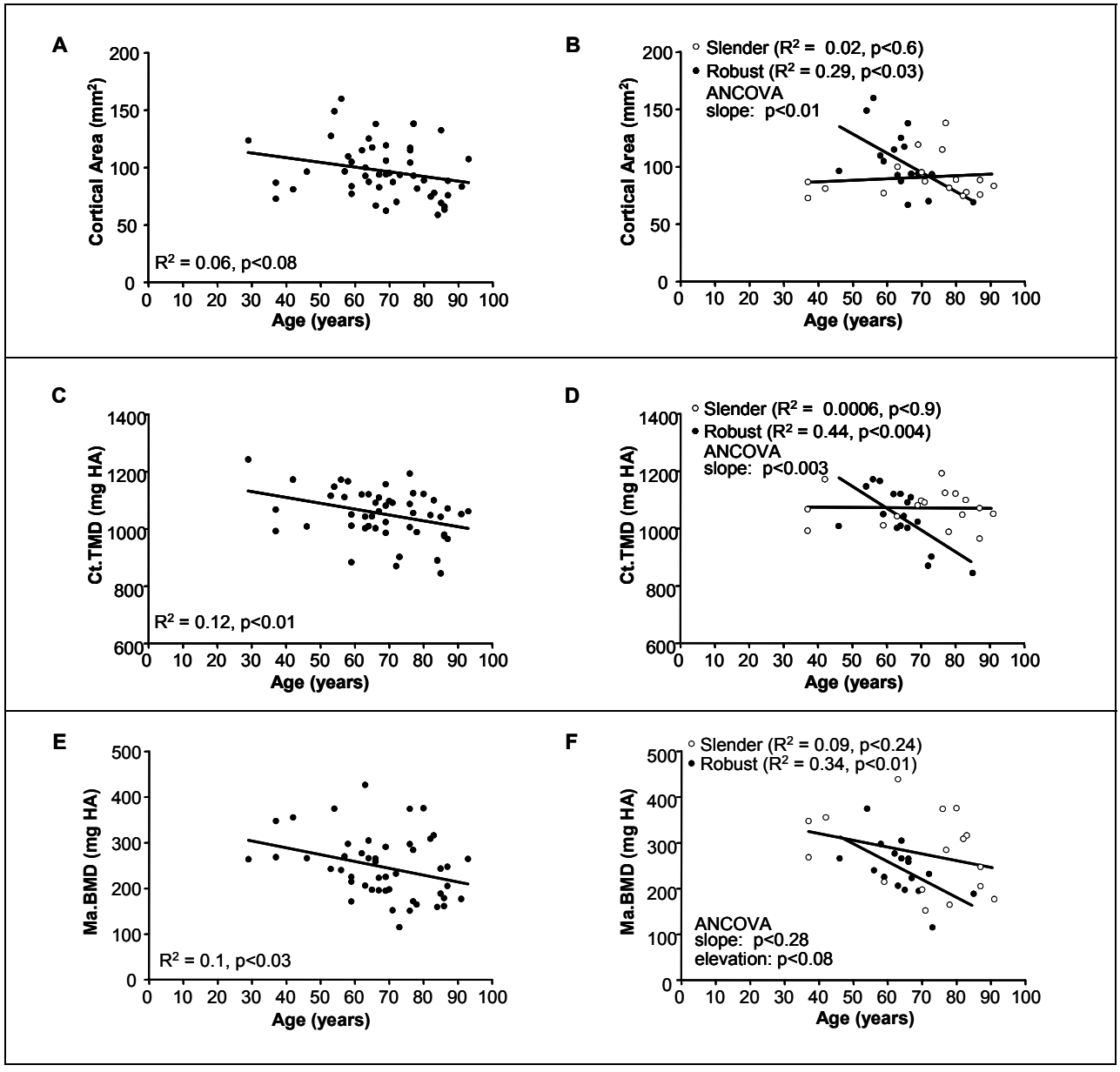

Figure 7. Age-changes in **A)** stiffness and **C)** maximum load measured in a fall to the side direction are shown for the entire cohort. The robust tertile showed a greater loss in **B)** stiffness and **D)** maximum load compared to slender. However, these regression were not significantly different.

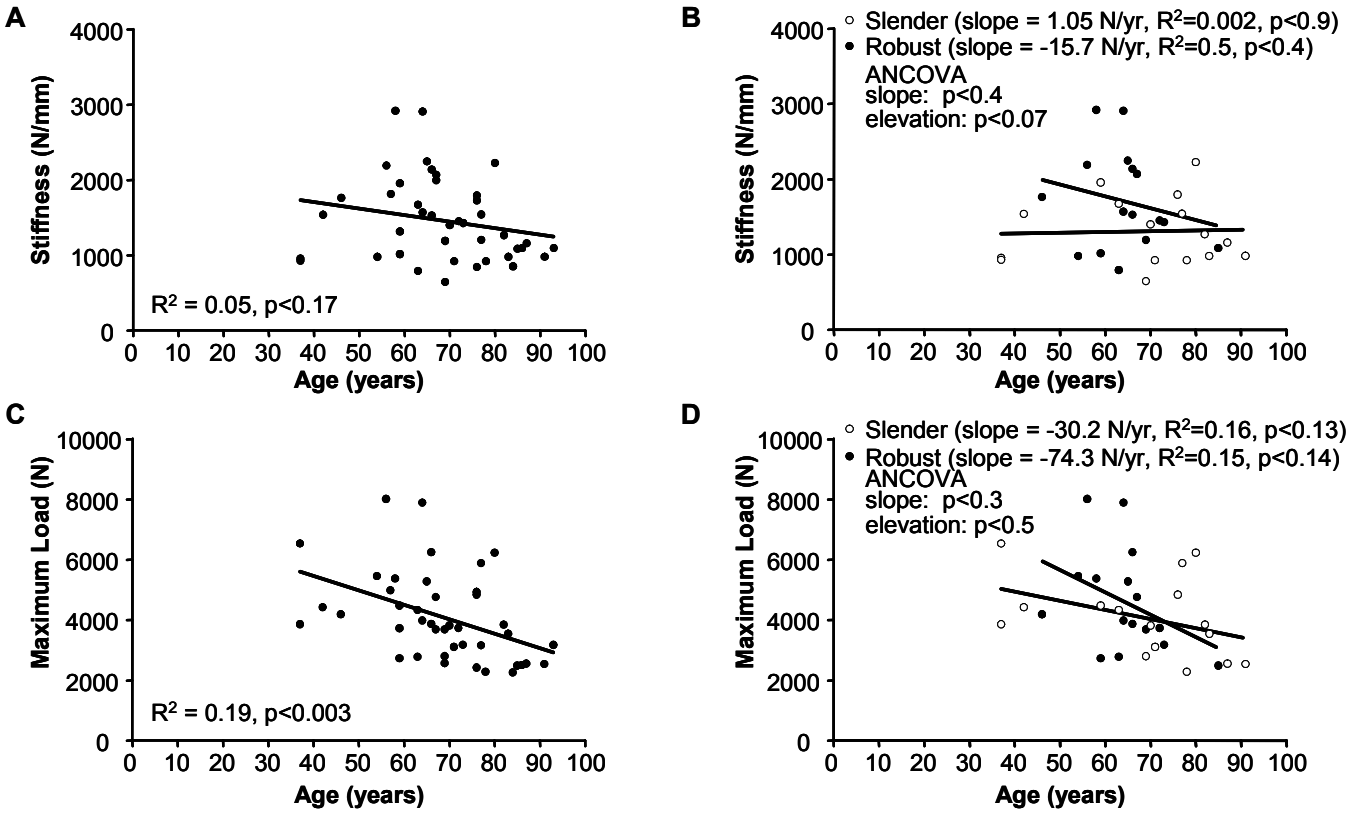

Appendix 2

Jepsen KJ, Centi A, Duarte GF, Galloway K, Goldman H, Hampson N, Lappe JM, Cullen DM, Greeves J, Izard R, Nindl BC, Kraemer WJ, Negus CH, Evans RK. Biological constraints that limit compensation of a common skeletal trait variant lead to inequivalence of tibial function among healthy young adults. *J Bone Miner Res,* in press, 2011

JBMR497

ORIGINAL ARTICLE

JBMR

Biological Constraints That Limit Compensation of a Common Skeletal Trait Variant Lead to Inequivalence of Tibial Function Among Healthy Young Adults

Karl J Jepsen,[1] Amanda Centi,[2] G Felipe Duarte,[1] Kathleen Galloway,[3] Haviva Goldman,[4] Naomi Hampson,[4] Joan M Lappe,[5] Diane M Cullen,[5] Julie Greeves,[6] Rachel Izard,[6] Bradley C Nindl,[2] William J Kraemer,[7] Charles H Negus,[8] and Rachel K Evans[2]

[1]Mount Sinai School of Medicine, NY, New York, USA
[2]U.S. Army Research Institute of Environmental Medicine, Natick, MA, USA
[3]Belmont University, Nashville, TN, USA
[4]Drexel University, Philadelphia, PA, USA
[5]Creighton University, Omaha, NE, USA
[6]HQ Army Recruiting and Training Division, Trenchard Lines, Upavon, UK
[7]University of Connecticut, Storrs, CT, USA
[8]L-3 Jaycor, San Diego, CA, USA

ABSTRACT

Having a better understanding of how complex systems like bone compensate for the natural variation in bone width to establish mechanical function will benefit efforts to identify traits contributing to fracture risk. Using a collection of pQCT images of the tibial diaphysis from 696 young adult women and men, we tested the hypothesis that bone cells cannot surmount the nonlinear relationship between bone width and whole bone stiffness to establish functional equivalence across a healthy population. Intrinsic cellular constraints limited the degree of compensation, leading to functional inequivalence relative to robustness with slender tibias being as much as two to three times less stiff relative to body size compared with robust tibias. Using path analysis, we identified a network of compensatory trait interactions that explained 79% of the variation in whole-bone bending stiffness. Although slender tibias had significantly less cortical area relative to body size compared with robust tibias, it was the limited range in tissue modulus that was largely responsible for the functional inequivalence. Bone cells coordinately modulated mineralization as well as the cortical porosity associated with internal BMU-based remodeling to adjust tissue modulus to compensate for robustness. Although anecdotal evidence suggests that functional inequivalence is tolerated under normal loading conditions, our concern is that the functional deficit of slender tibias may contribute to fracture susceptibility under extreme loading conditions, such as intense exercise during military training or falls in the elderly. Thus, we show the natural variation in bone robustness was associated with predictable functional deficits that were attributable to cellular constraints limiting the amount of compensation permissible in human long bone. Whether these cellular constraints can be circumvented prophylactically to better equilibrate function among individuals remains to be determined. © 2011 American Society for Bone and Mineral Research.

KEY WORDS: xxxx

Introduction

Physiological systems, like bone, tolerate many genetic and environmental factors by adjusting traits in a highly coordinated, compensatory manner to establish organ-level function. This ubiquitous process is critical for population-wide fitness and occurs at all levels of biological organization,[1–3] including interactions among systems.[4] Trait variants that are commonly expressed in a population are expected to be adequately compensated to have survived the pressures of natural selection.[5] However, the amount of variation in system function tolerated by a population is not fully understood.[6] For most systems, individual traits are nonlinearly related to organ-level function, and intrinsic

Received in original form June 6, 2011; revised form August 4, 2011; accepted August 18, 2011. Published online xxxx xx, 2011.
Address correspondence to: Karl J Jepsen, PhD, Leni and Peter W. May Department of Orthopaedics, Mount Sinai School of Medicine, Box 1188, One Gustave Levy Place, New York, NY, 10029, USA. E-mail: karl.jepsen1@gmail.com

Journal of Bone and Mineral Research, Vol. 9999, No. 9999, Month xxxx, pp 1–14
DOI: 10.1002/jbmr.497

boundaries on cellular activity could limit the degree to which adaptive processes can adjust traits, resulting in functional disparity or inequivalence among individuals. Functional inequivalence associated with a common trait variant could be a public health concern if system performance is limited and susceptibility to common diseases is increased for a predictable segment of the population.

We studied how biological constraints that limit compensation of a common skeletal trait variant lead to functional inequivalence among healthy, young adults. To be functional, bones must be sufficiently stiff and strong to support the loads incurred during daily activities. The adaptive process that adjusts traits to match bone stiffness with these loads occurs primarily during growth[7] with continued modifications throughout life.[8] This process is well understood for the population-average bone. However, two people with similar body sizes can acquire widely varying bone sizes, ranging from slender (narrow relative to length) to robust (wide relative to length) (Fig. 1). Bone robustness is a common, heritable[9] morphological variant established by approximately 2 years of age.[10] Because bone stiffness is proportional to the fourth power of width, small variations in width must be compensated by large, coordinated changes in other traits[11,12] to maximize stiffness while minimizing mass,[13] otherwise slender bones would be weak and prone to fracturing, whereas robust bones would be bulky and metabolically expensive to maintain and move through space. Slender bones are generally assumed to be less strong than robust bones,[14,15] but just how much variation in function is tolerated among healthy individuals and whether this variation stems from limited functional compensation are not known. We hypothesized that the nonlinear relationship between bone width and whole bone stiffness is too severe for bone cells to compensate slender and robust bones equivalently. Our goals were to determine if adaptive processes establish a uniform level of skeletal function across a healthy population and to identify biological constraints that limit the ability of the skeletal system to fully compensate the normal range in robustness.

Methods

Study participants

A total of 730 women (20.8 ± 3.1 years old) and men (21.4 ± 3.4 years old) from the United States and the United Kingdom volunteered to participate in this study, all with informed consent. The average BMI for those with recorded height was $23.4 \pm 2.9\ kg/m^2$ for women and $23.7 \pm 2.8\ kg/m^2$ for men. For the US cohort, 347 individuals (321 women, 26 men) were enrolled through the Naval Station Great Lakes (Great Lakes, Illinois, USA), the Physical Therapy Department at Oakland University (Rochester, Michigan, USA), and the University of Connecticut (Storrs, Connecticut, USA). Individuals were not quantitatively assessed for the amount of physical activity before enrolling in military training. Individuals recruited into the US cohort were healthy and had no prior participation in organized sports. For the UK cohort, 383 individuals were recruited through the Army Training Centre in Pirbright[Q6], England (148 women, 100 men) and the Infantry Training Centre in Catterick[Q7], England (135 men). The UK cohort was purely voluntary and did not exclude anyone based on prior training or participation in sports. All individuals passed rigorous medical entry assessments.

The primary criteria for excluding individuals from the study was image quality. A few individuals moved during pQCT scanning, resulting in tibial cross-sections with small streaks in the image. Each image was scored for image quality by one individual (CN)[Q8] before quantifying cross-sectional morphology. Those with motion artifacts near the region of interest were

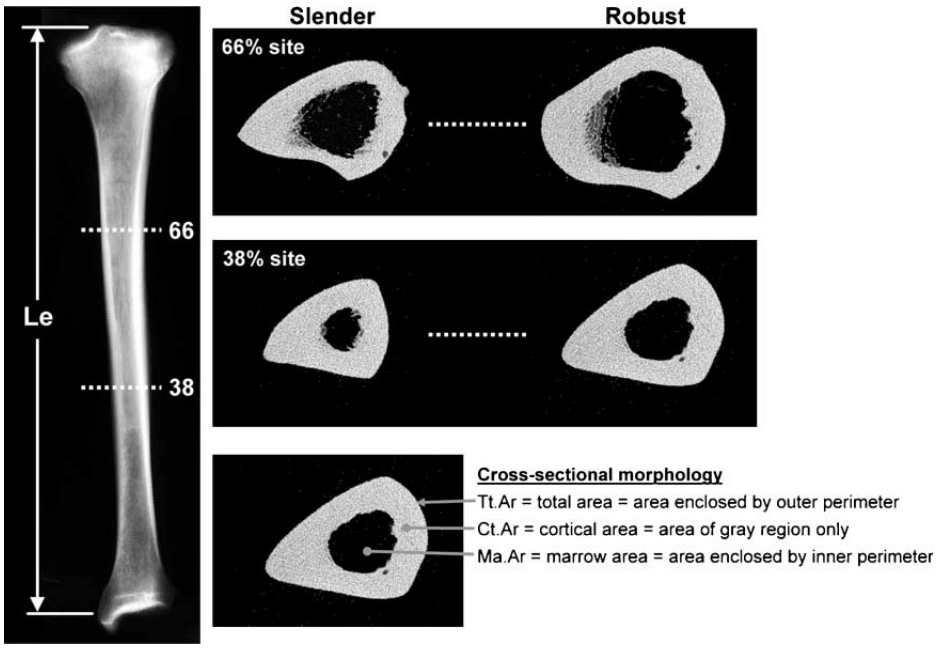

Fig. 1. Representative pQCT images of slender and robust tibial cross-sections taken at the 38% and 66% anatomical sites. Measures of morphology are shown for clarification.

removed from the analysis. In addition, data for one woman from the US cohort with unusually robust bones (> 5 standard deviations from the mean) were excluded, because her traits generated excessively large residuals that affected most regression analyses. Of the total number of individuals enrolled, 696 individuals (442 women, 254 men) had valid information regarding anthropometric and morphological traits that were absent of motion artifacts from which functional equivalence was tested. Individuals were from various racial and ethnic backgrounds, but were primarily white. All data sets were combined and segregated by sex only.

Bone morphology and tissue-mineral density

Morphological traits were quantified for tibial diaphyses using peripheral quantitative computed tomography, pQCT (XCT 2000 or 3000; Stratec Medizintechnik, Pforzheim, Germany), as described ~~above~~[Q9] [16] Although the systems were not cross-calibrated, the US and UK pQCT instruments were made by Stratec, and both were calibrated by the manufacturer and used similar manufacturer-provided calibration quality-assurance (QA) devices. Consequently, differences in instruments were corrected by converting attenuation to pQCT density using a common calibration device. A QA scan was conducted at least once every 24 hours to test for drift in the system calibration. The difference in measured and calibrated density values were less than 1%, ensuring that the system calibration did not drift over time and allowing us to compare data derived from the two systems. The XCT 2000 and 3000 were shown by others to generate equivalent trait values (total cross-sectional area, cortical area, cortical density) at multiple locations along the tibia, including the 8%, 50%, and 66% sites.[17] Tibial length (Le) was measured from the distal aspect of the medial malleolus to the proximal medial joint line. This measurement requires palpation of the skin to locate the bony landmarks, and the errors associated with this measurement could be on the order of a few millimeters. This measurement error, because it is only 1% to 2% of tibial length, had a minimal effect on the calculation of robustness. Further, a validation study using cadaveric tibias compared traits measured for three adjacent images (2.5 mm apart) at the 38% and 66% sites. Traits like Ct.Ar, Ct.TMD, and Ct.Th varied between 0.3% to 2.6% across the images, indicating that bone traits were not sensitive to small positioning errors.

The non-dominant leg of each volunteer was positioned in the gantry of the pQCT system and the distal tibial end plate was identified during a scout scan. Axial scans (0.4 or 0.5 mm pixel size) were acquired at sites located 38% and 66% proximal to the distal endplate. Grayscale values were converted to cortical tissue mineral density (Ct.TMD) for each cross-section using calibration constants. Cross-sectional morphology and Ct.TMD were quantified using Matlab software (MathWorks, Natick, MA, USA), as described above.[16] Images were rotated to standardize image orientation and thresholded to delineate bone voxels (800–1500 mg/cc) from nonbone voxels. Morphological traits included the total cross-sectional area (Tt.Ar), cortical area (Ct.Ar), and the area moments of inertia about the anteroposterior (I_{AP}) and mediolateral axes (I_{ML}). Robustness was calculated as Tt.Ar/Le to reflect the biological relationship between the growth in width, which increases by area, and the growth in length. The same individual (CN)[Q10] conducted all morphological analyses using BAMpack (Bone Alignment and Measurement package) software. Some of the data were reported ~~above~~.[18]

Functional equivalence

To test for functional equivalence, we determined whether the relationship between whole-bone bending stiffness and the applied loads ~~depend~~ on robustness. Whole bone stiffness and the applied loads are not directly measurable, but can be estimated from pQCT images and anthropometric traits, respectively. The loads applied to the tibia were calculated as the product of a force (body weight) and the distance about which the force acts (bone length).[7,19] By engineering convention, whole bone stiffness was calculated as the product of tissue modulus (E) and the cross-sectional area moment of inertia (I). The bending stiffness in the posteroanterior (P-A) direction was used in the functional equivalence analysis, given that tibias are loaded predominantly in this direction during ambulation.[20] Whole bone stiffness (EI) was calculated from the pQCT images by converting Ct.TMD to E based on a validation study described below[Q11] and then multiplying E by I_{ML}, which is the rectangular moment of inertia about the mediolateral axis. The product EI was adjusted using the linear regression derived from the validation study (see below) that compared EI estimated from pQCT with EI measured by subjecting cadaveric tibias to conventional bending tests. To test for functional equivalence, we regressed bending stiffness, EI, against robustness after accounting for body size (BW-Le) effects by partial regression analysis. The slope of the partial regression should not be significantly different from zero if slender and robust tibias exhibit the same stiffness relative to applied loads (ie, functional equivalence).

Biological constraints limiting compensation

To identify biological constraints limiting the degree of compensation permissible in human long bone, we first determined whether individuals in our study population used a similar strategy to compensate for a common, heritable trait like robustness. In general, bone cells are expected to coordinate traits in a nonrandom manner to establish function for any given person. If all individuals were to use a similar biological strategy to compensate for robustness, then functionally related traits would correlate across a population and, because many traits are involved, these correlations would resemble a network of trait interactions.[2,21,22] Prior work identified important interactions among robustness, relative cortical area (cortical area/total area), and tissue-stiffness for a small cohort of cadaveric tibias.[22] Path Analysis was conducted to test whether our large study population exhibited a common pattern in the way traits covary and to identify the relative contribution of each trait to whole bone stiffness. A path model was constructed by specifying the directed paths among select bone traits. As in prior work, we postulated that relationships occur in a particular order, such that slender bones (Tt.Ar/Le) are compensated by greater tissue-modulus (E) and a proportionally greater relative cortical area (RCA = Ct.Ar/Tt.Ar), whereas robust bones are compensated by reduced E and reduced RCA. We arranged the traits and specified

the direction of the arrows (interactions) among traits to provide a test of the compensatory interactions among traits and to determine how these traits together define the inter-individual variation in whole-bone stiffness. The primary difference from prior Path Models is that we allow the amount of bone (Ct.Ar) to vary independently of robustness. This was based on work in mouse bone showing that Ct.Ar and robustness are regulated by independent genes.[23] We found this model was sufficiently general to accommodate dimorphic growth patterns, allowing us to combine data for men and women. Path coefficients, which represent the magnitude of the direct and indirect relationships among traits, were calculated using standardized (Z-transformed) data (LISREL v.8.8; Scientific Software International, Lincolnwood, IL, USA). Structural equations were constructed using the path coefficients to specify the interconnected relationships. For traits with both direct and indirect paths, the structural equations were rederived in terms of the independent traits (BW-Le, robustness, cortical area). These are reported as the reduced form equations. Observed and model-implied covariance matrices were compared using maximum likelihood estimation. Chi-squared values with an associated p-value greater than 0.05 indicate the model adequately fits the data. The root mean square error of approximation (RMSEA), which is a measure of fit that is adjusted for population size and takes the number of degrees of freedom of the model into consideration, was also reported as an additional fit index. For RMSEA, the p-value represents the significance of fit with $p < 0.05$ indicating a close fit.[24]

Validation studies

Several validation studies were conducted using cadaveric tibias to confirm that whole-bone bending stiffness (EI) could be accurately estimated from pQCT images. This involved relating cortical tissue-mineral density derived from pQCT with matrix composition (mineralization), porosity, and tissue modulus, and then correlating EI derived from pQCT with EI measured directly after loading human tibias in four-point bending.

1. Correlating cortical tissue mineral density with ash content and porosity

The inter-individual variation in Ct.TMD measured using pQCT could result in part from differences in matrix mineralization and/or porosity, both of which are important determinants of tissue modulus.[25] We assessed this relationship by correlating Ct.TMD with ash content and porosity using a set of unfixed, cadaveric tibias ($n = 13$; 8 male, 5 female; age range = 17 to 54 years). Cross-sectional morphology and Ct.TMD were quantified at sites located 25%, 38%, 50%, 66%, and 75% proximal to the distal end-plates for the cadaveric tibias using the same pQCT protocols described above. The tibias were then sectioned (2.5 mm thickness) at each of the five anatomical sites using a diamond-coated band saw (Exakt Technologies, Inc; Oklahoma City, OK, USA). The ash content (ash weight/hydrated weight) for each cross-section was measured according to previously published protocols.[22]

To account for the effects of porosity on Ct.TMD, a second 2.5-mm-thick cross-section was obtained at the 38% and 66% sites adjacent to the ones used for ashing for 10 of the 13 tibias (six male, four female, age 37 +/− 8 years). Each cross-section was sectioned radially into six wedges, imaged using a Skyscan 1172 μCT (Skyscan, Kontich, Belgium) with a 1-mm-thick aluminum filter, and reconstructed at a 5-μm voxel size. This procedure captured vascular spaces (including primary vascular canals, Haversian canals, Volkmann's canals, and resorption bays), while excluding osteocyte lacunae. Noise was reduced by applying a 1-pixel median filter to the image stack using ImageJ, followed by a series of despeckling and morphological processing steps (opening) using the manufacturer's software. These procedures were standardized for all blocks; however, an additional processing step was added to some samples if visual inspection showed lingering noise. A region of interest (ROI) was manually selected to exclude cancellous bone (defined visually as regions with greater than ~50% porosity). The final ROI was shrink-wrapped to the very edge of the bone, and then eroded by 2 pixels to remove edge artifacts. Total tissue volume (Tt.V), total canal volume (Tt.Ca.V), and average 2-D pore number (Ct.Po.N) were measured. Porosity (Ct.Po, %) was calculated as canal volume normalized by total tissue-volume, and pore density (Ct.Po.Dn, 1/mm^2) was calculated as Ct.Po.N normalized by cross-sectional area. Data from each of the six wedges were combined to generate an average Ct.Po and Ct.Po.Dn for each cross-section.

2. Estimating tissue modulus from cortical tissue mineral density

To verify that [[[[Ok E?]]]]tissue modulus, E, can be accurately calculated from Ct.TMD measured using pQCT, we conducted traditional materials tests on bone samples machined from the intervening segments of the tibial diaphyses used to assess ash content and porosity. Diaphyseal segments greater than 40 mm in length were sectioned into regular prismatic beams using a diamond-coated wafering saw. Cortical bone samples ($n = 42$) from 9 cadaveric tibias were loaded to failure in four-point bending at 0.05 mm/s using a servohydraulic materials testing system (Instron model 8872, Instron Corp., Canton, MA, USA), as described[11] Tissue modulus was calculated from a linear regression of the initial portion of the stress-strain curve. For each bone sample, Ct.TMD assessed by pQCT was determined on a regional basis corresponding to the location of the machined bone sample. Linear regression analysis was conducted between tissue modulus and Ct.TMD to calculate the slope and y-intercept. Because tissue modulus and the associated Ct.TMD were measured in a site-specific manner rather than averaged over the entire cross-section (as is done for the study population), we used the maximum slope and y-intercept of the 95% confidence interval to convert Ct.TMD to E. We found this method was necessary to ensure that estimating E from Ct.TMD captured the full range in tissue modulus across the live human cohort. This relationship was confirmed by comparing the regressions of E (determined by pQCT) versus robustness for the live human cohort with the regression of E (determined by conventional four-point bending tests) versus robustness for the cadaveric samples. Slopes and y-intercepts were compared by ANCOVA.

3. Estimating whole-bone bending stiffness (EI) from pQCT data

To verify that EI calculated from pQCT accurately estimated whole-bone bending stiffness, intact tibias ($n = 13$), which were contralateral to those used for ashing and porosity, were subjected to whole bone four-point bending tests. The cadaveric tibias were imaged before mechanical testing using the same protocols described above, and EI was measured at 25%, 38%, 50%, 66%, and 75% sites proximal to the distal end-plate by calculating E from Ct.TMD and quantifying I_{ML} and I_{AP} from the cross-sectional images. To minimize rotation of the tibias during testing, the proximal and distal metaphyses were embedded in square aluminum channels filled with Bondo (3M; Maplewood, MN, USA). Parallel guides were used to ensure the proximal and distal aluminum pots were aligned relative to each other. Once the Bondo cured, the aluminum channels were removed and the tibias were placed in a four-point bending apparatus that was customized to include two parallel aluminum guides, similar to those used for embedding. The guides, which prevented rotation of the tibias during testing, were covered with Teflon tape to minimize frictional loads being applied to the metaphyses during the bending tests.

Tibias were loaded to preyield load-levels at 0.1 mm/s in the anteroposterior (AP), posteroanterior (PA), mediolateral (ML), and lateromedial (LM) directions to obtain stiffness values for each anatomical axis. Tibias were then loaded to failure in the LM direction at 0.1 mm/s. Difficulties in loading one sample in the LM direction resulted in poor estimates of whole bone stiffness. The LM stiffness value for this sample was excluded from the analysis.

All tests were conducted using a servohydraulic materials testing system (Instron model 8872, Instron Corp., Canton, MA, USA). The distance between the lower two supports (L) was adjusted for each tibia so the supports contacted the bone at the 25% and 75% anatomical sites. The upper-two loading points were placed at one-third and two-thirds of the lower-support span length. Load-deflection graphs were analyzed for stiffness, failure load, postyield deflection, and work-to-fracture. Deflection was corrected for system compliance. A validation study confirmed this loading procedure estimated the modulus of steel and aluminum bars to within 1% of textbook values. The bending stiffness (EI) of each tibia was calculated by correcting load and deflection for the geometry of the loading setup according to the following equation:

$$EI = (P/y)(a^3/3 - a^2L/4),$$

where, P/y = stiffness from the load-deflection curve, L = span length of the lower two supports, a = span of the upper loading points = one-third L. Linear regression analysis and the Bland Altman analysis were used to determine whether EI estimated from pQCT from one of the five anatomical sites accurately predicted whole-bone bending stiffness measured directly from four-point bending tests. Our goal was to identify an anatomical site from which the linear regression between EI derived from pQCT images and EI measured from four-point bending had a high R^2-value, was significant, and had a slope close to 1. Further, this site also had to have a Bland Altman plot with a low bias regarding whether EI estimated from pQCT predicted bending stiffness consistently across all stiffness values.

Results

Validation studies

Because whole-bone bending stiffness depends on both morphology and tissue-quality, a validation study was conducted using cadaveric tibias to determine how Ct.TMD determined by pQCT relates to matrix mineralization and porosity, both of which affect X-ray attenuation and define tissue modulus. A linear regression analysis revealed that none of the traits of interest (robustness, Tt.Ar, Ct.Ar, Ma.Ar, Ct.TMD, Le, J, E) changed significantly with age ($R^2 = 0.0 - 0.1$, p-value $= 0.1 - 0.9$), and this was true for the 25%, 38%, 50%, 66%, and 75% anatomical sites. Linear regression analysis showed that Ct.TMD correlated positively with ash content ($R^2 = 0.34$, $p < 0.007$) and negatively with porosity ($R^2 = 0.51$, $p < 0.0004$) and pore density ($R^2 = 0.35$, $p < 0.006$). Pore density correlated significantly with porosity ($R^2 = 0.40$, $p < 0.003$), as expected. Multiple linear regression analysis showed that 63% of the variation in Ct.TMD was explained by ash content, porosity, and pore density (Table 1). Tissue modulus determined by conventional four-point bending tests correlated positively with Ct.TMD ($R^2 = 0.27$, $p < 0.0004$), as expected.

Further examination revealed significant negative correlations between robustness and Ct.TMD (Fig. 2*A*) and ash content (Fig. 2*B*), as expected. Surprisingly, a significant positive correlation was observed between porosity and robustness (Fig. 2*C*), which remained significant after accounting for age effects by partial regression analysis ($R^2 = 0.42$, $p < 0.04$). The slope of the tissue modulus versus robustness regression (Fig. 2*D*) was not significantly different between the live human cohort and the cadaveric data ($p < 0.84$, ANCOVA), confirming that our method of estimating E from Ct.TMD replicated the full range of variation in tissue modulus expected for the live human cohort. A small difference in the *y*-intercepts between regressions was expected because of differences in attenuation associated with imaging cadaveric tibias in water compared with acquiring images for tibias of living humans with surrounding muscle, fat, and skin.

Finally, the whole bone four-point bending tests showed that EI measured at the 38% site correlated best (ie, slope closest to 1) with bending stiffness measured in the PA and LM directions (Fig. 2*E*). This was confirmed by conducting a Bland Altman analysis, which compared the difference between EI measured

Table 1. Multiple Linear Regression Analysis

Equation	R^2 (adj)	p-value
Ct.TMD = 668 − 7.20%Porosity + 977%Ash Content	0.60	0.0001
Ct.TMD = 657 − 4.84%Porosity + 1046%Ash Content − 2.70 Ct.Po.N	0.63	0.0001

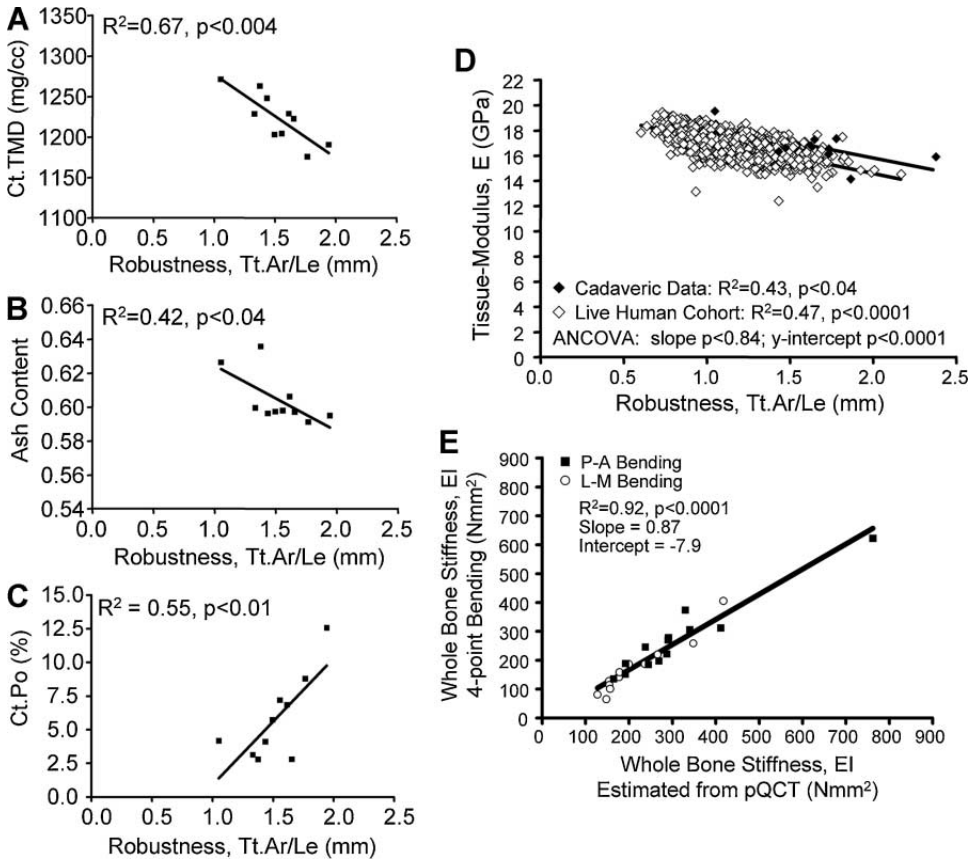

Fig. 2. (*A*) Ct.TMD, (*B*) ash content, and (*C*) porosity correlated significantly with tibial robustness measured at the 66% anatomical site. (*D*) Tissue modulus measured directly for the cadaveric tibias correlated negatively with robustness. The slope of this line was not significantly different from that of the entire live human cohort ($p < 0.84$, ANCOVA), where E was estimated from Ct.TMD measured by pQCT. (*E*) Bending stiffness (EI), estimated from pQCT images acquired at the 38% site, accurately predicted whole-bone bending stiffness of cadaveric tibias ($n = 13$) loaded to failure in conventional four-point bending tests in the posteroanterior (PA) and lateromedial (LM) directions. Tissue stiffness, E, was estimated from tissue-mineral density (Ct.TMD), and I was calculated about the PA and ML axes from the pQCT images.

directly by four-point bending to EI measured by pQCT at each of the five anatomical sites. The data points for the 25% and 38% sites were on average 0.3 SD away from the average of the two methods, whereas data for the 50%, 66%, and 75% sites were on average 1.0, 2.4, and 3.4 SDs, respectively, from the average of the two methods. The regression between the difference and the average showed that the 38% site had the lowest R^2-value ($p < 0.1$) and the p-value was not significant ($p < 0.11$). This regression was borderline significant for the 25% site (negative slope, $R^2 = 0.14$, $p < 0.06$) and highly significant (all positive slopes, $R^2 = 0.72$–0.92, all $p < 0.0001$) for the 50%, 66%, and 75% sites, indicating that stiffer bones were underestimated by pQCT data measured at the 25% site and overestimated by pQCT data measured at the 50%, 66%, and 75% sites. Thus, EI measured at the 38% site was the only site to show good agreement between methods and consistent predictability across all stiffness values. Thus, we show that EI calculated from pQCT images accurately estimated whole-bone bending stiffness.

Functional equivalence

Tibial robustness (total cross-sectional area/tibial length) was normally distributed ($p > 0.10$, Kolmogorov-Smirnov test) and varied ~2-fold among men and women (Fig. 3*A*). Further, robustness increased modestly with BW-Le (Fig. 3*B*), and significant differences in the y-intercept ($p < 0.0001$, ANCOVA) indicated the greater tibial robustness for men was independent of a measure of body size, consistent with sexually dimorphic growth patterns.

Whole bone stiffness increased with applied loads (Fig. 3*C*), and the R^2-values suggested our study population tolerated a modest degree of variation in bone stiffness. Because the slope of the regressions for EI versus robustness was significantly different between men and women ($p < 0.017$, ANCOVA), we tested for sex-specific effects by correcting EI for BW-Le by regression analysis. When men and women were compared at a common BW-Le (260.2 kg cm), male tibias were 40.9% stiffer relative to applied loads compared with female tibias ($p < 0.0001$, t-test). Importantly, bone stiffness correlated significantly with robustness for both sexes after accounting for BW-Le (Fig. 3*D*). Tibias that were slender relative to BW-Le were as much as two to three times less stiff relative to applied loads compared with robust tibias. This analysis confirmed that the variation in robustness was not fully compensated by the underlying biology, resulting in functional inequivalence among individuals, as hypothesized.

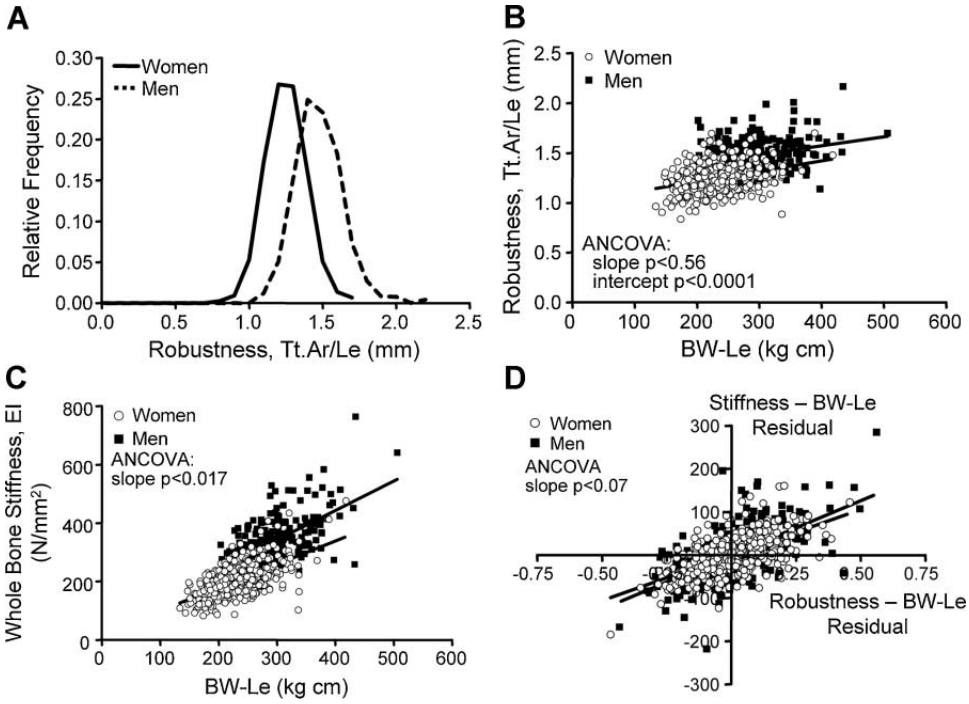

Fig. 3. Tibial robustness (Tt.Ar/Le) measured at the 66% anatomical site (*A*) varied widely among women (solid line) and men (dashed line), and (*B*) increased modestly with BW-Le for women ($R^2 = 0.10$) and men ($R^2 = 0.08$). Differences in the *y*-intercept (ANCOVA, $p < 0.0001$) indicated that men have more robust tibias relative to BW-Le compared with women. (*C*) Whole-bone bending stiffness (EI) increased significantly with BW-Le for women ($R^2 = 0.38$) and men ($R^2 = 0.38$). (*D*) Whole-bone bending stiffness correlated significantly with robustness for women ($R^2 = 0.40$) and men ($R^2 = 0.37$) after accounting for BW-Le by partial regression analysis. All linear regressions were significant at $p < 0.0001$.

Interactions among traits contributing to whole bone stiffness

Robustness, relative cortical area (cortical area/total area), and tissue-stiffness, which are functionally interacting traits shown previously to contribute to long bone function, exhibited a well-defined trajectory in a 3-D plot (Fig. 4*A, B*). Path Analysis was used to determine how this pattern of trait interactions contributed to the variation in whole bone stiffness. The significant goodness-of-fit criteria for the Path Model (chi-square

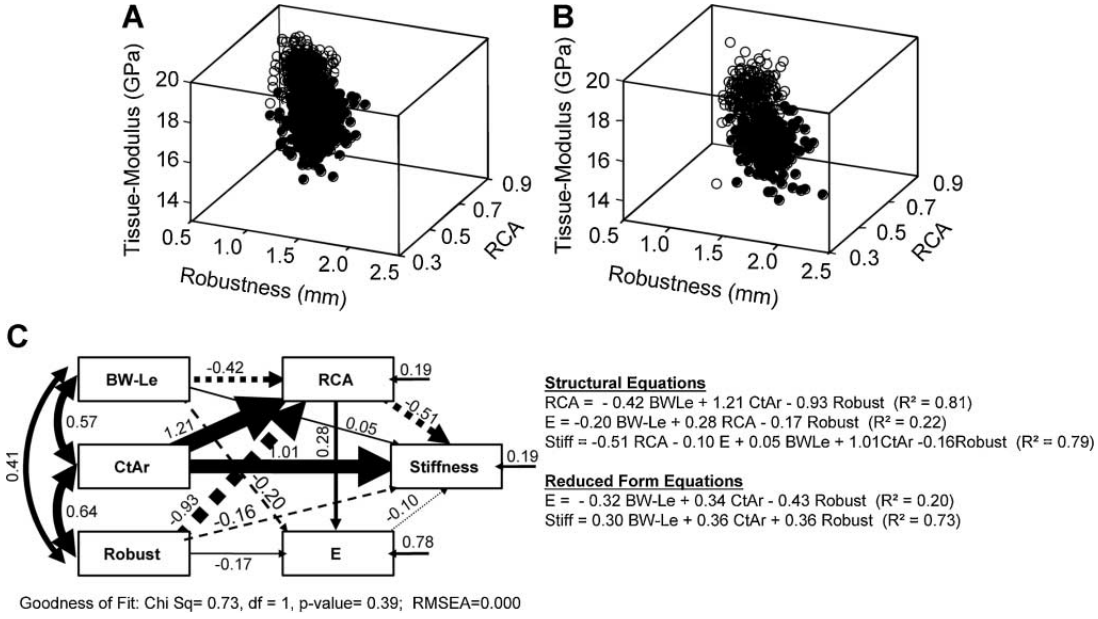

Fig. 4. An emergent trajectory was observed among robustness, tissue stiffness, and relative cortical area for (*A*) women and (*B*) men. Symbols: open circles = 38% anatomical site; filled circles = 66% anatomical site. (*C*) The path model, which included data for both men and women, showed significant goodness-of-fit criteria. The reduced structural equations revealed that 73% of the variation in whole bone stiffness was explained by BW-Le, robustness, and cortical area. Arrows: solid = positive association; dashed = negative association. Abbreviations: E = tissue-stiffness; Ct.Ar = cortical area; RCA = relative cortical area = Ct.Ar/Tt.Ar; Tt.Ar = total cross-sectional area.

test p-value = 0.39; RMSEA = 0.000) confirmed that traits covaried in a highly consistent manner among individuals (Fig. 4*C*). Similar networks were found when analyzing the male and female data separately (not shown). Some trait-trait interactions were expected based on mathematical associations (eg, the interactions among Ct.Ar, Robustness, and RCA), whereas other interactions were indicative of biological associations (eg, the interaction between RCA and E). Removing or reversing the arrow between RCA and E resulted in loss of goodness-of-fit for the model, suggesting the interaction between the amount of bone and tissue modulus is a critical component of the functional adaptation process. The network and the reduced structural equations indicated that individuals with slender bones relative to BW-Le acquired a proportionally greater relative cortical area and tissue modulus to establish stiffness, whereas individuals with robust bones established stiffness by acquiring a proportionally lower relative cortical area and tissue modulus. The reduced form equations showed that the network of trait interactions explained 73% of the variation in whole bone stiffness and that Ct.Ar and robustness had similar relative contributions to whole-bone bending stiffness.

Biological constraints limiting compensation

Because the Path Analysis indicated that individuals in our study population utilized a similar biological strategy to mechanically compensate robustness, we could identify common boundaries on cellular activity or "biological constraints" that limited the degree of compensation permissible in human long bone and that were responsible for the functional inequivalence. The two major compensatory traits contributing to function included the amount of bone (cortical area) and tissue modulus. Cortical area measured at the 38% (women $R^2 = 0.36$, men $R^2 = 0.38$) and 66% (women $R^2 = 0.25$, men $R^2 = 0.31$) anatomical sites correlated positively with BW-Le for both sexes ($p < 0.0001$ for all regressions). Men exhibited a significantly greater amount of bone (10% to 11%) compared with women across the full range in body size (ANCOVA, intercept $p < 0.0001$). After accounting for BW-Le, we found that cortical area correlated positively with robustness at both the 38% (Fig. 5*A*) and 66% sites (Fig. 5*B*), indicating that tibias that were slender relative to BW-Le were constructed with less bone tissue relative to BW-Le compared with robust tibias. To further compensate for robustness, osteoblasts and osteoclasts must also adjust tissue modulus. Both men and women showed significant negative correlations between tissue modulus and robustness (Fig. 5*C*), indicating that osteoblasts compensated slender tibias with greater tissue-modulus. We estimated the regression between tissue modulus and robustness required to equilibrate function among individuals by iteratively modifying the relationship between tissue modulus and Ct.TMD until the slope of the partial regression between EI and robustness was not significantly different from zero or the R^2 value was less than 0.01 (ie, satisfying the null hypothesis). The regressions required to establish functional equivalence for men and women are shown in Fig. 5*C*. These regressions do not represent biologically realistic outcomes, because they would result in excessively large tissue-modulus values for slender bones and extremely low tissue-modulus values for robust bones.

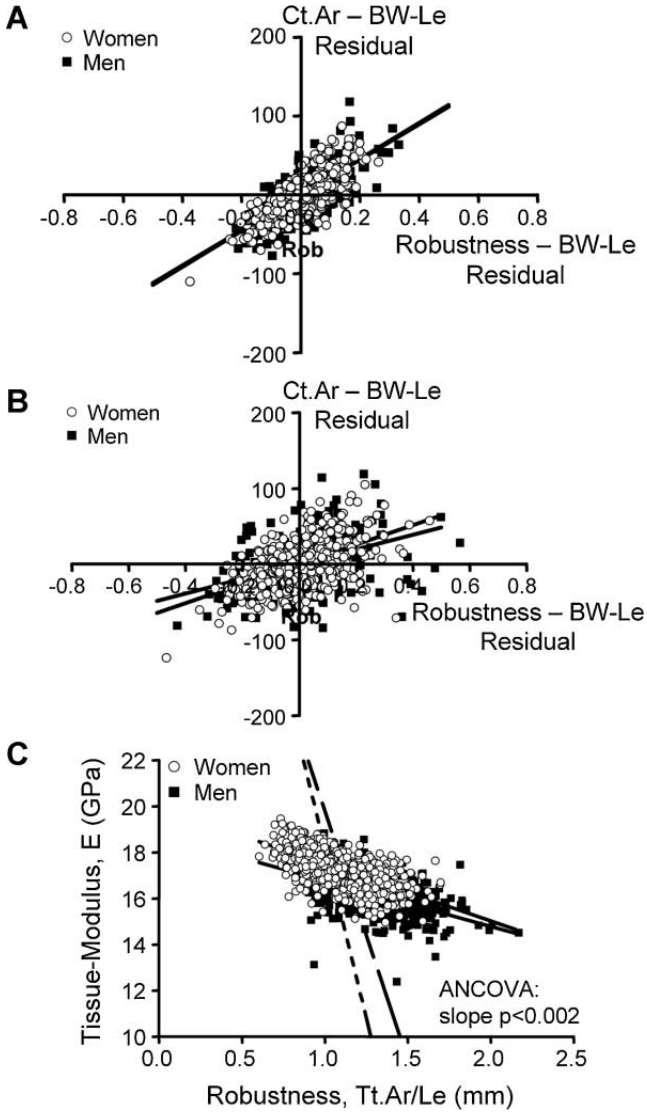

Fig. 5. Cortical area correlated positively with robustness for both the (*A*) 38% (women $R^2 = 0.58$, men $R^2 = 0.53$) and (*B*) 66% (women $R^2 = 0.29$, men $R^2 = 0.17$) anatomical sites, after accounting for BW-Le by partial regression analysis. All linear regressions were significant at $p < 0.0001$. (*C*) Tissue-modulus estimated from pQCT correlated negatively with robustness at the 38% and 66% sites for women ($R^2 = 0.42$) and men ($R^2 = 0.33$). The relationship between tissue modulus and robustness required to establish functional equivalence is shown for women (short-dashed line) and men (long-dashed line). All linear regressions were significant at $p < 0.0001$.

Discussion

Functional compensation is a biological process critical for system health and homeostasis, because it allows individuals to tolerate many genetic and environmental factors leading to variation in one trait through coordinated, compensatory changes in other traits. Approximately 70 years ago, Waddington proposed that functional compensation or

"buffering" suppresses phenotypic variation and establishes functional equivalence, or "constancy of the wild type," across a population.[5] However, we now know this concept cannot be generalized to all physiological systems, as inter-individual variation in lung size,[4,26] heart size,[27] and arterial morphology[28,29] are associated with disparity in system performance, overall fitness, and disease risk. The current results were consistent with these studies, showing that compensation of tibial robustness, a common, heritable morphological variant, was imperfect and led to functional inequivalence among nearly 700 young adult women and men, as hypothesized. In contrast to prior studies showing functional equivalence of mastication among different species of soricid shrews expressing variable mandibular morphologies,[30] herein we found functional inequivalence when studying the inter–individual variation in morphology of long bones within a single species.

The functional inequivalence was predictable based on robustness and the amount of disparity among individuals was substantial; tibias that were slender for BW–Le were as much as two to three times less stiff relative to BW–Le compared with tibias that were robust relative to BW–Le. The relationship between whole bone stiffness and the applied loads is important because it defines tissue–level strains, which are thought to drive functional adaptation. ([31] Although BW-[illegible] traditionally used as a measure of the loads applied to bone,[32] other aspects of activity (eg, type, intensity, duration, age of onset of training) that are thought to be involved in the functional adaptation process during growth are expected to vary among individuals. Whether activity levels during growth varied predictably with bone robustness for members of our study population and would explain a portion of the functional inequivalence observed here, however, remains unclear. Functional inequivalence relative to robustness means that bone cells could not adjust traits like cortical area and tissue-modulus to the degree needed to fully compensate the nonlinear relationship between bone width and whole-bone bending stiffness. The functional inequivalence reported in Fig. 3*D* was not limited to bending loads, but was also found when assuming tibias were loaded in compression (data not shown). Although long bones of modern populations are comparatively more slender and weaker than archaeological populations,[33,34] it is unclear if the degree of functional inequivalence has changed over time and whether modern diets and exercise habits contributed to the substantial disparity in function observed for the young adult population examined here. Further, the vast majority of individuals in our study population were white, and it remains to be determined if the degree of functional inequivalence varies with race or ethnic background. Future work could also include measuring the amount of subcortical bone and determining whether this compartment varies in a predictable way with robustness and may reduce some of the functional equivalence reported here.

The results provided important insight into the biological constraints that limited the degree of compensation. The disparity in cortical area relative to robustness (Fig. 5*A, B*) may affect measures like BMD, but would contribute only modestly to the functional inequivalence because further addition of mineralized tissue to the inner surface of slender tibias would have minimal mechanical benefits. The limited range in tissue modulus (range/average = 36.7%) did not fully compensate for the wide range in moment of inertia (279%) and thus was an important determinant of the functional inequivalence reported here (Fig. 5*C*). Limited compensation at this level of biological organization may be a public health concern, not only because it means a predictable segment of the population has a functional deficit, but also because it remains to be determined to what extent prophylactic treatments can circumvent these intrinsic cellular constraints to establish a higher degree of functional equivalence among individuals.

Our analysis indicated that bone cells adjusted tissue modulus to compensate for robustness, but only within a very narrow range compared with that observed for bones from different species with widely varying loading demands.[35] This constraint, however, may be advantageous, because extracellular matrix modifications that increase tissue modulus (eg, mineralization) generally occur at the expense of increased tissue brittleness. Slender tibias would be extremely brittle if mineralized to the degree needed to establish the same level of functionality as robust tibias (Fig. 5*C*). Thus, the skeletal system may have evolved to tolerate a modest degree of functional inequivalence relative to robustness, possibly to avoid developing an excessively fragile bone that is prone to fracturing under daily activities and that would decrease individual fitness and survival. This biomechanical trade-off may be an important factor defining the range in robustness values and the degree of functional inequivalence tolerated by a modern population.

The significant correlation between EI derived from pQCT and EI measured directly from four-point bending of cadaveric tibias (Fig. 2*E*) confirmed that we accurately estimated whole-bone bending stiffness for our study population. We used EI as the measure of bending stiffness, rather than the more commonly used strength-related parameters like bone mineral density (BMD), section modulus, the bone strength index (BSI), and the strength-strain index (SSI). BMD is useful clinically for diagnosing osteoporosis, but does not provide the details of structure and tissue quality required to assess functional inequivalence. Morphological indices like section modulus do not consider the variation in tissue quality, which we show in the current study and in prior work[11,12] is a critical component of the functional adaptation process. Both BSI and SSI incorporate Ct.TMD as a measure of tissue-quality. However, because small changes in bone density correspond to large changes in tissue modulus,[25] it was important to use EI as a measure of bending stiffness to test whether the variation in E was sufficiently large to compensate the variation in moment of inertia. We found that EI measured at the 38% site was an accurate predictor of whole-bone bending stiffness (Fig. 2*E*), which is consistent with prior work showing that tibial architecture at the 33% site was well adapted to anterior-posterior bending loads.[36] Although further work is needed to establish a standard conversion between Ct.TMD and E, our method replicated the range in E for the live human cohort and confirmed the relationship between robustness and E was accurately estimated from pQCT (Fig. 2*D*). The small difference in the *y*-intercept between the regressions for the cadaveric data and the live human cohort did not affect the outcome of our study, because the partial regression

analysis and the path analysis relied on the variation in E relative to robustness, not the magnitude of E.

Although functional inequivalence was observed for both sexes, we also found functional disparity between men and women (Fig. 3*C*), consistent with prior work.[36] The stiffness of tibias relative to BW-Le was 40.9% lower for women compared with men, indicating that the 14.8% reduction in robustness of female tibias was not compensated to the same degree as male tibias, despite a 7% greater tissue-modulus for female tibias (Fig. 5*C*; $p < 0.0001$, *t*-test). Consistent with the results of others,[37] our study found that women showed 10% to 11% less Ct.Ar relative to BW-Le compared with men, which contributed in part to the functional disparity between sexes. This disparity in tibial stiffness relative to body size may help explain why women sustain approximately five times more stress fractures than men during gender-integrated military training regimens,[7,38] and why fracture incidence is greater for elderly women compared with men.[39] Prior work by others showed that sex-differences in strength-related morphological parameters are not fully eliminated even after adjusting for body size.[37,40]

Anecdotally, young adult men and women expressing the full range in bone robustness successfully perform daily activities (eg, walk, run, stand), indicating that functional inequivalence is generally tolerated, probably because bone has large safety factors that minimize fracture risk under normal loading conditions.[41] However, our concern is that safety factors are often exceeded under extreme loading conditions, such as falls in the elderly and the intense, repetitive exercise combined with prolonged load carriage typical of military training. Young adults with reduced stiffness relative to body size have proportionally weaker bones that would be expected to experience greater tissue strains during intense exercise, increasing matrix damage and the probability of developing a stress fracture.[42] This functional inequivalence may help explain why having a slender tibia relative to body size is an important risk factor for stress fractures in military recruits[14,15] and athletes.[43] Although slender bones are generally assumed to be weaker than robust bones,[14,15] it was important to formally test this assumption in the context of the skeletal system's ability to compensate a common trait variant. Prior work did not consider the compensatory changes in morphology and tissue quality that accompany the natural variation in robustness. Functional inequivalence may also be problematic in the ever-growing elderly population, because it means individuals begin the aging process at different starting points. Individuals with slender bones relative to body size would be expected to reach a fracture-risk threshold earlier in life if they lose bone mass on a structure with a pre-existing functional deficit. To the extent that functional inequivalence in the tibial diaphysis extends to other skeletal sites, our results may help explain why bone slenderness is a consistent indicator of fracture risk in the elderly.[44,45] However, to generalize the results of this study to the hip, which shows a high incidence of age-related fragility fractures, would require testing how cortical and trabecular traits are adjusted to compensate for the natural variation in femoral neck width, whether proximal femora with slender and robust necks have the same strength during a fall to the side, and whether proximal femora with slender necks show the same age-related bone loss pattern as proximal femora with robust necks.

Our analysis also showed that nearly 700 young adult men and women with different genetic backgrounds and life histories exhibited highly significant functional trait interactions. The network of trait interactions shown in the path model (Fig. 4*C*) highlighted the biological complexity of a relatively simple, tubular system. Unlike multivariate approaches such as multiple regression or principal components analysis, which make no specific assumption about the underlying biology, we used path analysis to test whether traits that are functionally related during growth would show correlations among adult structures consistent with the idea that bone maximizes stiffness using minimum mass.[13] The network, which explained 79% of the variation in whole bone stiffness and was consistent with that reported for a small cadaveric cohort,[22] indicated that young adult men and women in our study population acquired highly predictable trait sets during growth and thus shared important aspects of a negative feedback control mechanism responsible for coordinating traits to establish function. In contrast to man-made systems, where highly variable morphologies and materials are combined to establish function, biological systems like bone work with limited resources and must adjust the amount, location, and organization of a narrow range of building blocks (eg, mineral, collagen, proteoglycan, water) to achieve the degree of variation in morphology and tissue quality required to establish function across a population. These cellular constraints, which were responsible for functional inequivalence, also appear to limit the number of possible functional trait sets that can be acquired during growth. That is, individuals with slender bones coordinated Ct.Ar and tissue modulus in fairly similar ways to establish function; likewise, the same can be said for individuals with robust bones. The limited range in functional trait sets acquired during growth explained why we saw a consistent pattern in the way traits covaried across a young adult population. Although the larger number of traits in corticocancellous structures increases the possibility that compensation of robustness can occur using a wider range of trait sets, relatively similar functional trait-interactions have been observed for the human femoral neck[46] and mouse vertebral body.[47]

The Path Model also showed that variation in compensatory traits were superimposed on the variation in robustness. This is an important outcome of this study and one worth illustrating to better convey the concept. Fig. 6 was constructed to illustrate how cortical area varied among individuals. A similar diagram could be constructed for tissue modulus. First, cortical area varied relative to robustness, with slender tibias having less Ct.Ar compared with robust tibias. Second, there was inter-individual variation in Ct.Ar for any given robustness value. This is important because it means that traits like Ct.Ar should be adjusted for body size and robustness to identify genetic factors, environmental factors, or both affecting the inter-individual variation in measures related to bone mass.[23] Although the path analysis revealed a highly predictable pattern for nearly 700 individuals, additional data from a more diverse population would be required to establish norms for these compensatory relationships. It is important to note that having slender bones does not

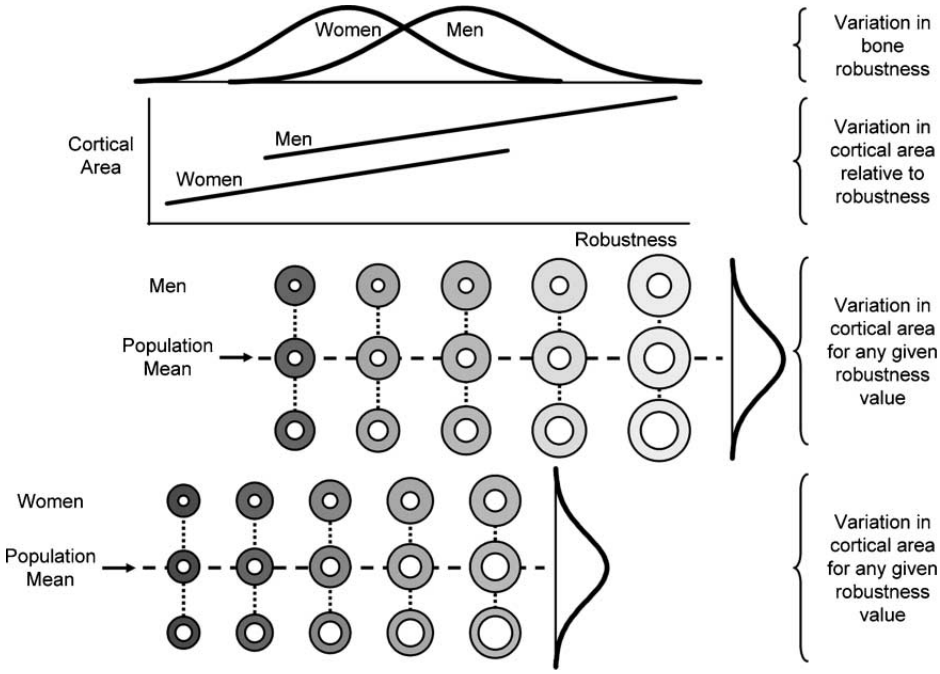

Fig. 6. A schematic diagram was constructed based on the results of the path model (Fig. 4*C*) and the association between Ct.Ar and robustness (Fig. 5*A, B*) to illustrate how variation in cortical area is superimposed on the variation in robustness. Tibial diaphyses are represented as idealized circular cross-sections, with gray values representing the variation in tissue modulus. With body size effects removed, cortical area varies with robustness, with slender tibia showing lower Ct.Ar than robust tibia. In addition, there is variation in Ct.Ar for any given robustness value. These relationships hold for men and women, despite sex-specific differences in robustness and Ct.Ar. Thus, the natural variation in robustness is associated with specific changes in cortical area and tissue-modulus that need to be considered when seeking genomic factors, and environmental factors, or both regulating bone function.

necessarily indicate a failure to adapt. Although periosteal expansion during early growth may be modified by extreme loading conditions,[48] it is unclear to what extent variation in the normal range of loading affects an individual's skeletal robustness. Based on our data, we would argue that genetic variants, environmental variants, or both that impair the functional adaptation process may affect robustness, but would primarily affect the compensatory traits that accompany robustness, that is, Ct.Ar and E. Thus, a poorly adapted bone, whether slender or robust, would have reduced Ct.Ar and reduced E compared with the population mean for that particular robustness value. Identifying individuals with poorly adapted bones would require establishing population norms for how traits covary relative to external size and then adjusting an individual's acquired trait set for their robustness.

Although the limited range in E was an important determinant of the functional inequivalence (Fig. 5*C*), the path model showed that E was not a major determinant of the inter-individual variation in whole-bone bending stiffness. This is probably because the variation in E at a single anatomical site is small compared with the variation in cortical area. Further, prior work in mouse bone showed that E covaries closely with periosteal expansion rate early in life.[49] Consequently, the contribution of E to the variation in whole bone stiffness may be masked in the multivariate model by its association with robustness. In contrast, Ct.Ar develops throughout growth and may be more susceptible to environmental perturbations, thereby showing greater inter-individual variation relative to robustness and making a dominant contribution to the variation in whole bone stiffness.[50,51]

The validation study provided important insight into the manner by which the skeletal system adjusts tissue quality to compensate for robustness. Variation in Ct.TMD depended on both mineralization and porosity, consistent with expectations of acquiring pQCT images with a 0.4- to 0.5-mm pixel size. Although 63% of the variation in Ct.TMD was explained by ash content, porosity, and pore density (Table 1), we suspect the 37% ~~of the~~ unexplained variance ~~in part could be because of~~ measurement error, particularly for ash content and Ct.TMD. Although these two particular traits vary predictably with bone size, they show little variation among individuals. Consequently, small measurement errors would contribute substantially to the unexplained variance. The unexplained variance could also be explained by properties that were not measured. In addition to ash content and porosity, X-ray attenuation could be affected by material heterogeneity, components of mineralization not accounted for by traditional ash content measures, and possibly the organic component of bone tissue. The negative correlations between robustness and Ct.TMD (Fig. 2*A,B*) and between robustness and E (Fig. 2*D*, 5*C*) are consistent with prior work.[11,12,22] A surprising outcome was finding that porosity was also highly significantly correlated with robustness (Fig. 2*C*). Unlike prior work,[22,52] we assessed porosity and robustness at the same anatomical site in the current study, enabling us to see a strong association between these two traits that remained significant after correcting for age. Thus, the higher tissue-modulus of slender bones resulted from increased mineralization and reduced porosity, whereas at the other extreme the reduced tissue-modulus of robust bones resulted from reduced mineralization and increased porosity. This suggested that bone cells

coordinately modulate both mineralization and porosity to regulate tissue modulus, thereby expanding the range of variation in E that can be achieved across a population beyond a strict dependence on varying matrix mineralization alone. Because tissue density correlated positively with ash content (not shown), modulating tissue quality by varying mineralization and porosity would have the added benefit of increasing the mass of slender bones while minimizing the mass of robust bones.[13] It is unclear from our current study if there are additional levels of compensation that modulate tissue modulus, such as collagen orientation[53,54] and cross-linking,[55] but certainly these factors should be examined in future work. The validation study was limited to available young adult and middle-aged tibias, which are difficult to acquire. The limited number of samples did not allow us to test for a sex-specific effect.

Because our analysis purposely selected vascular pores from within the cortex, the positive correlation between porosity and robustness (Fig. 2*C*) suggested that internal BMU-based remodeling may be suppressed in slender bones and stimulated in robust bones. These results suggested that internal remodeling may not only be regulated locally by factors such as matrix damage,[56] but also globally by factors associated with the compensation of bone robustness. This intriguing outcome is worth confirming with a larger collection of tibias combined with histological techniques that provide dynamic measures of bone turnover.[57] Whether the internal remodeling of slender tibias is suppressed during the intense physical exercise typical of military training and contributes to stress fracture incidence has yet to be tested.

Although individuals who enroll into the military are from the general population and are thus expected to represent the diverse range in physical fitness and general health expected for the US and the UK populations, these individuals must pass a rigorous medical screening to be permitted into military training. Thus, our results do not incorporate skeletal traits for individuals with poor health. We suspect the functional adaptation process would be impaired in these later individuals, and consequently, a randomized study of the general population would result in greater variation in the degree to which bone traits are adapted relative to an individuals robustness value. However, excluding individuals with poor health would not be expected to affect the concept of functional inequivalence. Rather, we suspect that inclusion of individuals with poorly adapted trait sets may exaggerate the degree of functional inequivalence across the population.

In conclusion, intrinsic limitations on cellular activity and biomechanical trade-offs established boundaries on tissue modulus and cortical area that prevented adaptive processes from fully compensating the nonlinear relationship between tibial width and whole-bone bending stiffness. The limited variation in trait values constrained the range of functional trait sets that could be acquired by individuals with diverse genetic backgrounds and life histories, resulting in an emergent network of trait interactions. Susceptibility to common, heritable diseases is generally thought to originate at the genetic level, and most studies seek genomic variants or altered molecular networks to develop novel diagnostics and treatments to reduce disease risk.[58] Herein, we showed that predictable functional deficits may also arise at a higher level of biological organization, a phenomenon that may be difficult to predict from genetic information alone, because it involved biomechanical trade-offs, constraints on cellular activity, regulation of internal remodeling, and a network of compensatory trait interactions defining organ-level function. Limited compensation at this level of biological organization may be a public health concern, and it remains to be determined how the functional inequivalence reported in this study relates to fracture susceptibility.

Disclosures

All the authors have no conflict of interest.

Acknowledgments

We are grateful to D Catrambone, P Nasser, N Gendron, R Ghillani, B Spering[Q15], H Isome, M Lester, N Andarawis-Puri, M Faillace, and CJ Terranova for materials and discussion. This work was supported by grants from the US Department of Defense (W81XWH-09-2-0113, W81XWH-07-C-0097). The opinions or assertions contained herein are the private views of the authors and are not to be construed as official or as reflecting the views of the U.S. Army or the Department of Defense.

Authors' roles: K Jepsen, C Negus, and R Evans were responsible for establishing the hypotheses. K Jepsen was responsible for analyzing the data and writing the manuscript. GF Duarte conducted the validation study. H Goldman and N Hampson were responsible for analyzing the porosity data for the cadaveric tibias validation study. A Centi, BC Nindl, WJ Kraemer, K Galloway, J Lappe, D Cullen, and R Evans were responsible for recruiting subjects and acquiring pQCT data for the US cohort. J Greeves and R Izard were responsible for recruiting subjects and acquiring pQCT data for the UK cohort. C Negus was responsible for analyzing the pQCT images using the BAMpack software that he designed.

References

1. Rutherford SL, Lindquist S. Hsp90 as a capacitor for morphological evolution. Nature. 1998;396(6709):336–42.
2. Nadeau JH, Burrage LC, Restivo J, Pao YH, Churchill G, Hoit BD. Pleiotropy, homeostasis, and functional networks based on assays of cardiovascular traits in genetically randomized populations. Genome Res. 2003;13(9):2082–91.
3. Marder E, Goaillard JM. Variability, compensation and homeostasis in neuron and network function. Nat Rev Neurosci. 2006;7(7):563–74.
4. Hopkins SR, Harms CA. Gender and pulmonary gas exchange during exercise. Exerc Sport Sci Rev. 2004;32(2):50–6.
5. Waddington CH. Canalization of development and the inheritance of acquired characters. Nature. 1942;14:563–5.
6. Goaillard JM, Taylor AL, Schulz DJ, Marder E. Functional consequences of animal-to-animal variation in circuit parameters. Nat Neurosci. 2009;12(11):1424–30.
7. Ruff C. Growth tracking of femoral and humeral strength from infancy through late adolescence. Acta Paediatr. 2005;94(8):1030–7.
8. Smith RW, Walker RR. Femoral expansion in aging women: Implications for osteoporosis and fractures. Science. 1964;145:156–7.

9. Susanne C, Defrise-Gussenhoven E, Van Wanseele P, Tassin A. Genetic and environmental factors in head and face measurements of Belgian twins. Acta Genet Med Gemellol (Roma). 1983;32(3–4): 229–38.
10. Pandey N, Bhola S, Goldstone A, Chen F, Chrzanowski J, Terranova CJ, Ghillani R, Jepsen KJ. Inter-individual variation in functionally adapted trait sets is established during post-natal growth and predictable based on bone robusticity. J Bone Miner Res. 2009; 24(12):1969–80.
11. Tommasini SM, Nasser P, Schaffler MB, Jepsen KJ. Relationship between bone morphology and bone quality in male tibias: implications for stress fracture risk. J Bone Miner Res. 2005;20(8): 1372–80.
12. Jepsen KJ, Hu B, Tommasini SM, Courtland H-W, Price C, Terranova CJ, Nadeau JH. Genetic randomization reveals functional relationships among morphologic and tissue-quality traits that contribute to bone strength and fragility. Mamm Genome. 2007;18(6–7):492–507.
13. Currey JD, Alexander RM. The thickness of the walls of tubular bones. Journal of Zoology, London. 1985;206:453–68.
14. Milgrom C, Giladi M, Simkin A, Rand N, Kedem R, Kashtan H, Stein M, Gomori M. The area moment of inertia of the tibia: a risk factor for stress fractures. J Biomech. 1989;22(11–12):1243–8.
15. Beck TJ, Ruff CB, Shaffer RA, Betsinger K, Trone DW, Brodine SK. Stress fracture in military recruits: gender differences in muscle and bone susceptibility factors. Bone. 2000;27(3):437–44.
16. Evans RK, Negus C, Antczak AJ, Yanovich R, Israeli E, Moran DS. Sex differences in parameters of bone strength in new recruits: beyond bone density. Med Sci Sports Exerc. 2008;40 (11 Suppl): S645–53.
17. Burrows M, Cooper DM, Liu D, McKay HA. Bone and muscle parameters of the tibia: agreement between the XCT 2000 and XCT 3000 instruments. J Clin Densitom. 2009;12(2):186–94.
18. Lester ME, Urso ML, Evans RK, Pierce JR, Spiering BA, Maresh CM, Hatfield DL, Kraemer WJ, Nindl BC. Influence of exercise mode and osteogenic index on bone biomarker responses during short-term physical training. Bone. 2009;45(4):768–76.
19. Selker F, Carter DR. Scaling of long bone fracture strength with animal mass. J Biomech. 1989;22(11–12):1175–83.
20. Peterman MM, Hamel AJ, Cavanagh PR, Piazza SJ, Sharkey NA. In vitro modeling of human tibial strains during exercise in micro-gravity. J Biomech. 2001;34(5):693–8.
21. Wright S. Correlation and causation. Journal of Agricultural Research. 1921;20:557–85.
22. Tommasini SM, Nasser P, Hu B, Jepsen KJ. Biological Co-adaptation of Morphological and Composition Traits Contributes to Mechanical Functionality and Skeletal Fragility. J Bone Miner Res. 2008;23(2):236–46.
23. Jepsen KJ, Courtland H-W, Nadeau JH. Genetically-determined phenotype covariation networks control bone strength. J Bone Miner Res. 2010;25(7):1581–93.
24. MacCallum RC, Hong S. Power analysis in covariance structural modeling using GFI and AGFI. Multivariate Behavioral Research. 1997;32(2):193–210.
25. Currey JD. Effects of differences in mineralization on the mechanical properties of bone. Philos Trans R Soc Lond B Biol Sci. 1984;304(1121): 509–18.
26. Tawhai MH, Hoffman EA, Lin CL. The lung physiome: merging imaging-based measures with predictive computational models. Wiley Interdiscip Rev Syst Biol Med. 2009;1(1):61–72.
27. Nash M, Hunter P. Computational mechanics of the heart. J Elasticity. 2000;61:113–41.
28. Lee SW, Antiga L, Spence JD, Steinman DA. Geometry of the carotid bifurcation predicts its exposure to disturbed flow. Stroke. 2008; 39(8):2341–7.
29. Markl M, Wegent F, Zech T, Bauer S, Strecker C, Schumacher M, Weiller C, Hennig J, Harloff A. In vivo wall shear stress distribution in the carotid artery: effect of bifurcation geometry, internal carotid artery stenosis, and recanalization therapy. Circ Cardiovasc Imaging. 2010;3(6):647–55.
30. Young RL, Haselkorn TS, Badyaev AV. Functional equivalence of morphologies enables morphological and ecological diversity. Evolution. 2007;61(11):2480–92.
31. Frost HM. Bone "mass" and the "mechanostat": a proposal. Anat Rec. 1987;219(1):1–9.
32. Ruff C. Growth in bone strength, body size, and muscle size in a juvenile longitudinal sample. Bone. 2003;33(3):317–29.
33. Ruff CB. Mechanical determinants of bone form: insights from skeletal remains. J Musculoskelet Neuronal Interact. 2005;5(3):202–12.
34. Nowlan NC, Jepsen KJ, Morgan EF. Smaller, weaker, and less stiff bones evolve from changes in subsistence strategy. Osteoporos Int. 2011;22(6):1967–80.
35. Currey JD. Mechanical properties of bone tissues with greatly differing functions. J Biomech. 1979;12(4):313–9.
36. Rittweger J, Beller G, Ehrig J, Jung C, Koch U, Ramolla J, Schmidt F, Newitt D, Majumdar S, Schiessl H, Felsenberg D. Bone-muscle strength indices for the human lower leg. Bone. 2000;27(2):319–26.
37. Nieves JW, Formica C, Ruffing J, Zion M, Garrett P, Lindsay R, Cosman F. Males have larger skeletal size and bone mass than females, despite comparable body size. J Bone Miner Res. 2005; 20(3):529–35.
38. Friedl KE. Biomedical research on health and performance of military women: accomplishments of the Defense Women's Health Research Program (DWHRP). J Women's Health (Larchmt). 2005;14(9): 764–802.
39. Cummings SR, Kelsey JL, Nevitt MC, O'Dowd KJ. Epidemiology of osteoporosis and osteoporotic fractures. Epidemiol Rev. 1985;7:178–208.
40. Looker AC, Beck TJ, Orwoll ES. Does body size account for gender differences in femur bone density and geometry?. J Bone Miner Res. 2001;16(7):1291–9.
41. Currey JD. How well are bones designed to resist fracture?. J Bone Miner Res. 2003;18(4):591–8.
42. Burr DB, Forwood MR, Fyhrie DP, Martin RB, Schaffler MB, Turner CH. Bone microdamage and skeletal fragility in osteoporotic and stress fractures. J Bone Miner Res. 1997;12(1):6–15.
43. Franklyn M, Oakes B, Field B, Wells P, Morgan D. Section modulus is the optimum geometric predictor for stress fractures and medial tibial stress syndrome in both male and female athletes. Am J Sports Med. 2008;36(6):1179–89.
44. Albright F, Smith PH, Richardson AM. Post-menopausal osteoporosis. Its clinical features. JAMA. 1941;116:2465–74.
45. Szulc P, Munoz F, Duboeuf F, Marchand F, Delmas PD. Low width of tubular bones is associated with increased risk of fragility fracture in elderly men—the MINOS study. Bone. 2006;38(4):595–602.
46. Zebaze RM, Jones A, Knackstedt M, Maalouf G, Seeman E. Construction of the femoral neck during growth determines its strength in old age. J Bone Miner Res. 2007;22(7):1055–61.
47. Tommasini SM, Hu B, Nadeau JH, Jepsen KJ. Phenotypic integration among trabecular and cortical bone traits establishes mechanical functionality of inbred mouse vertebrae. J Bone Miner Res. 2009; 24(4):606–20.
48. Kannus P, Haapasalo H, Sankelo M, Sievanen H, Pasanen M, Heinonen A, Oja P, Vuori I. Effect of starting age of physical activity on bone mass in the dominant arm of tennis and squash players. Ann Intern Med. 1995;123(1):27–31.
49. Jepsen KJ, Hu B, Tommasini SM, Courtland H-W, Price C, Cordova M, Nadeau JH. Phenotypic integration of skeletal traits during growth

buffers genetic variants affecting the slenderness of femora in inbred mouse strains. Mamm Genome. 2009;20(1):21–33.

50. Liu D, Manske SL, Kontulainen SA, Tang C, Guy P, Oxland TR, McKay HA. Tibial geometry is associated with failure load ex vivo: a MRI, pQCT and DXA study. Osteoporos Int. 2007;18(7):991–7.
51. Kontulainen SA, Johnston JD, Liu D, Leung C, Oxland TR, McKay HA. Strength indices from pQCT imaging predict up to 85% of variance in bone failure properties at tibial epiphysis and diaphysis. J Musculoskelet Neuronal Interact. 2008;8(4):401–9.
52. Ural A, Vashishth D. Interactions between microstructural and geometrical adaptation in human cortical bone. J Orthop Res. 2006; 24(7):1489–98.
53. Skedros JG, Dayton MR, Sybrowsky CL, Bloebaum RD, Bachus KN. The influence of collagen fiber orientation and other histocompositional characteristics on the mechanical properties of equine cortical bone. J Exp Biol. 2006;209(Pt 15):3025–42.
54. Goldman HM, Bromage TG, Thomas CD, Clement JG. Preferred collagen fiber orientation in the human mid-shaft femur. Anat Rec. 2003;272A(1):434–45.
55. Brama PA, TeKoppele JM, Bank RA, Barneveld A, van Weeren PR. Biochemical[Q16] development of subchondral bone from birth until age eleven months and the influence of physical activity. Equine Vet J. 2002;34(2):143–9.
56. Bentolila V, Boyce TM, Fyhrie DP, Drumb R, Skerry TM, Schaffler MB. Intracortical remodeling in adult rat long bones after fatigue loading. Bone. 1998;23(3):275–81.
57. Goldman HM, McFarlin SC, Cooper DM, Thomas CD, Clement JG. Ontogenetic patterning of cortical bone microstructure and geometry at the human mid-shaft femur. Anat Rec (Hoboken). 2009; 292(1):48–64.
58. Schadt EE. Molecular networks as sensors and drivers of common human diseases. Nature. 2009;461(7261):218–23.

AUTHOR QUERY FORM

JOURNAL: JOURNAL OF BONE AND MINERAL RESEARCH
Article: jbmr_497

Dear Author,

During the copyediting of your paper, the following queries arose. Please respond to these by annotating your proofs with the necessary changes/additions.

- If you intend to annotate your proof electronically, please refer to the E-annotation guidelines.
- If you intend to annotate your proof by means of hard-copy mark-up, please refer to the proof mark-up symbols guidelines. If manually writing corrections on your proof and returning it as a scanned pdf via email, do not write too close to the edge of the paper. Please remember that illegible mark-ups may delay publication.

Whether you opt for hard-copy or electronic annotation of your proofs, we recommend that you provide additional clarification of answers to queries by entering your answers on the query sheet, in addition to the text mark-up.

Query No.	Query	Remark
Q1	Please supply a running title above the article title.	
Q2	Here and throughout this list, please supply the names of the departments right after the superscript numbers.	
Q3	"L-3/Jaycor"? Is this name correct?	
Q4	Please be sure that all acronyms are spelled out at first cite, followed by the abbreviation in parentheses.	
Q5	Please supply five key words.	
Q6	Add Surrey to this address?	
Q7	Add North Yorkshire to the address?	
Q8	Delete here and work this into the second paragraph of the Acknowledgments?	
Q9	Be more specific where "above" appears throughout? If so, section titles should be in roman and in quotation marks.	
Q10	Delete here and add more detail to the second paragraph of the Acknowledgments?	
Q11	Specify sections where "below" appears throughout?	
Q12	Please verify names of companies (including use of upper- and lowercase), throughout.	
Q13	Specify where described?	
Q14	Please verify that this is correct.	
Q15	See "Spiering" in note 18, and please verify spelling.	
Q16	In #55, is "TeKoppele" correct as spelled?	